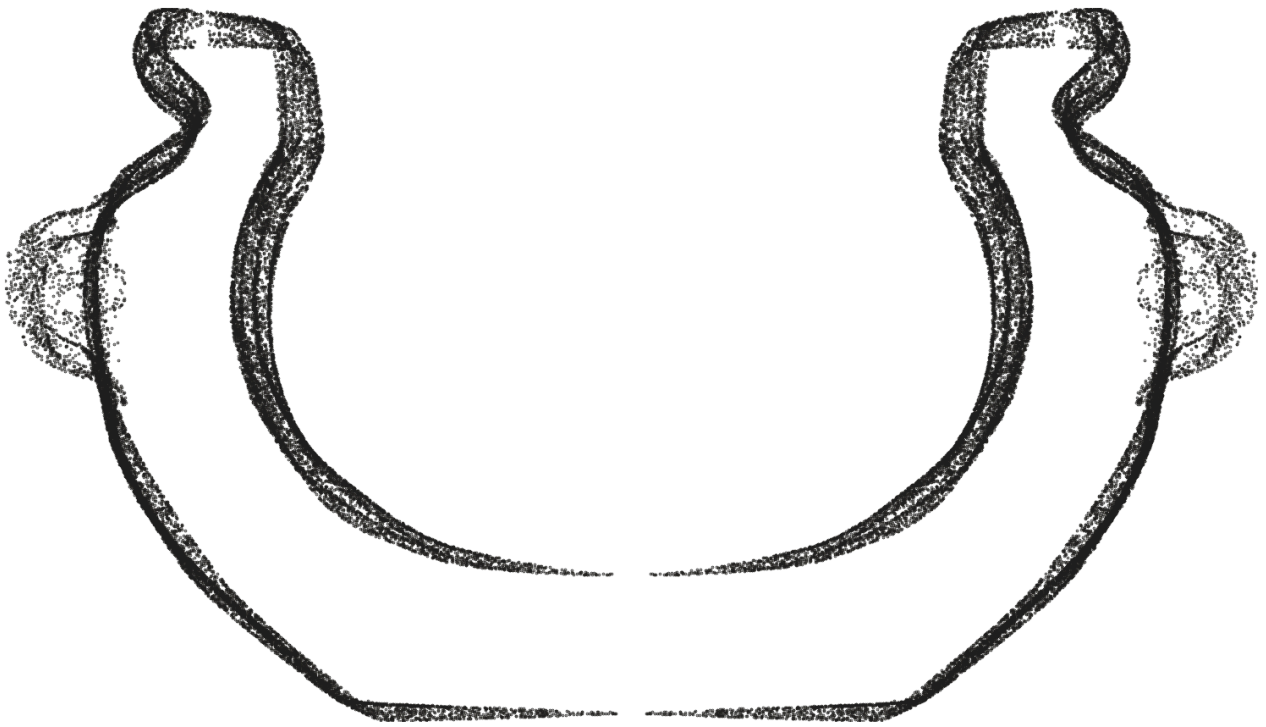


RV003 - Squat Shouldered Jar

An Exploration of Precision



Author: Stine Gerdes, arcsai.org

License: Creative Commons BY-NC-SA 4.0

Date: 2025-07-21

Version: 01.20



Scientists Against Myths

Contents

Artifact Information	2
Alignment In The Cartesian Coordinate System	3
Statistics used throughout the report	5
Precision	6
Circularity	6
Concentricity	32
Coaxiality	47
Surface Variability	51
Precision Score Of The Artifact	60
Analysis Roadmap	62
Appendix A - Comparison Of Circularity Measurements (Z-plane vs. surface-perpendicular)	63
Appendix B - Comparison Of Concentricity Measurements (Z-plane vs. surface-perpendicular)	73

Artifact Information

Artifact Data

Collection	In private collection
Provenance ¹	NA
Provenience ²	NA
Attribution	NA

Art dealer information

Ref.	
Description	Modern replica - Produced by Olga Vdovina and Yulia Gukasova in collaboration with Scientists Against Myths
URL	https://www.youtube.com/watch?v=dC3Z_DBNcp8

Maijers vessel classification³

Short classification	Squat Shouldered Jar
Long classification	The vessel is created in a closed form classified as a squat jar with a shouldered shape, a raised blunt rim.

Physical properties

Precision score ⁴	1.46
Height (approximate)	83 mm 3.27 in
Width (approximate)	126 mm 4.96 in
Material	Marble breccia
Mohs Hardness ⁵	5 - 7 (Breccia)
Weight	

Scan information

Source	Scanned by Scientists Against Myths
Source file name	SAM_Vaza_2_Model_00.obj
Scan method	Photogrammetry
Scanner	Unknown
Rated scan accuracy	Not specified
Scan date	Unknown
Scanned by	Unknown

Mesh decimation	Unknown
Number of vertices	261 712
Mesh density ⁶	342 µm 13.47 thou
Max vertex distance	978 µm 38.496 thou
Min vertex distance	0 µm 0.000 thou
Vertices per cm ²	265 (approximated)
Vertices per in ²	1709 (approximated)

¹The verifiable chain of custody of an artifact

²The location or site where an artifact was recovered

³Vessel artifact classification developed by W. Arnold Maijer and described in his publication Masters of Stone, ISBN 978-90-829212-0-5

⁴The precision score metric is described in Precision Score Of The Artifact, p. 61

⁵The Mohs scale is an ordinal scale, from 1 to 10, describing the materials resistance to abrasion (the ability of harder material to scratch softer material)

⁶Median distance between vertices

Alignment In The Cartesian Coordinate System

For precise and valid measurements of the vessel's geometry to be possible, the points of the scanned dataset must first and foremost be placed optimally in a Cartesian coordinate system. Several alignment methods and algorithms have been tested on a number of different vessels to determine the best way to achieve optimal alignment.

Any misalignment of the artifact will increase the error of the precision measurements, due to the distortion/wobble effect caused by the misaligned object. To visualize this distortion, we can consider a representation of the three-dimensional point cloud data, folded to a two-dimensional plane. This folded representation is obtained by rotating all scanned points around an assumed center axis to $y = 0, x > 0$, thus resulting in a two-dimensional profile representation of all scanned vertices in the object.

Figure 1 illustrates this effect on a ideal ellipsoid. In the first image, the ellipsoid is perfectly aligned, resulting in a narrow and precise two-dimensional folded profile. As misalignments are introduced, the two-dimensional profile increases in width, visually showing the distortion, causing the error in the precision measurements to increase. While easy to understand visually, this distortion can also be objectively quantified, and as such used to compare the fitness of different assumed center axes against each other, and further to create an automated and solid process for optimal Cartesian alignment of the scan data.

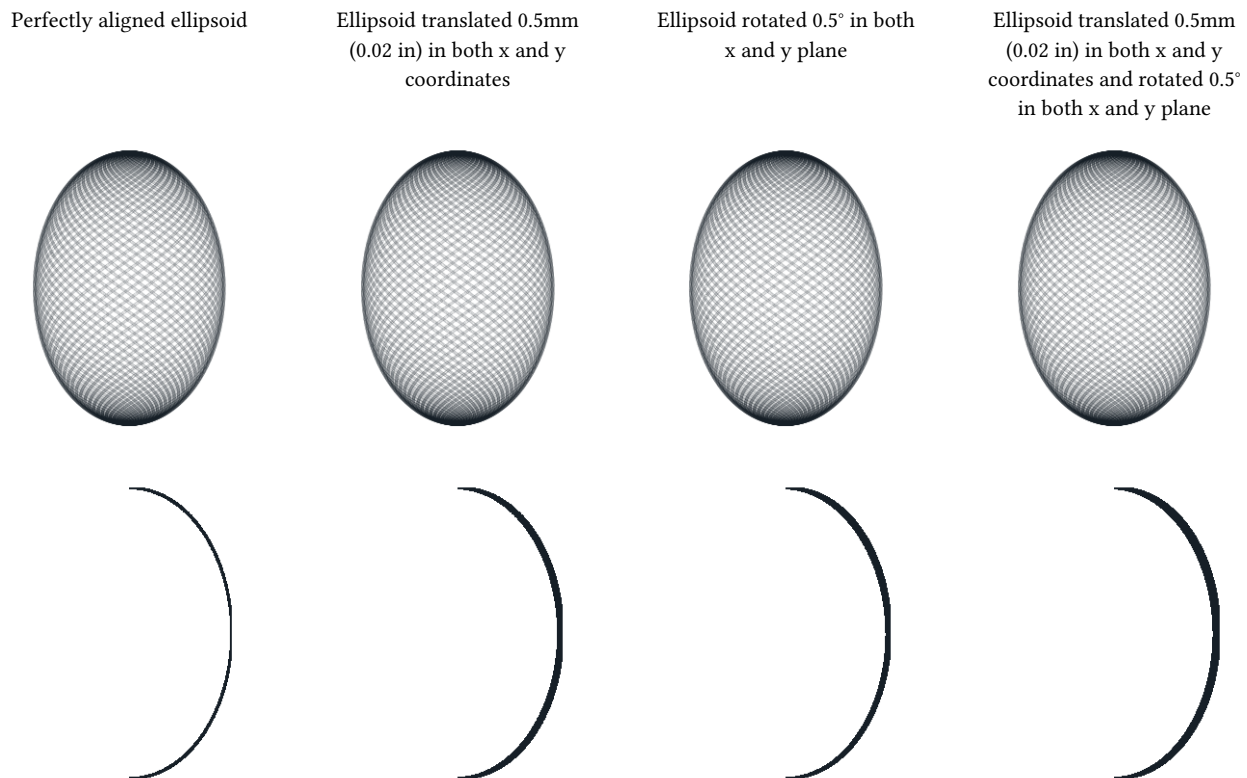


Figure 1: Distortion caused by a misalignment of the artifact

In contemporary metrology analysis of modern production objects, it is common to align the object in a Cartesian coordinate system by fitting a flat surface of the object to a reference plane in the coordinate system, cylindrical features to an ideal cylinder etc., or by using specific markers placed on the object in the design process. This methodology, however, is inadequate for the ancient objects in question. Most scanned artifacts, do not have a valid flat surface which could be aligned to a plane in the Cartesian coordinate system; most surfaces seem to be curved. Some artifacts do have a flat base, however this is often a worn area of the artifact and practical tests have shown that alignment to such surfaces will not produce optimal alignment of the scan data.

As conventional methods of alignment do not always yield good results with these types of artifacts, a more adequate method of alignment has been developed to enable precise measurements and statistical analysis of the scan data.

To find the optimal position of the vessel in the coordinate system, a range of rotation and translation tests are carried out to find the best fit of the central axis.

Based on the assumption that the analyzed object was created using a rotational process, and thus have symmetry around a central axis, the alignment of the artifact is carried out in a two-step process. An overview of this process is given below.

The artifact is placed in a Cartesian coordinate system, in an initially unaligned state. The first step in the alignment process estimates the central rotational axis of the vessel, by analyzing the coaxiality of thin cross-section slices of the vessel. The slices will be as thin as possible based on the mesh density of the scan, while still ensuring enough data points in each slice to be statistically valid.

For each slice, circular regression⁷ (estimate of best fit circle) is used to estimate the center point of this slice. Combined over the total Z-axis range of the vessel, these center points provide us with an indicator of the incline and position of the vessel's central axis.

The next step will optimize the center axis alignment by progressively minimizing the deviation (perpendicular to the surface curvature) of the two-dimensional profile, see Figure 1. By ascertaining and comparing the resulting fit of many thousands of different potential rotations, the best fit alignment of the scan data can be estimated, and an optimal center axis (in relation to the data points) can be reconstructed. The actual three-dimensional point-cloud is then aligned to this axis, by rotating and translating the scanned data points to match the Z-axis of the Cartesian coordinate system.

To enable extensive analysis of the full surface of the artifact, the mesh is split into exterior and interior surfaces. The exterior surface is aligned independently of interior data points, providing a baseline for exterior quality assessment. The interior surface is represented by two alignments:

- Aligned with the exterior mesh to analyze concentricity, and
- Aligned separately to assess its precision and compare the true tilt/displacement between interior and exterior surfaces.

⁷Circle regression algorithm used: Kenichi Kanatani, Prasanna Rangarajan, "Hyper least squares fitting of circles and ellipses" Computational Statistics & Data Analysis, Vol. 55, pages 2197-2208, (2011)

Statistics used throughout the report

This section provides an overview of the key statistical and model-evaluation metrics employed throughout the report to analyze dataset variability, model fit, and predictive accuracy.

Each measure is introduced with its mathematical formulation, practical interpretation, and explicit reference to how it is calculated in the context of the evaluated models and residuals. Together, these metrics quantify:

- Data variability (e.g., MAD, Standard Deviation, Range).
- Model accuracy (e.g., MSD, RMSD).
- Robustness vs. sensitivity to extreme values and central tendencies.

Mean Squared Deviation (MSD), also known as Mean Squared Error (MSE).

$$\text{MSD} = \frac{\sum_{i=1}^n (y_i - \hat{y})^2}{n}$$

The Mean Squared Deviation (MSD) measures the average magnitude of squared differences between observed (y_i) and predicted (\hat{y}) values, calculated as the mean of squared residuals, and is used as a measure of discrepancy in regression and model-fitting contexts.

This measure amplifies the influence of larger deviations through squaring, emphasizes imperfections in the observed data, but retains sensitivity to outliers.

Root Mean Squared Deviation (RMSD), also known as Root Mean Squared Error (RMSE).

$$\text{RMSD} = \sqrt{\frac{\sum_{i=1}^n (y_i - \hat{y})^2}{n}}$$

The Root Mean Square Deviation (RMSD) measures the magnitude of differences between observed (y_i) and predicted (\hat{y}) values by calculating the square root of the average of squared residuals.

RMSD is a commonly used measure of discrepancy in regression and model-fitting contexts. It quantifies the average magnitude of residuals while retaining sensitivity to larger deviations (via squaring), making it particularly useful for evaluating model accuracy.

Standard Deviation (SD)

$$s = \sqrt{\frac{\sum_{i=1}^n (y_i - \bar{y})^2}{n - 1}}$$

The Standard Deviation measures the spread of data (y_i) around the mean (\bar{y}) by calculating the square root of the average of squared differences between each value and the mean.

It is sensitive to outliers as it amplifies their influence through squaring, in contrast to MAD.

Throughout this report, the Standard Deviation is calculated using the absolute residuals from regression models.

Median Absolute Deviation (MedianAD)

$\text{MedianAD} = \text{median}(|y_i - \text{median}(y)|)$ The Median Absolute Deviation (MAD) measures the spread of data around the median by calculating the median of absolute differences between each value and the median.

MAD is a robust measure of spread, analogous to the interquartile range (a robust measure centered on the middle 50% of data), and differs from the standard deviation in that it minimizes the impact of outliers.

Throughout this report, the MAD is calculated using the absolute values of residuals from regression models.

Range

$$\max(y_i) - \min(y_i)$$

The Range measures the spread of a dataset by calculating the difference between the maximum and minimum values.

The Range is a simple measure of spread, capturing the full extent of variability. Range is very sensitive to extreme values, as it is entirely determined by the two most extreme data points.

Throughout this report, the Range is calculated using the full range of residuals from regression models.

Precision

To explore the manufacturing precision of the artifact in depth, the following analysis have been carried out:

- Circularity around the axis of symmetry is examined in detail at selected cross-sections.
- Overall circularity around the axis of symmetry is measured for the full height of the vessel (areas of the vessel with extensive damage are not taken into account for this metric).
- Concentricity of the vessel between selected cross-sections are examined in detail to determine if the existence of an axis of rotation in the manufacture of the object can be established.
- The coaxiality of the vessel is analyzed to explore the precision of the central axis of the object.
- The surface variability is analyzed and visualized on through a heatmap.

Circularity

Circularity is the measurement of how round the surface of an object is, optionally in reference to a datum axis. The *circularity tolerance* is the radial distance of two circles, each with their centers in the datum axis, and each of them conforming, respectively, to the minimum and maximum deviations of the data-set to a true circle, see Figure 2.

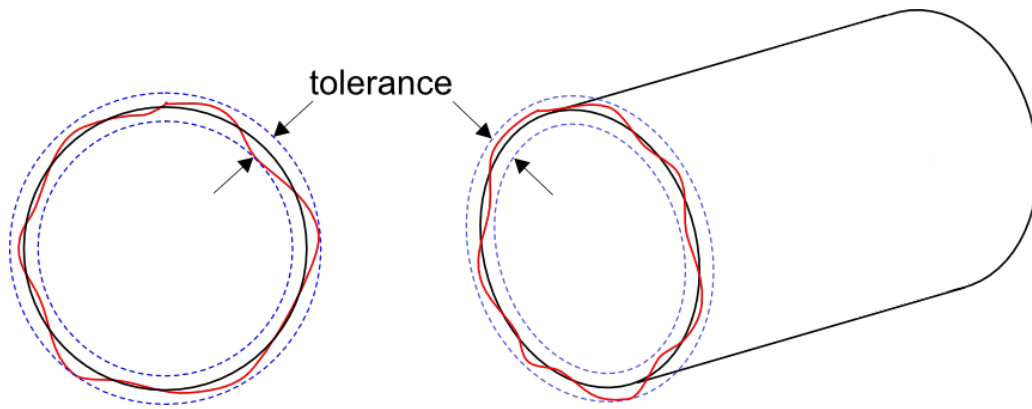


Figure 2: Circularity tolerance.

Circularity is examined at different cross-sections of the vessel, using the established Z-axis as the datum axis (axis of symmetry). The distance between the scanned points in the local datum plane is measured to determine the range between the two concentric circles encompassing the measured points, see Figure 3.

Referencing all of the individual circularity measurements to the global (reconstructed) axis of symmetry of the object, allows us to ascertain not only circularity of local features of the object, but how well circularity was *maintained* over the entire manufacturing process. This is an important distinction, which may be able to provide valuable insights into requirements of the construction methods. For reference, and seeing that the variance in local circularity also holds interest, measurements of circularity of the vessel without reference to the axis of symmetry can additionally be found in the Concentricity, p. 33.

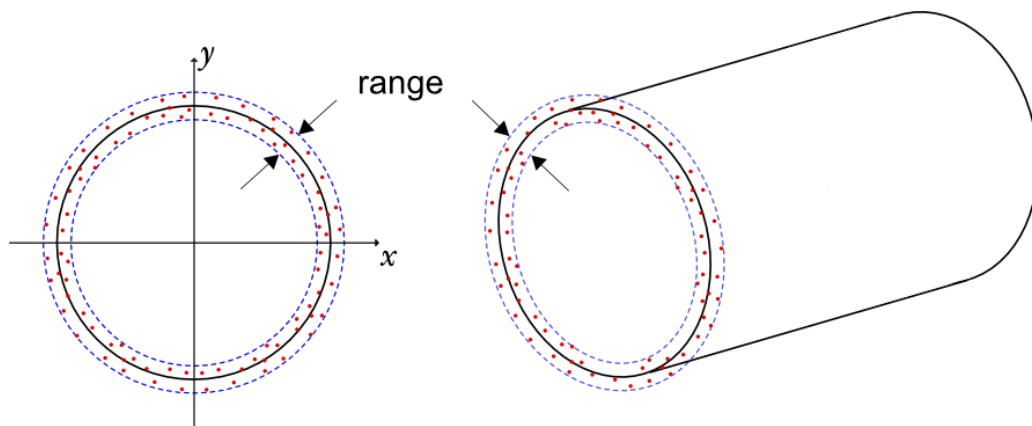


Figure 3: Circularity measurements.

If the circularity is determined from slices of the vessel exclusively in the *Z-plane* (actually measuring the cylindricity of a very thin slices of the vessel, in an attempt to approximate circularity), this would - in some areas - introduce significant distortion (increasing measurement errors) in the samples, due to the curvature of the vessel's surface.

Each sample slice of the vessel is therefore obtained perpendicular to the surface curvature, see Figure 6 to Figure 18. The measurements are taken conservatively without filtration of potential outliers.

To explore the potential distortion caused by obtaining samples in the Z-plane only, please refer to Appendix A, where measurements in the Z-plane and measurements perpendicular to surface curvature are compared side by side.

Detailed circularity measurements of selected points

Circularity measurements across a range of selected slices of the vessel (see Table 1) have been analyzed in-depth, and detailed plots of each measurement is provided. Furthermore, full circularity measurements are shown for each available scanned surface including a detailed plot to visualize the circularity of all areas of the vessel.

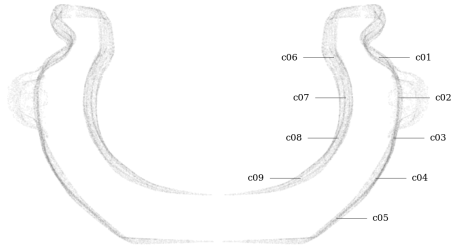


Figure 4: Circularity measurement sample locations, full mesh aligned with exterior surface



Figure 5: Circularity measurement sample location, separately aligned interior mesh

Metric

Tag	Area	Measured deviation ⁸	Residuals				Sample size	Slice		
			Range	RMSD ⁹	MAD ¹⁰	SD		Height	Z coord.	Radius ¹¹
		mm	mm	mm	mm	mm		mm	mm	mm
c01	exterior	Ø111.834±1.722	3.282	1.085	0.389	0.446	162	0.200	63.743	55.917
c02	exterior	Ø125.763±1.700	2.704	0.651	0.248	0.361	149	0.200	49.799	62.882
c03	exterior	Ø121.976±0.926	1.694	0.450	0.232	0.255	307	0.200	35.856	60.988
c04	exterior	Ø109.485±2.013	2.747	0.740	0.187	0.490	242	0.200	21.912	54.743
c05	exterior	Ø82.190±0.936	1.817	0.511	0.207	0.276	139	0.200	7.969	41.095
c06	interior	Ø80.516±3.192	5.489	1.433	0.416	0.687	273	0.200	63.743	40.258
c06_s	interior sep.	Ø80.571±1.770	3.326	0.974	0.405	0.471	339	0.200	63.743	40.285
c07	interior	Ø88.855±2.447	4.734	1.529	0.764	0.768	276	0.200	49.799	44.428
c07_s	interior sep.	Ø89.099±1.262	1.992	0.507	0.180	0.259	305	0.200	49.799	44.549
c08	interior	Ø83.652±1.798	3.373	1.115	0.299	0.438	329	0.200	35.856	41.826
c08_s	interior sep.	Ø83.803±1.076	1.766	0.438	0.189	0.247	290	0.200	35.856	41.902
c09	interior	Ø57.403±1.549	2.884	0.925	0.381	0.409	86	0.200	21.912	28.701
c09_s	interior sep.	Ø57.052±1.098	2.194	0.724	0.263	0.330	98	0.200	21.912	28.526

Imperial

Tag	Area	Measured deviation ⁸	Residuals				Sample size	Slice		
			Range	RMSD ⁹	MAD ¹⁰	SD		Height	Z coord.	Radius ¹¹
		in	in	in	in	in		in	in	in
c01	exterior	Ø4.4029±0.0678	0.1292	0.0427	0.0153	0.0176	162	0.0079	2.5096	2.2014
c02	exterior	Ø4.9513±0.0669	0.1065	0.0256	0.0098	0.0142	149	0.0079	1.9606	2.4756
c03	exterior	Ø4.8022±0.0365	0.0667	0.0177	0.0091	0.0101	307	0.0079	1.4116	2.4011
c04	exterior	Ø4.3105±0.0793	0.1081	0.0291	0.0074	0.0193	242	0.0079	0.8627	2.1552
c05	exterior	Ø3.2358±0.0368	0.0715	0.0201	0.0082	0.0109	139	0.0079	0.3137	1.6179
c06	interior	Ø3.1699±0.1257	0.2161	0.0564	0.0164	0.0270	273	0.0079	2.5096	1.5850
c06_s	interior sep.	Ø3.1721±0.0697	0.1309	0.0384	0.0160	0.0186	339	0.0079	2.5096	1.5860
c07	interior	Ø3.4982±0.0963	0.1864	0.0602	0.0301	0.0302	276	0.0079	1.9606	1.7491
c07_s	interior sep.	Ø3.5078±0.0497	0.0784	0.0200	0.0071	0.0102	305	0.0079	1.9606	1.7539
c08	interior	Ø3.2934±0.0708	0.1328	0.0439	0.0118	0.0172	329	0.0079	1.4116	1.6467
c08_s	interior sep.	Ø3.2993±0.0424	0.0695	0.0173	0.0074	0.0097	290	0.0079	1.4116	1.6497
c09	interior	Ø2.2599±0.0610	0.1135	0.0364	0.0150	0.0161	86	0.0079	0.8627	1.1300
c09_s	interior sep.	Ø2.2461±0.0432	0.0864	0.0285	0.0104	0.0130	98	0.0079	0.8627	1.1231

Table 1: Detailed circularity measurements at selected samples of RV003.

Figure 6 to Figure 18 shows a detailed plots of each circularity measurement.

⁸Sample diameter Ø± maximum measured deviation from measured radius

⁹Root mean square deviation (RMSD) also called Root mean square error (RMSE)

¹⁰Median absolute deviation

¹¹Median sample radius from z-axis

Graphical overview of circularity measurement c01

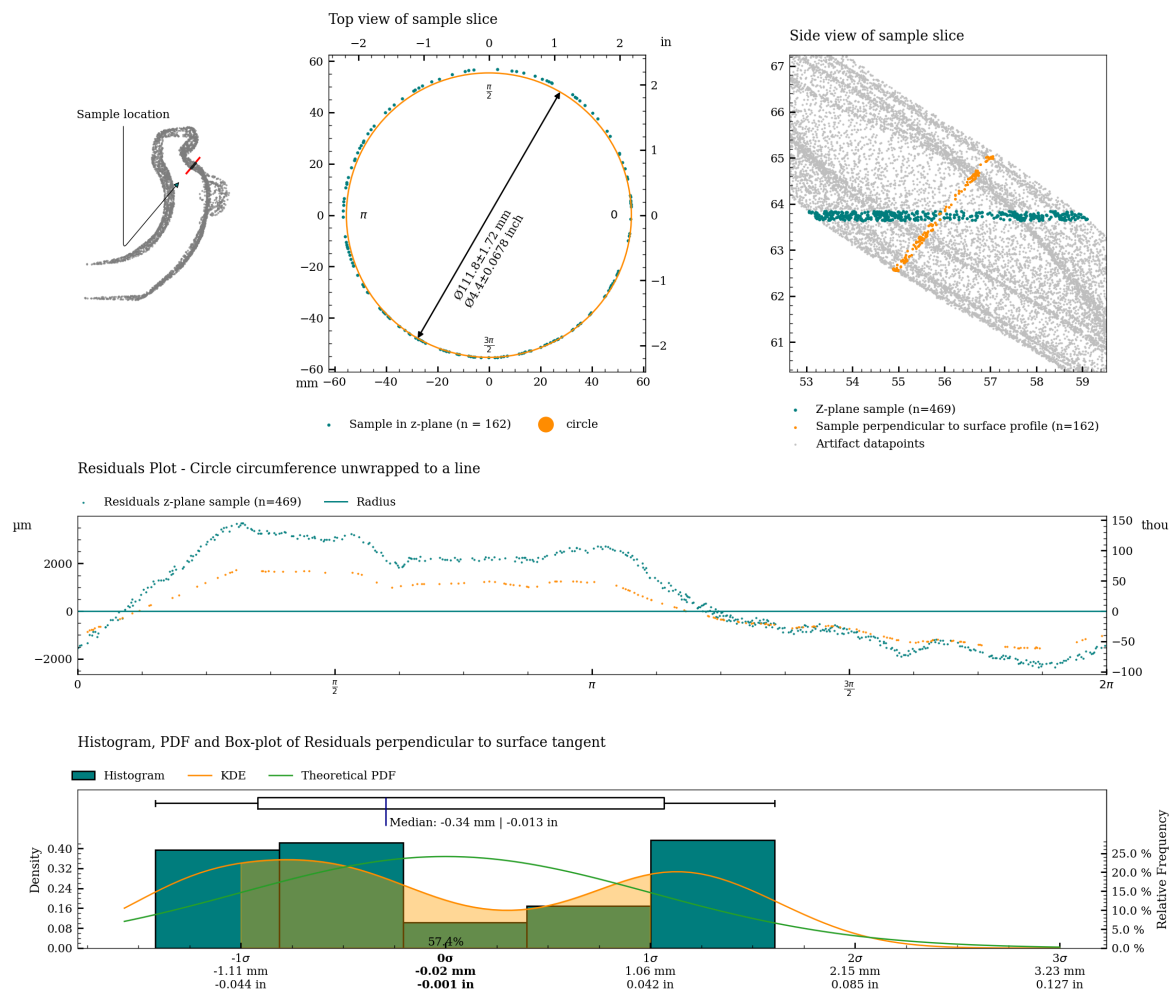


Figure 6: Charts with statistics for the measurement of c01.

Graphical overview of circularity measurement c02

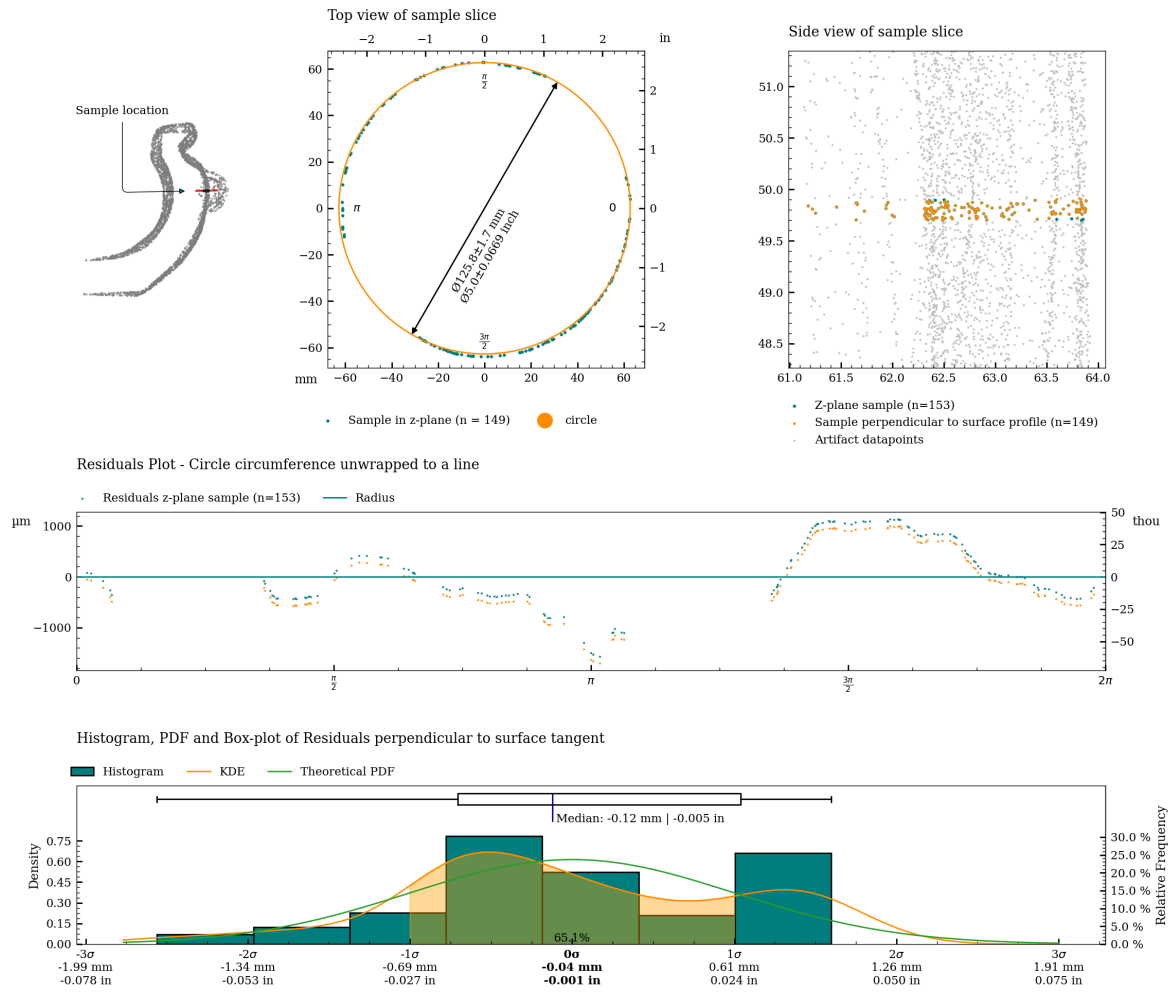


Figure 7: Charts with statistics for the measurement of c02.

Graphical overview of circularity measurement c03

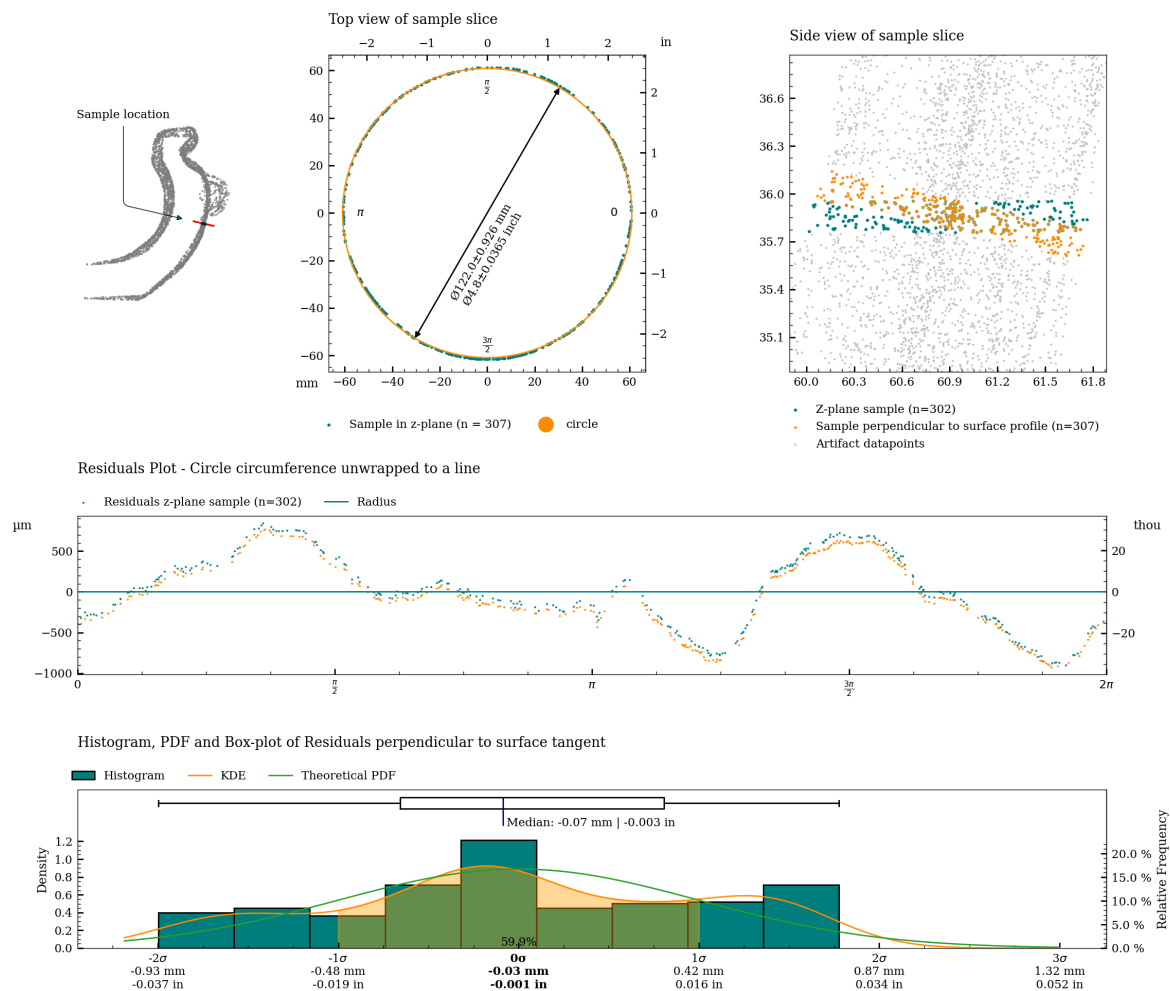


Figure 8: Charts with statistics for the measurement of c03.

Graphical overview of circularity measurement c04

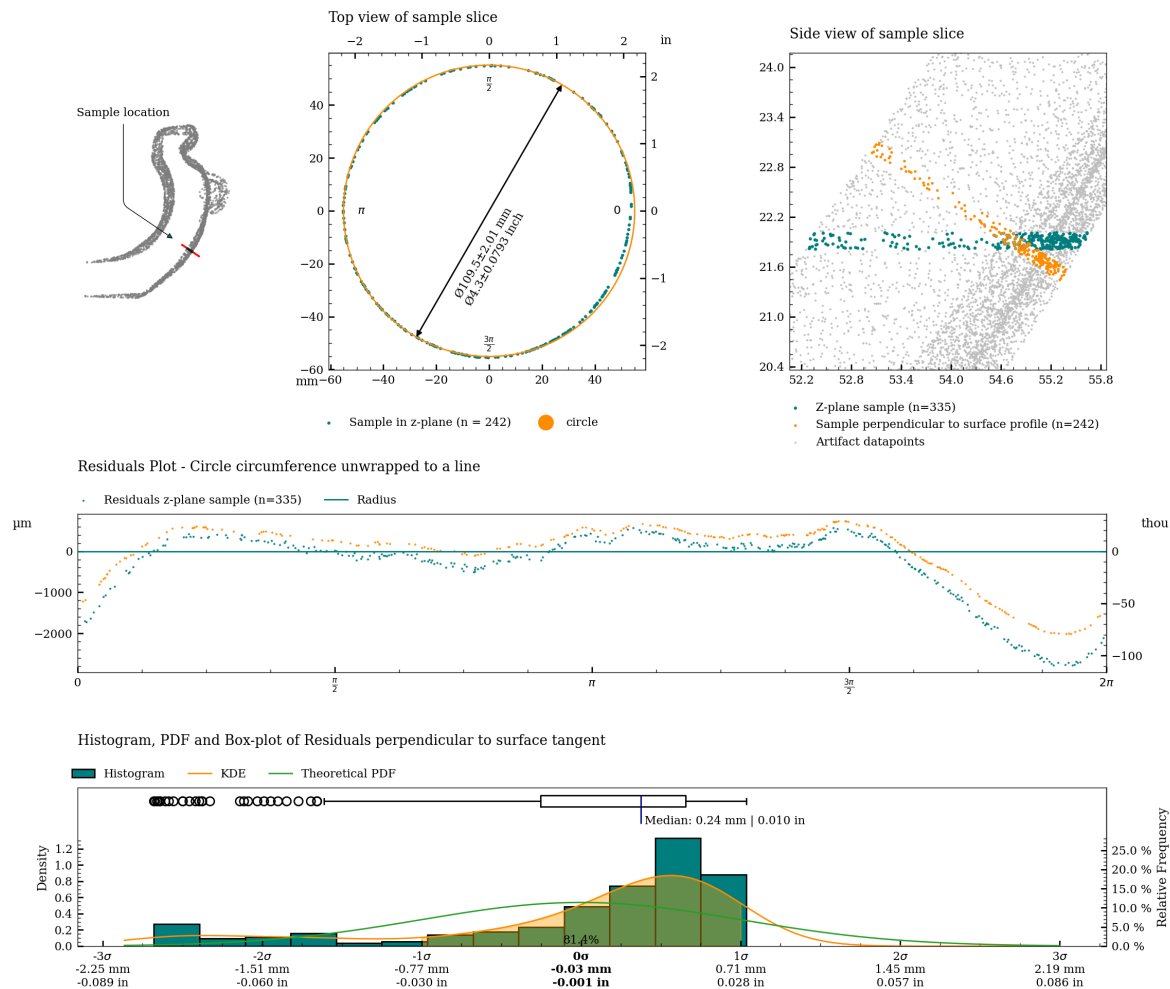


Figure 9: Charts with statistics for the measurement of c04.

Graphical overview of circularity measurement c05

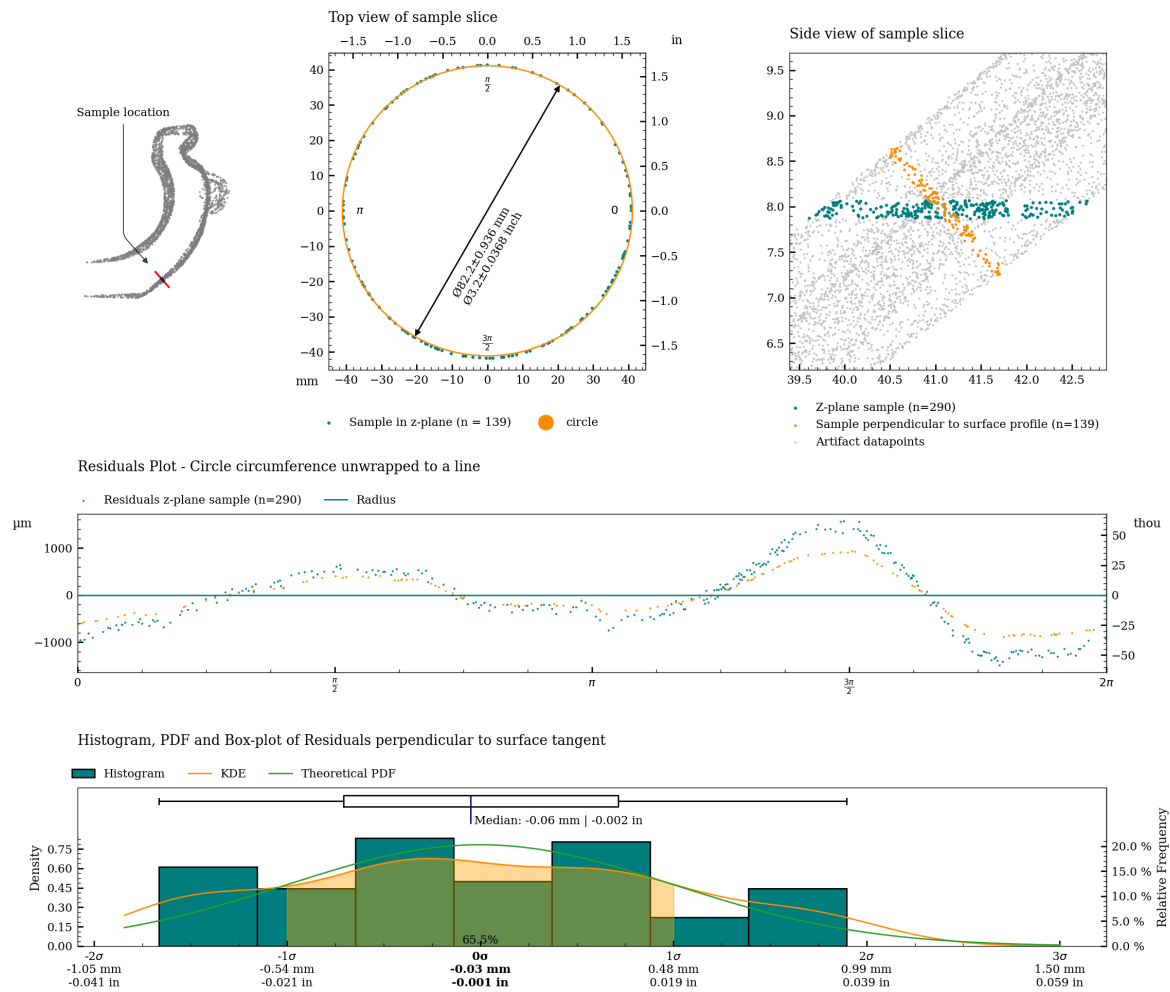


Figure 10: Charts with statistics for the measurement of c05.

Graphical overview of circularity measurement c06

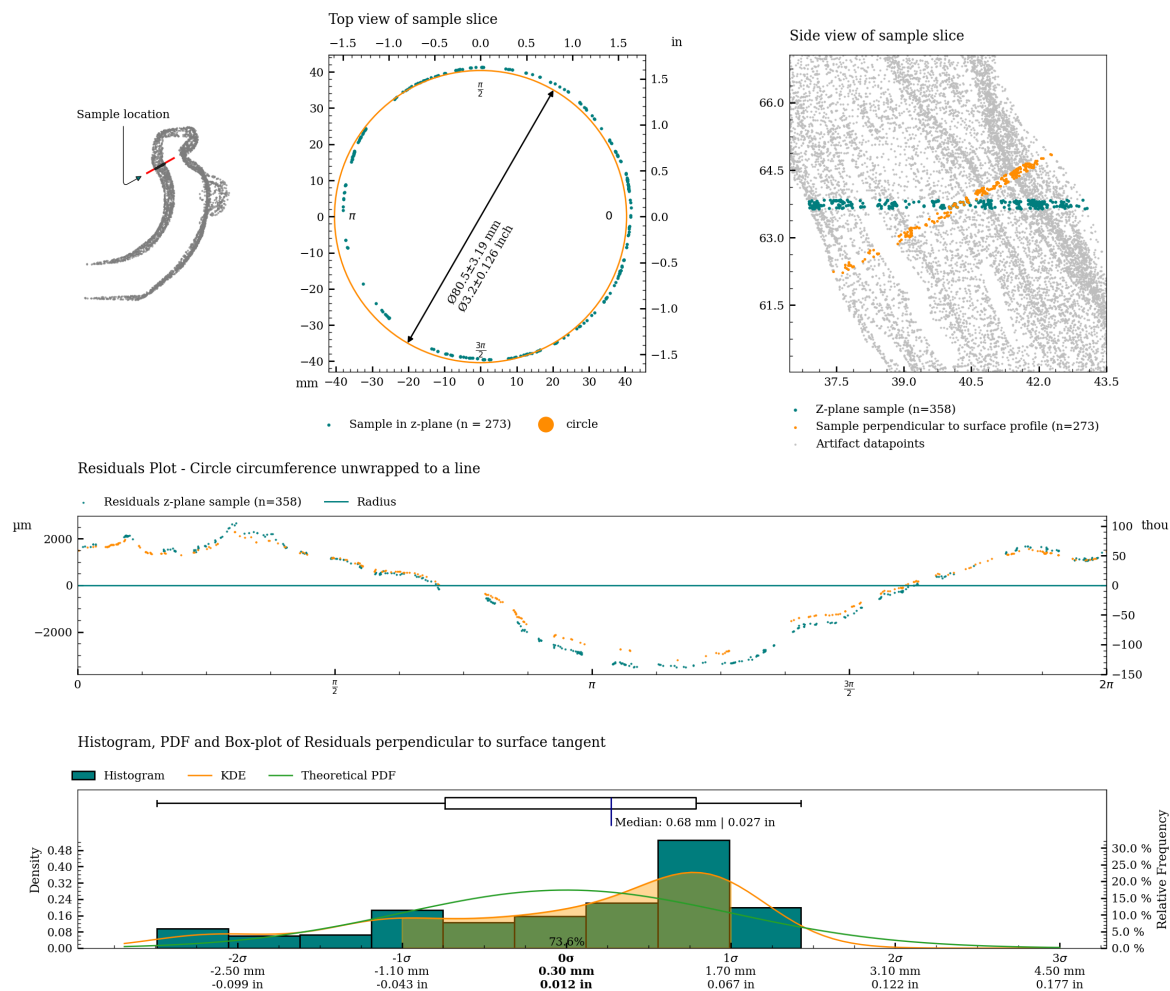


Figure 11: Charts with statistics for the measurement of c06.

Graphical overview of circularity measurement c06_s

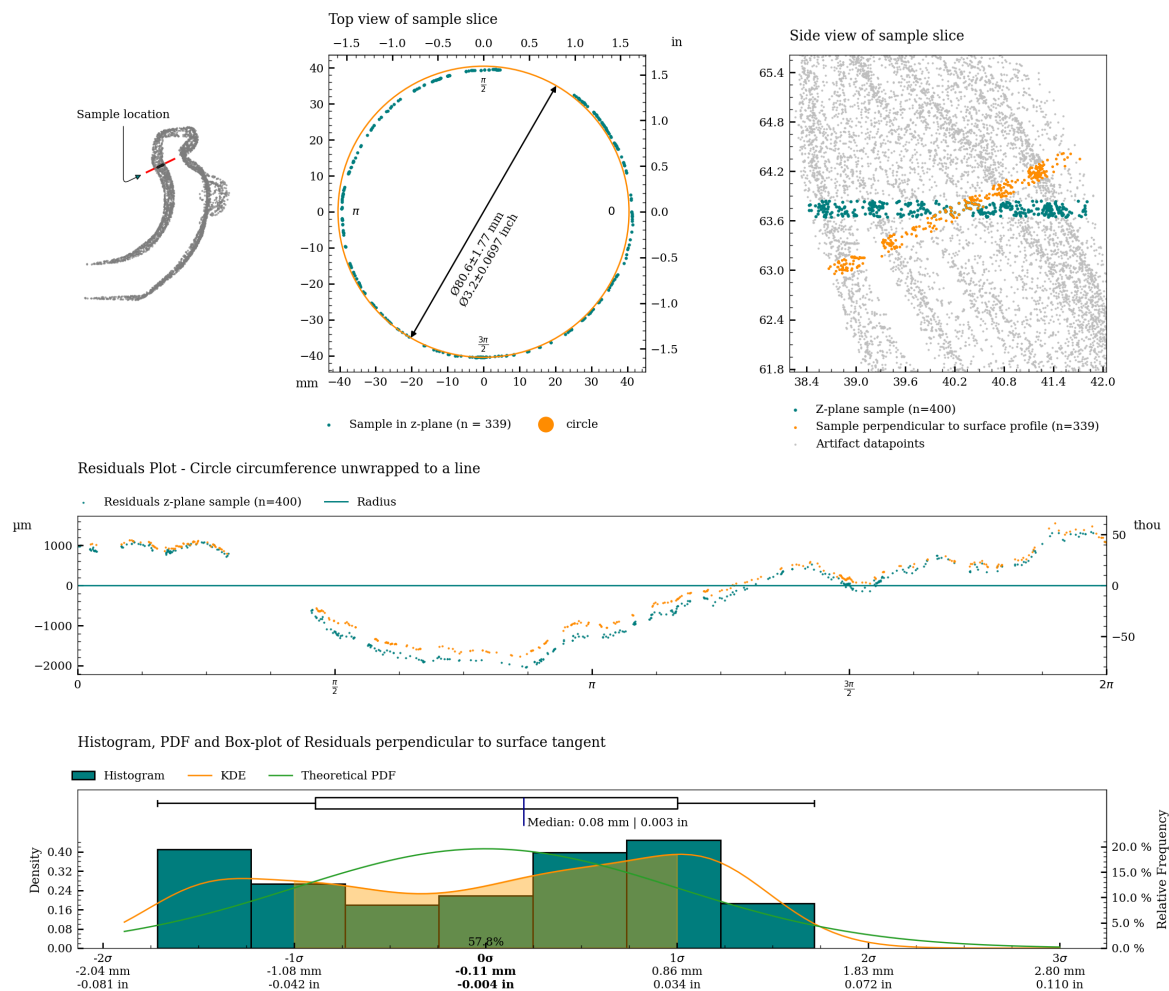


Figure 12: Charts with statistics for the measurement of c06_s.

Graphical overview of circularity measurement c07

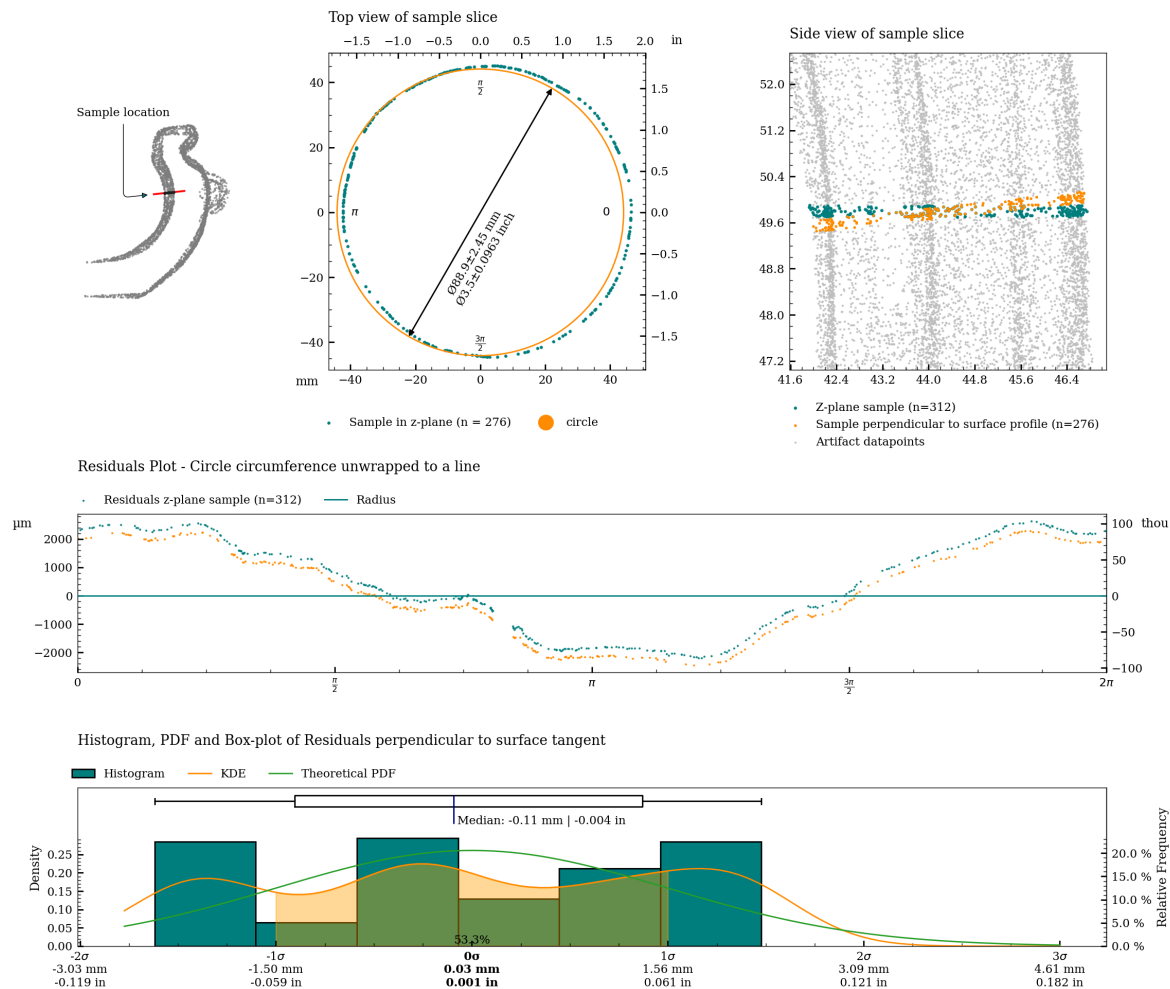


Figure 13: Charts with statistics for the measurement of c07.

Graphical overview of circularity measurement c07_s

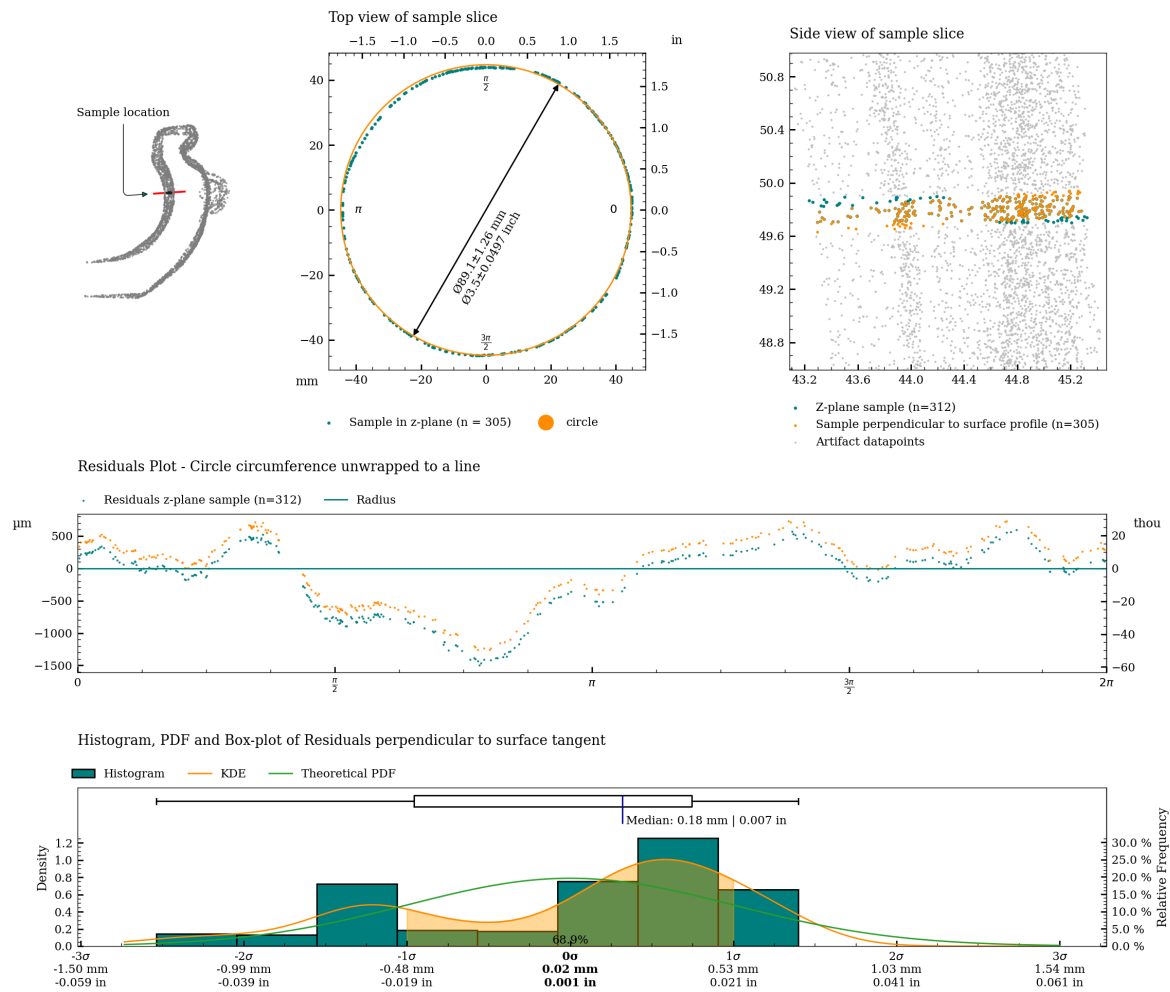


Figure 14: Charts with statistics for the measurement of c07_s.

Graphical overview of circularity measurement c08

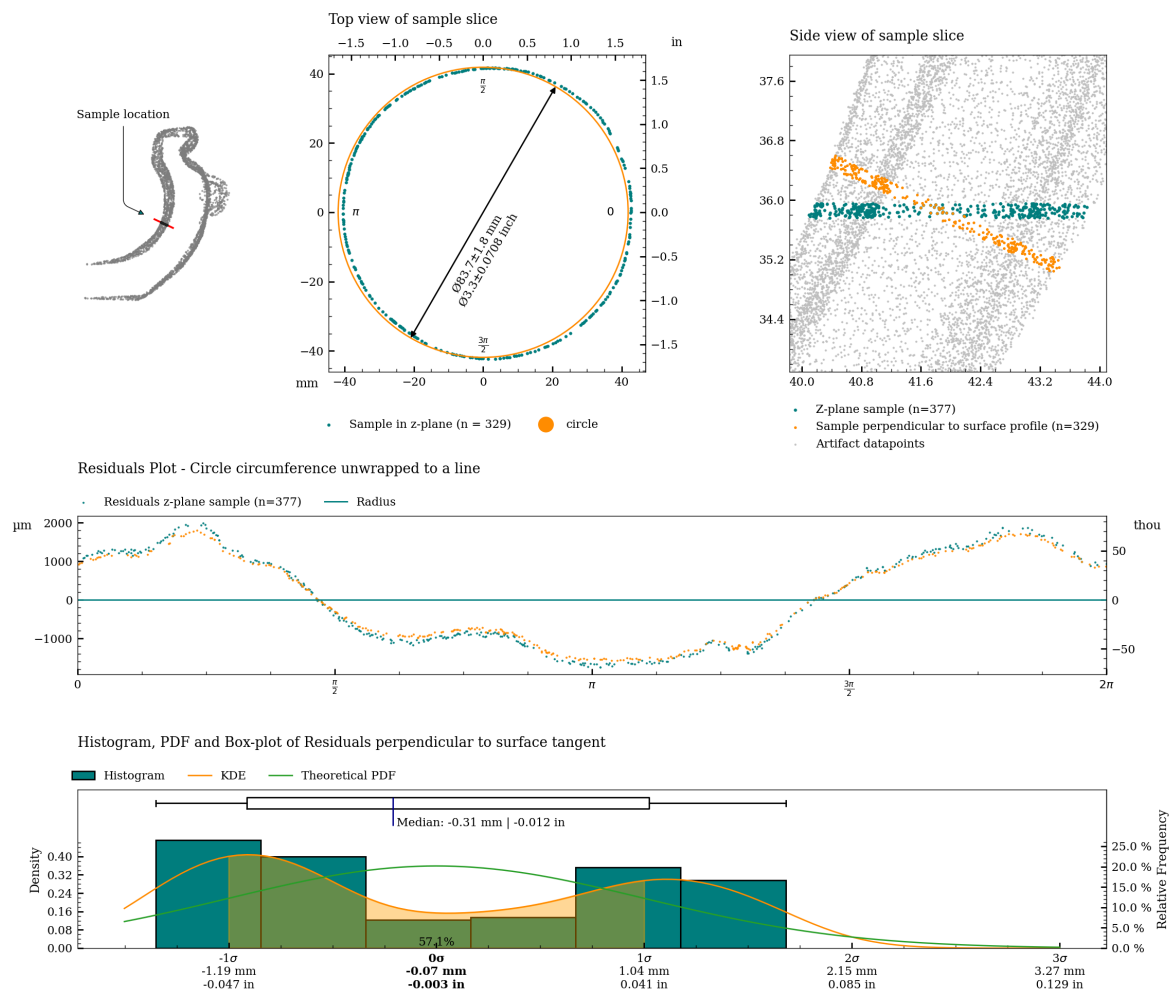


Figure 15: Charts with statistics for the measurement of c08.

Graphical overview of circularity measurement c08_s

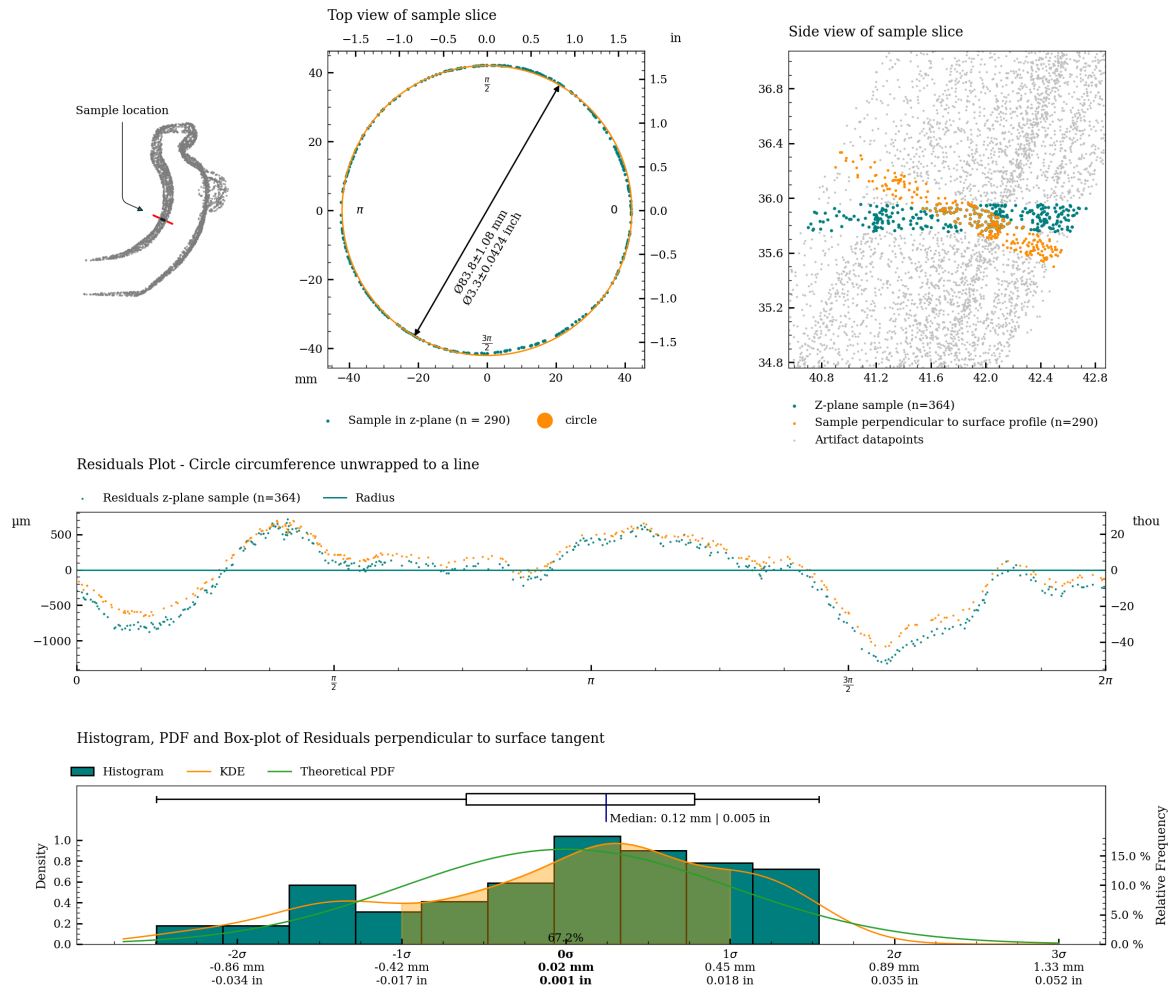


Figure 16: Charts with statistics for the measurement of c08_s.

Graphical overview of circularity measurement c09

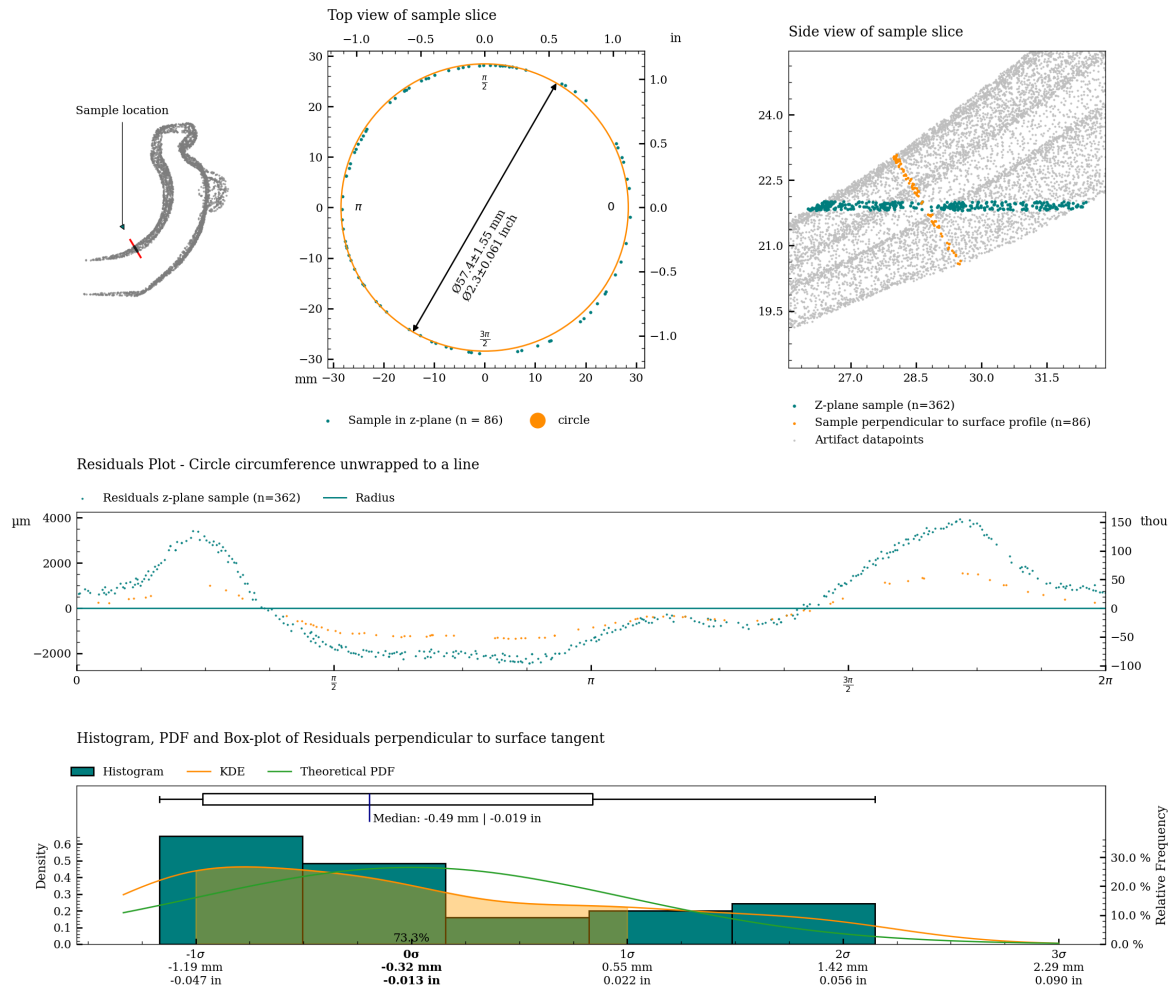


Figure 17: Charts with statistics for the measurement of c09.

Graphical overview of circularity measurement c09_s

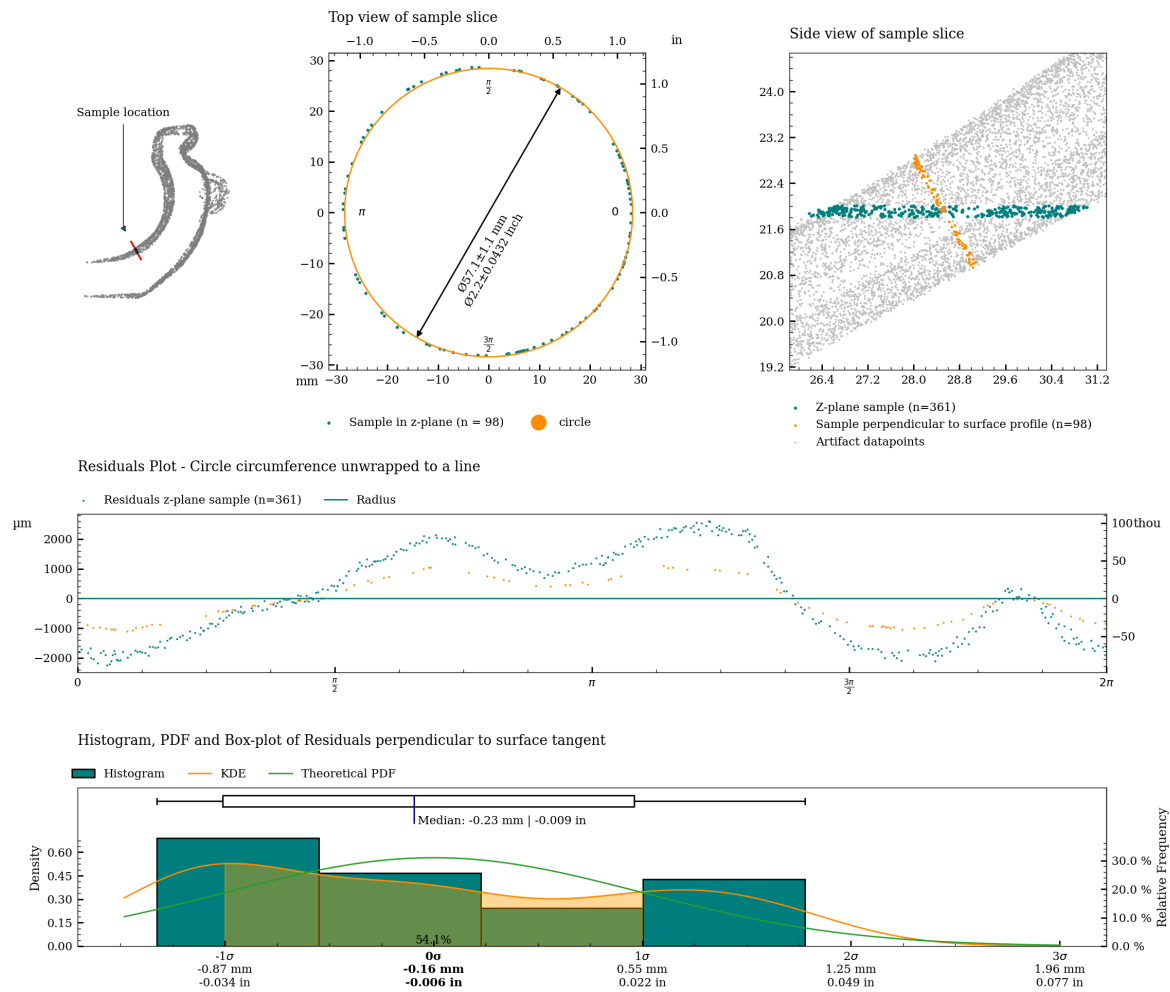


Figure 18: Charts with statistics for the measurement of c09_s.

Table 2 shows statistical measures of the circularity of the vessel, measured along the full height (areas on the artifact scan containing damaged parts have been removed to the best extent possible to reduce the influence of the measurement).

Metric											
Area	Range			Standard Deviation			RMSD			Slices	Slice height
	Median	Min.	Max.	Median	Min.	Max.	Median	Min.	Max.		
	mm	mm	mm	mm	mm	mm	mm	mm	mm		
Exterior	1.913	1.205	3.721	0.251	0.140	0.489	0.457	0.235	0.916	269	0.200
Interior	4.381	1.959	5.168	0.636	0.254	0.857	1.374	0.549	1.739	213	0.200
Interior separate	1.962	1.070	3.129	0.266	0.118	0.603	0.501	0.314	1.057	235	0.200

Imperial											
Area	Range			Standard Deviation			RMSD			Slices	Slice height
	Median	Min.	Max.	Median	Min.	Max.	Median	Min.	Max.		
	in	in	in	in	in	in	in	in	in		
Exterior	1.913	1.205	3.721	0.251	0.140	0.489	0.457	0.235	0.916	269	0.200
Interior	4.381	1.959	5.168	0.636	0.254	0.857	1.374	0.549	1.739	213	0.200
Interior separate	1.962	1.070	3.129	0.266	0.118	0.603	0.501	0.314	1.057	235	0.200

Table 2: Perpendicular Circularity analysis of RV003.

Circularity analysis of exterior surface

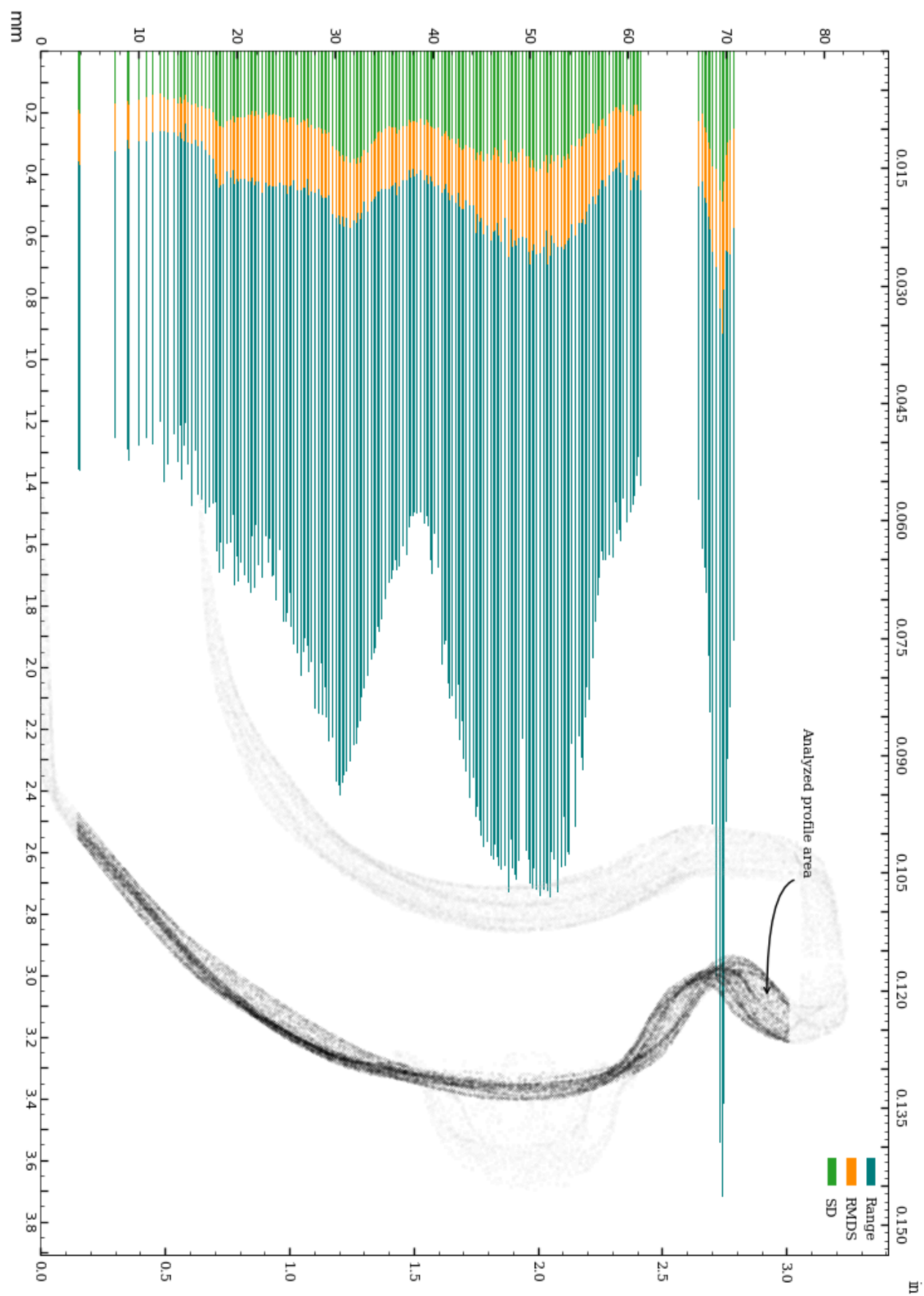


Figure 19: Circularity of exterior surface.

Circularity analysis of exterior surface, Standard Deviation and Root Mean Squared Deviation

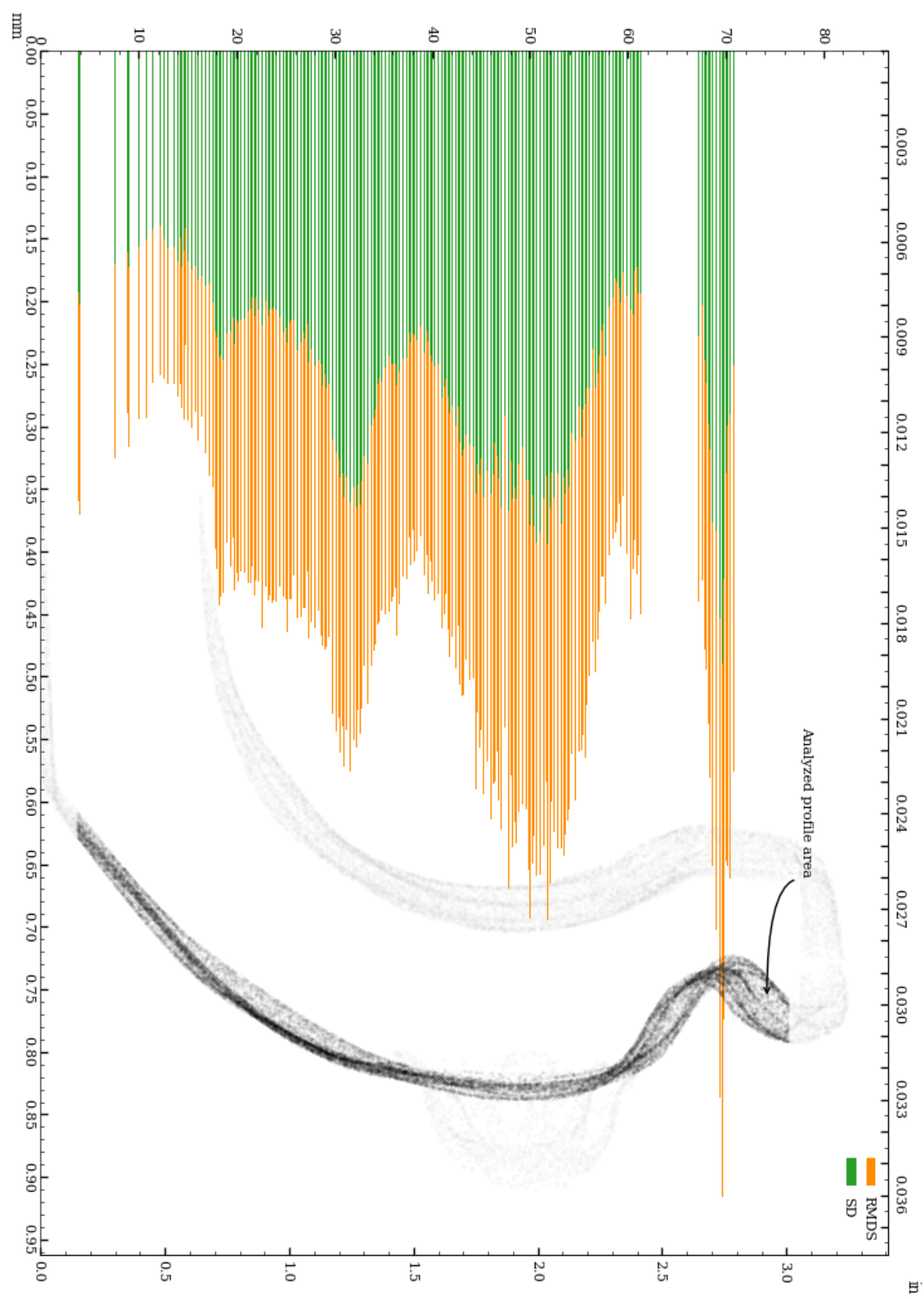


Figure 20: Vessel circularity of exterior surface, standard deviation and median absolute deviation.

The distributions of the circularity measurements across 269 slices of the exterior surface are shown below.

Range measurement distribution across 269 slices of exterior surface

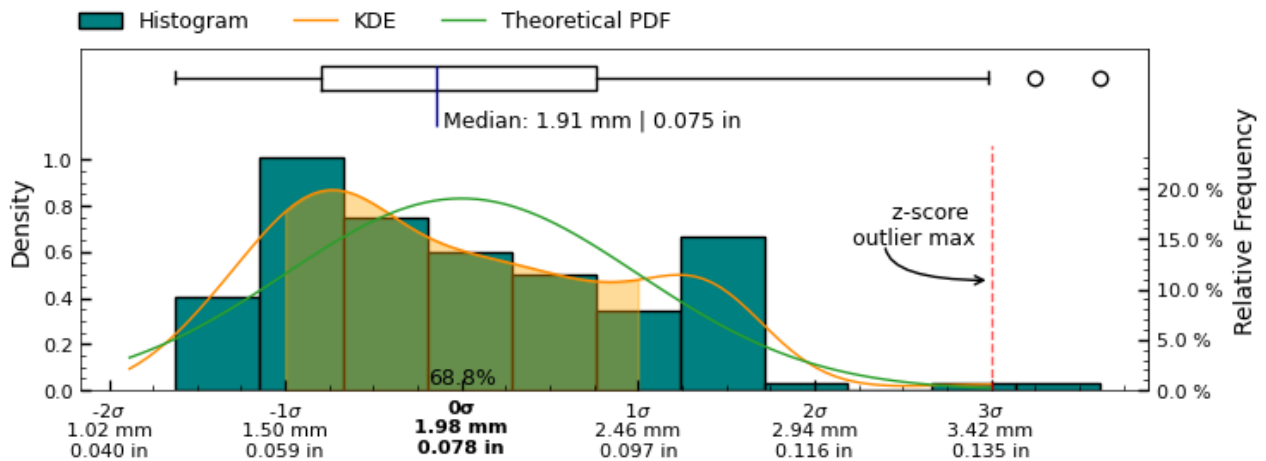


Figure 21: Range measurement distribution across measured slices of exterior surface

Standard Deviation measurement distribution across 269 slices of exterior surface

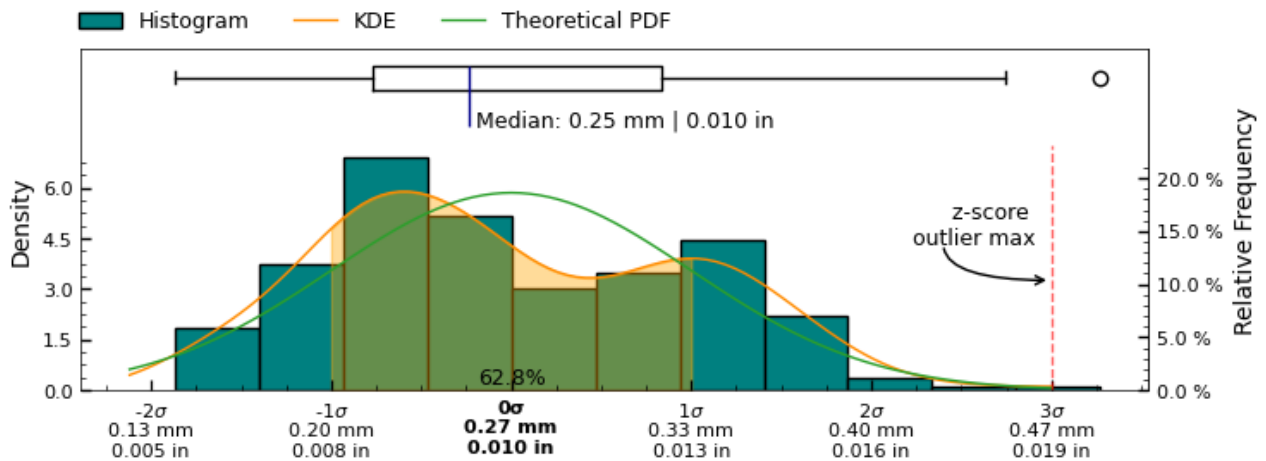


Figure 22: Standard Deviation measurement distribution across measured slices of " + exterior + " surface

Root Mean Squared Deviation measurement distribution across 269 slices of exterior surface

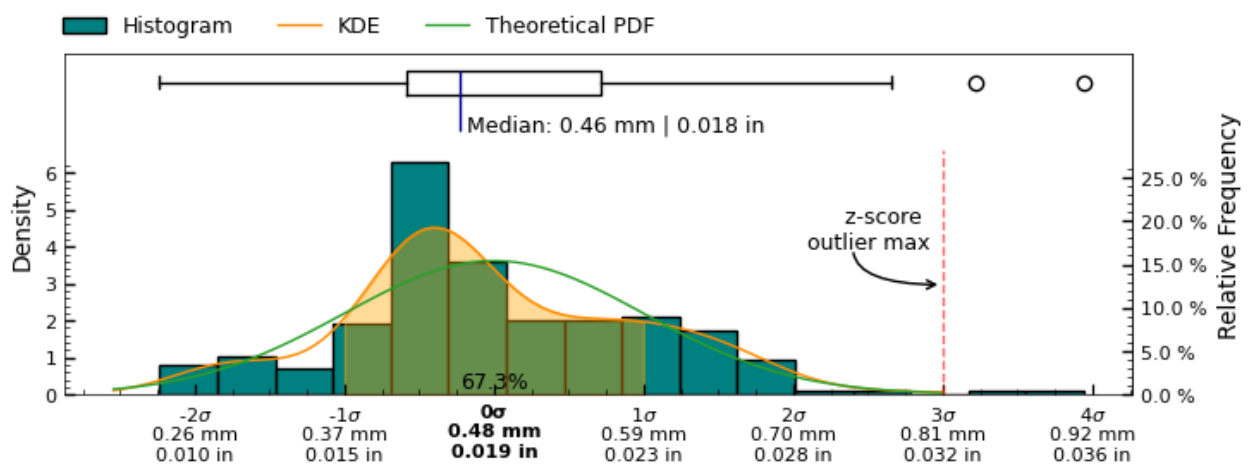


Figure 23: Root Mean Squared Deviation measurement distribution across measured slices of exterior surface

Circularity analysis of interior surface

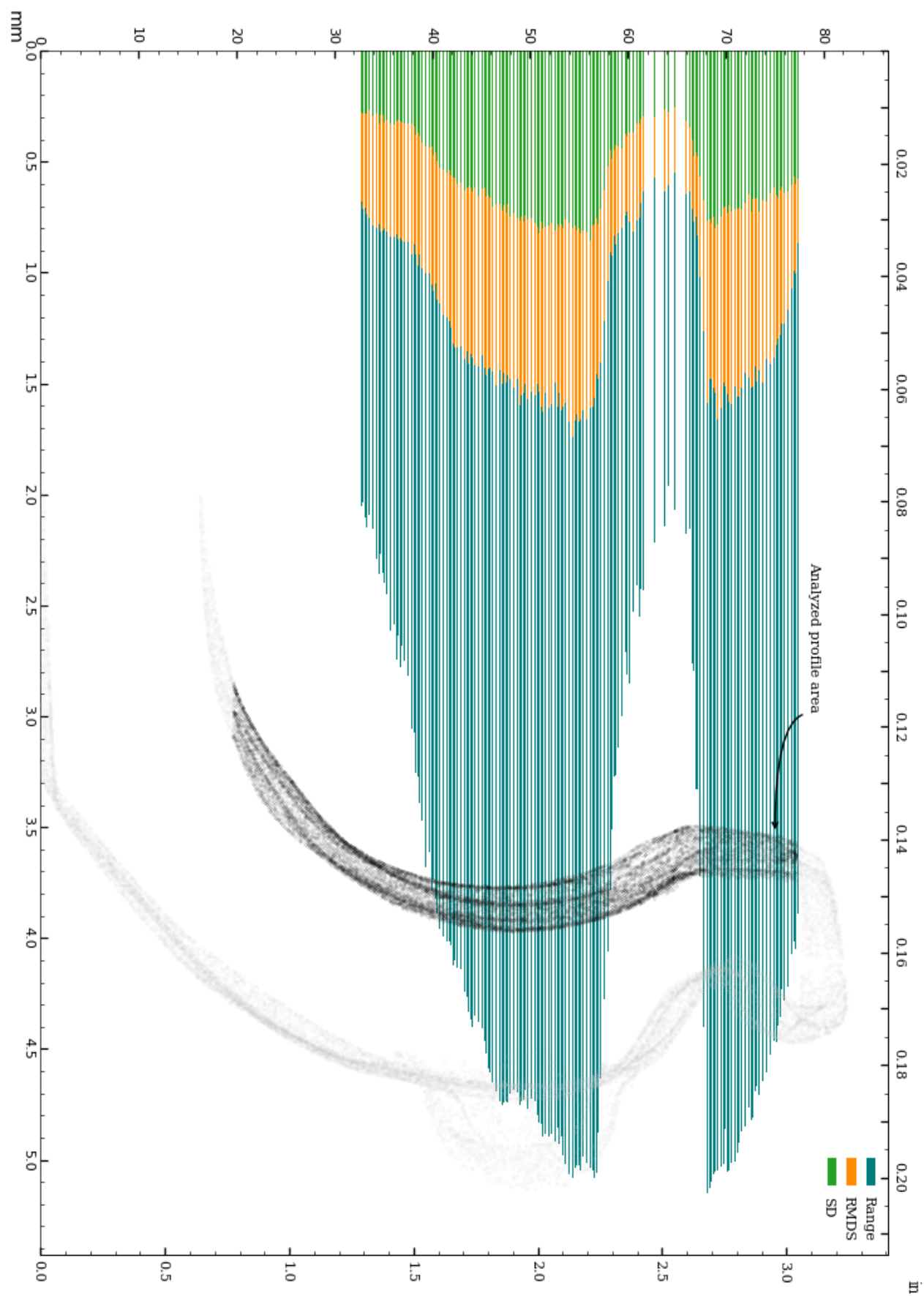


Figure 24: Circularity of interior surface.

Circularity analysis of interior surface, Standard Deviation and Root Mean Squared Deviation

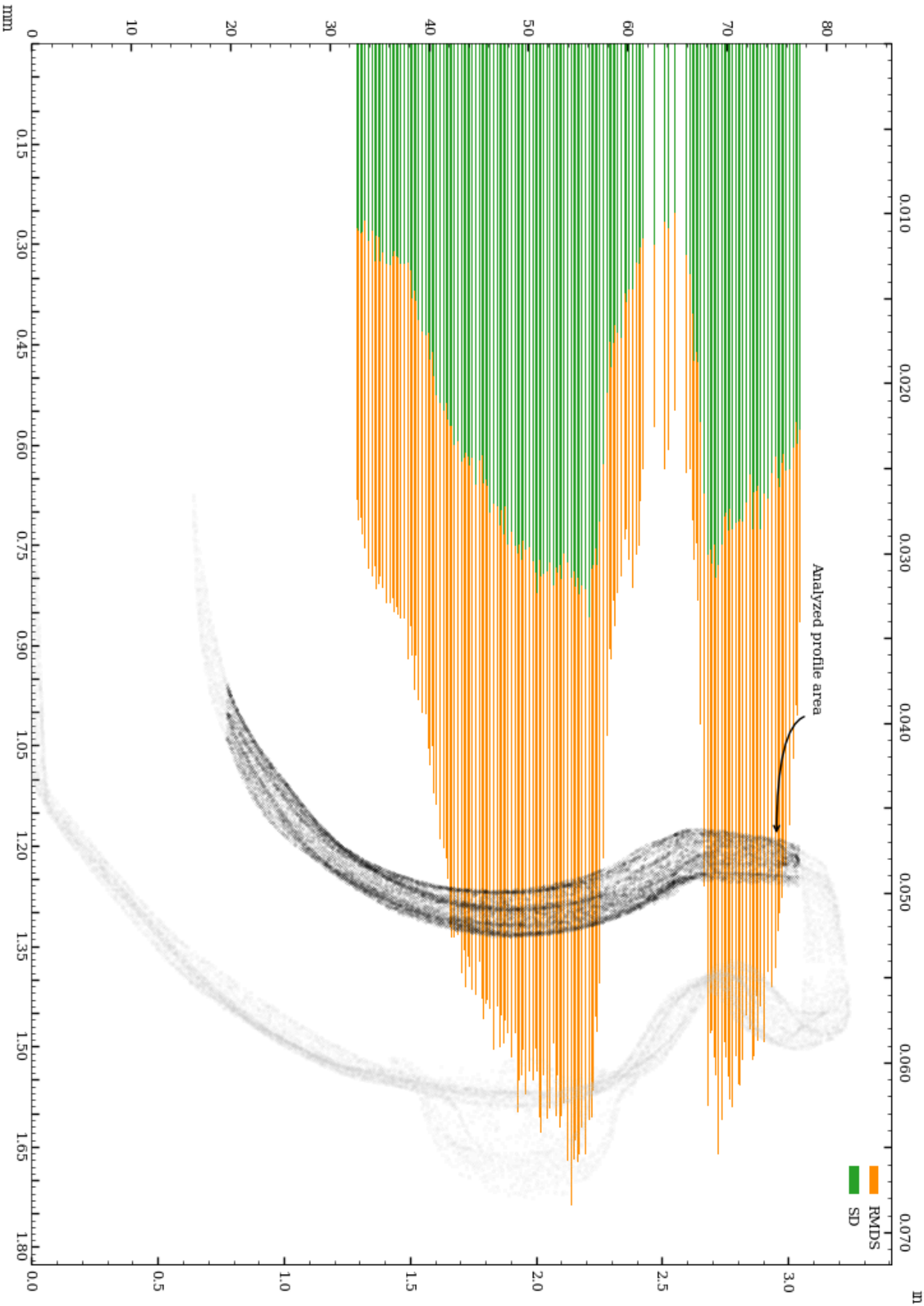


Figure 25: Vessel circularity of interior surface, standard deviation and median absolute deviation.

The distributions of the circularity measurements across 213 slices of the interior surface are shown below.

Range measurement distribution across 213 slices of interior surface

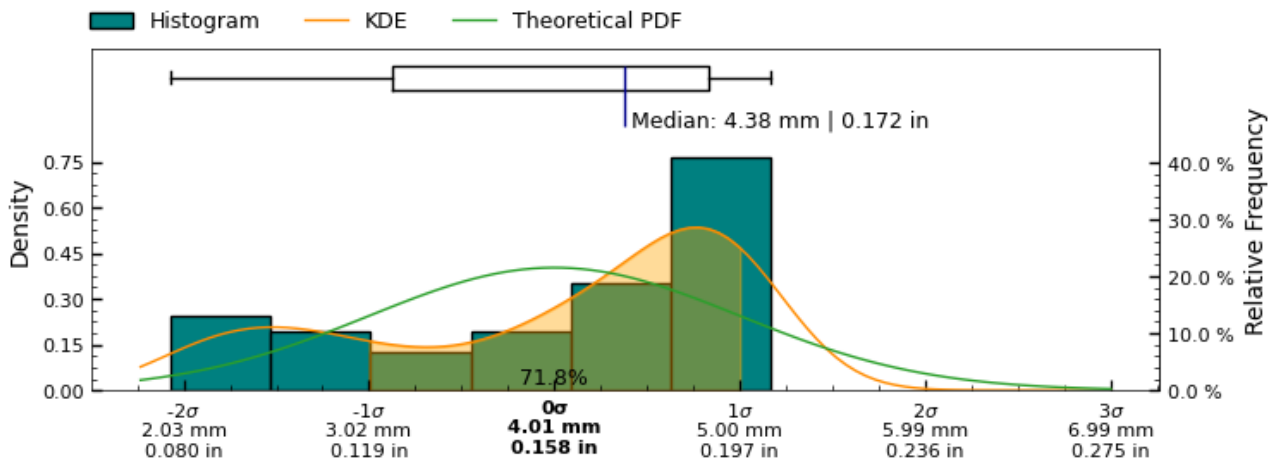


Figure 26: Range measurement distribution across measured slices of interior surface

Standard Deviation measurement distribution across 213 slices of interior surface

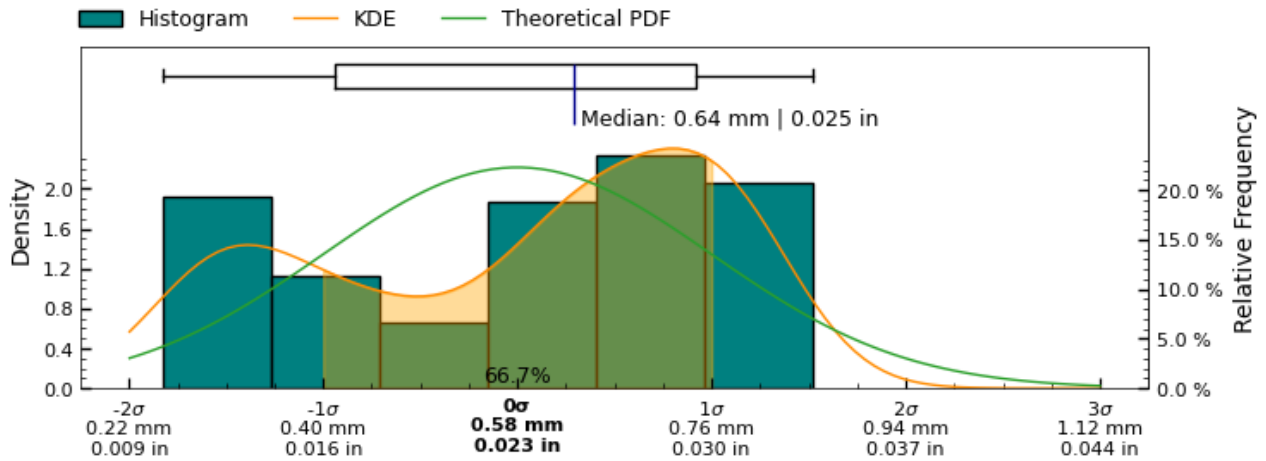


Figure 27: Standard Deviation measurement distribution across measured slices of " + interior + " surface

Root Mean Squared Deviation measurement distribution across 213 slices of interior surface

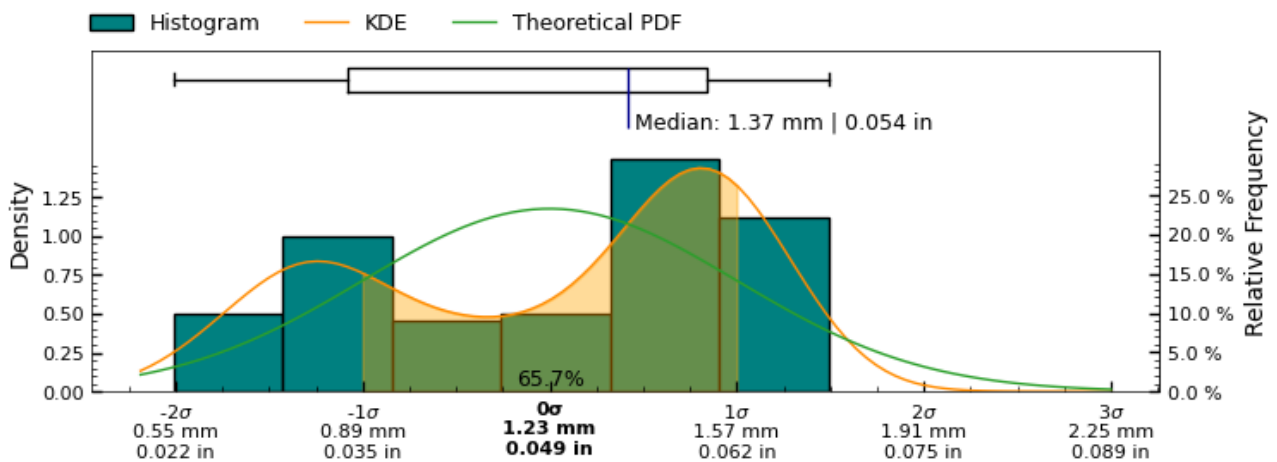


Figure 28: Root Mean Squared Deviation measurement distribution across measured slices of interior surface

Circularity analysis of interior separately aligned surface

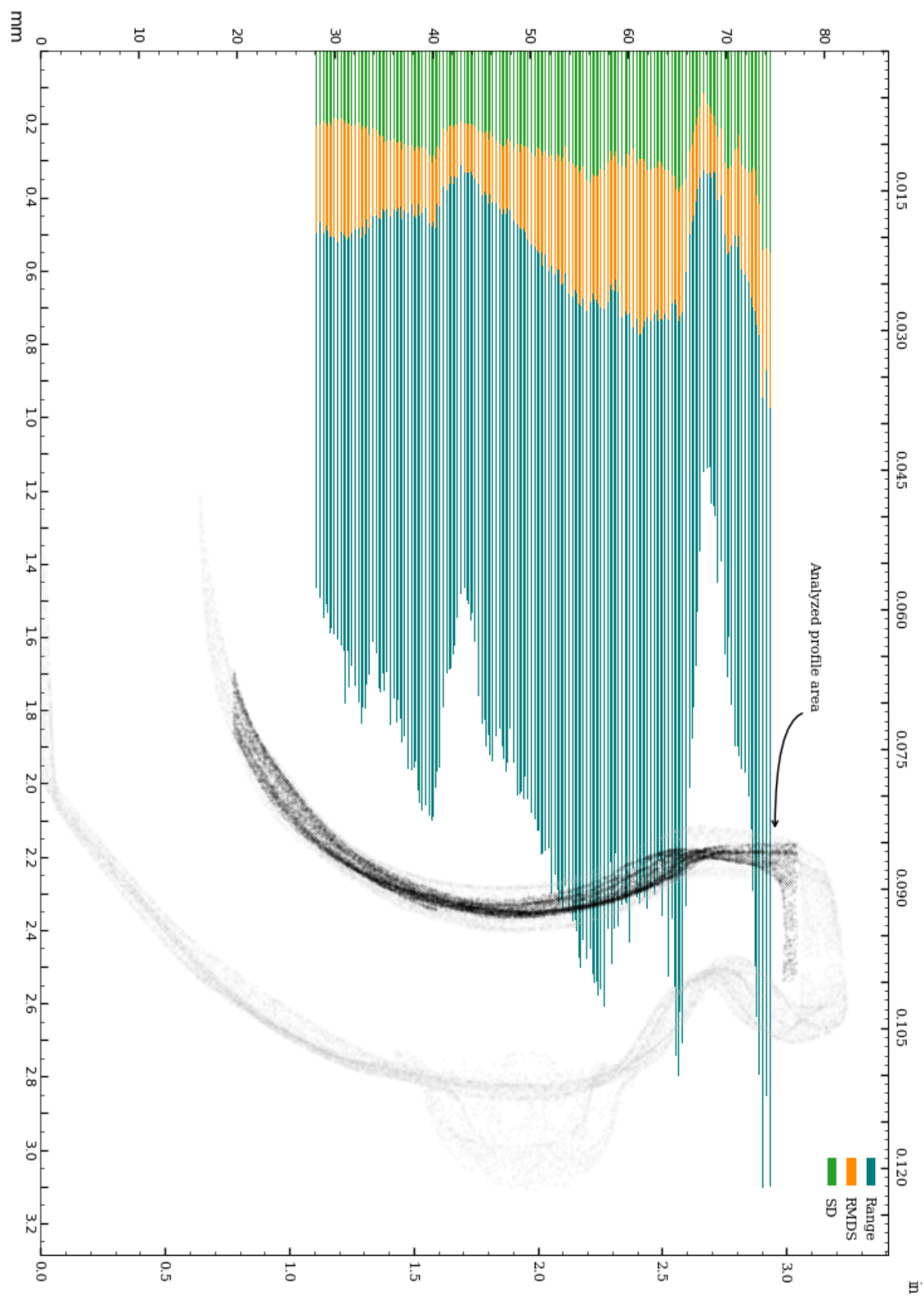


Figure 29: Circularity of interior_separate surface.

Circularity analysis of interior separately aligned surface, Standard Deviation and Root Mean Squared Deviation

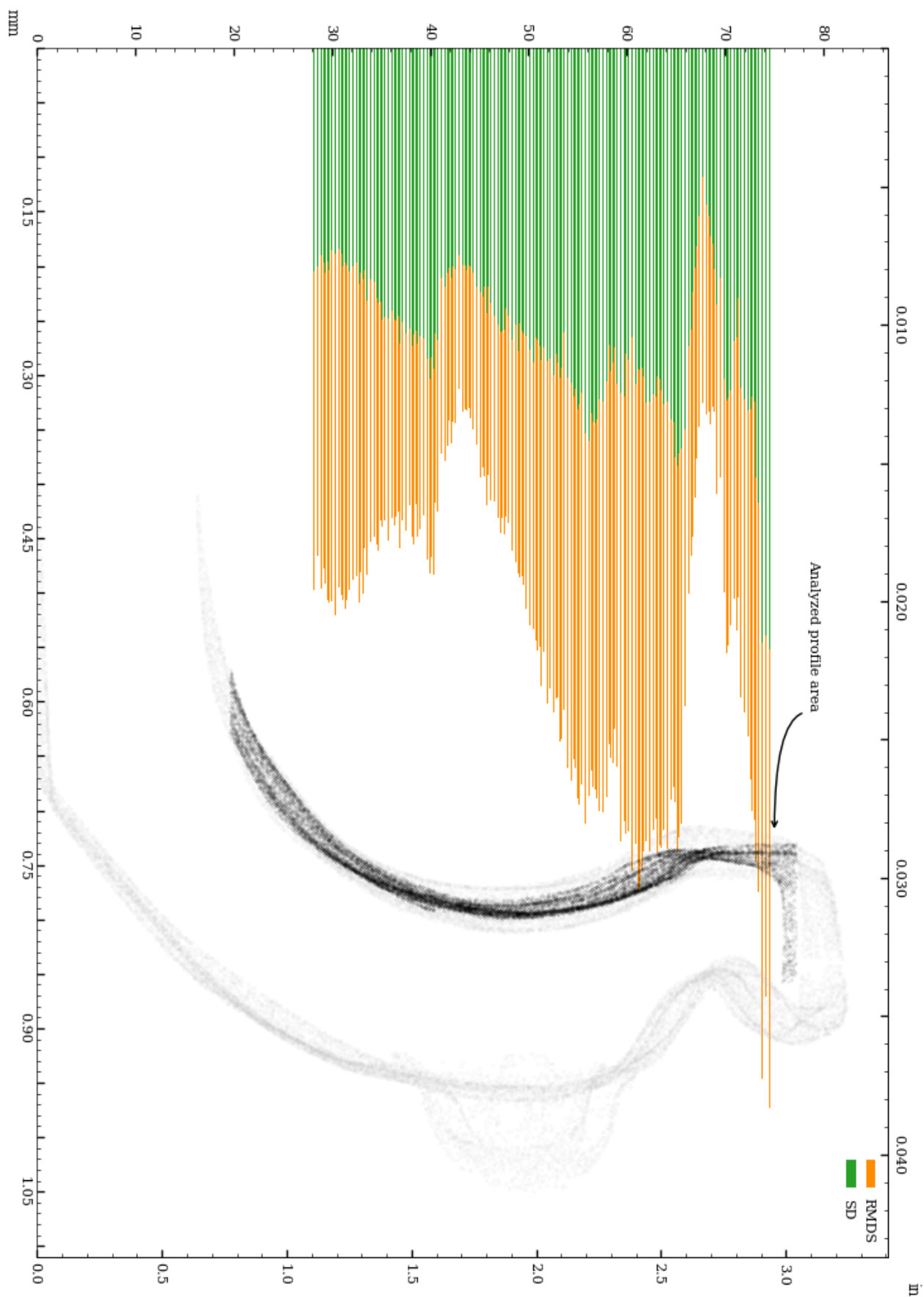


Figure 30: Vessel circularity of interior_separate surface, standard deviation and median absolute deviation.

The distributions of the circularity measurements across 235 slices of the interior_separate surface are shown below.

Range measurement distribution across 235 slices of interior separately aligned surface

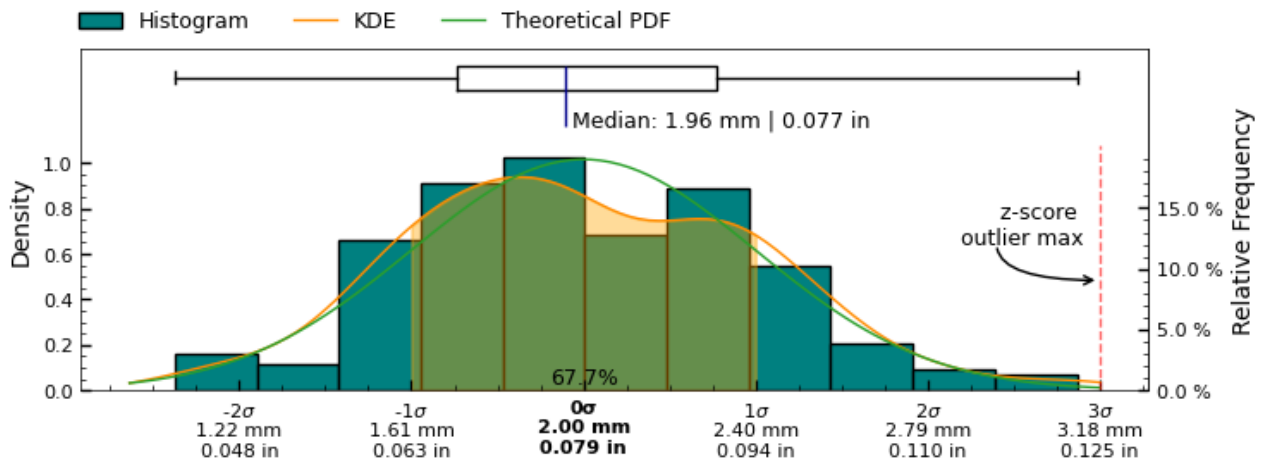


Figure 31: Range measurement distribution across measured slices of interior_separate surface

Standard Deviation measurement distribution across 235 slices of interior separately aligned surface

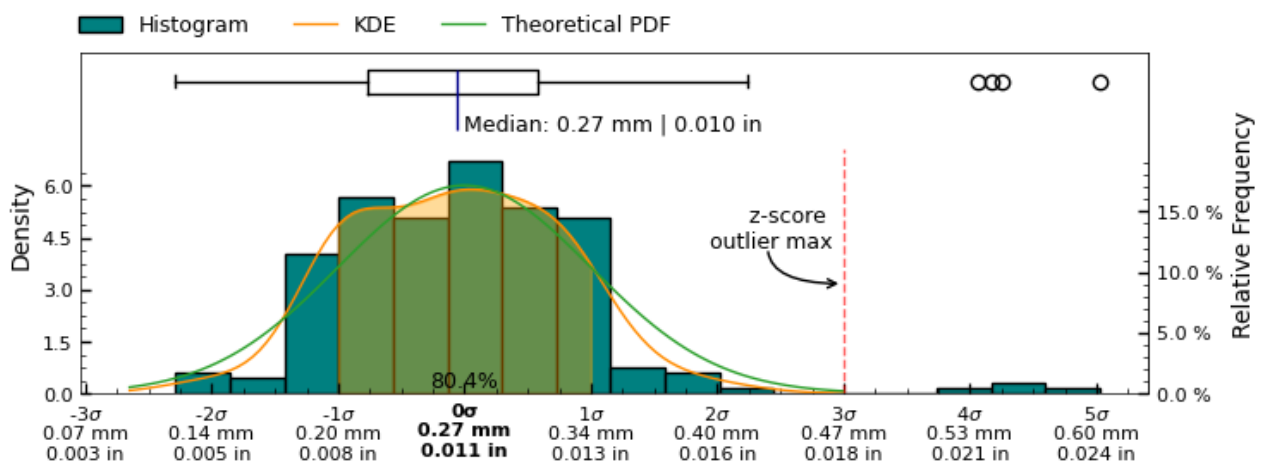


Figure 32: Standard Deviation measurement distribution across measured slices of " + interior_separate + " surface

Root Mean Squared Deviation measurement distribution across 235 slices of interior separately aligned surface

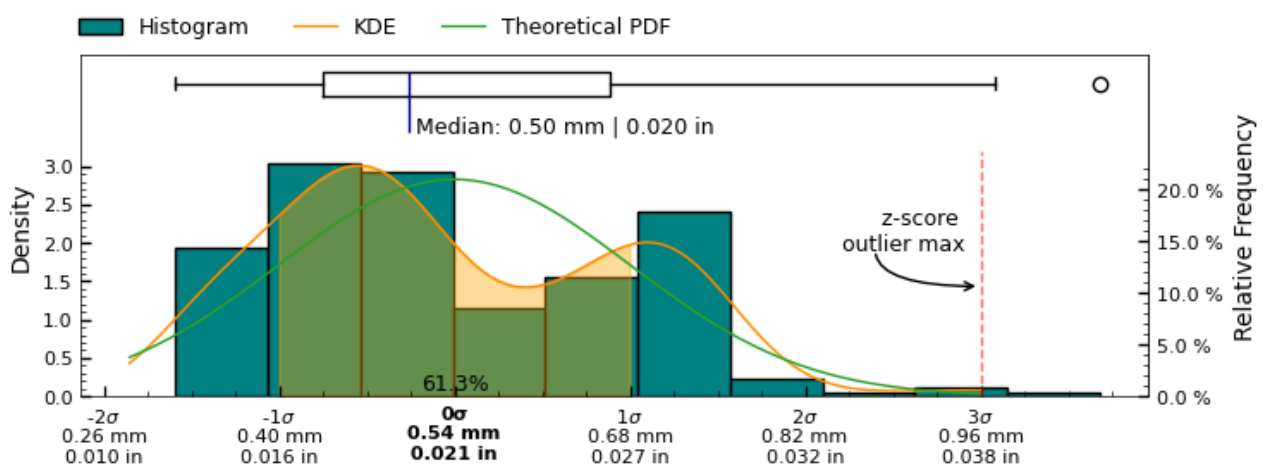


Figure 33: Root Mean Squared Deviation measurement distribution across measured slices of interior separately aligned surface

Concentricity

The concentricity metric describes the deviation in the center-point of the referenced features. As such, it is a measure to determine if several features of the object share the same center point/axis, and how closely. See Figure 34 for a visual representation of this metric.

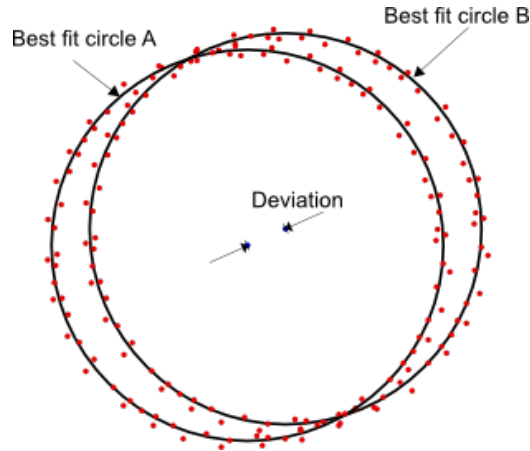


Figure 34: Concentricity measures the deviation (distance) between the center of two circles.

Determination of concentricity has been carried out by establishing the best fit circles of sample slices, using RANSAC (Random sample consensus) algorithm for outlier detection of a least squares circle regression on the scanned data-points at each cross-section, to estimate centers of each cross-section.

The concentricity between both the interior and exterior circular cross-sections is explored for cross-section measurements with the same Z-coordinates.

Additionally, the concentricity between each cross-section measurement defined in Figure 4 and the datum axis $(x, y) = (0, 0)$ has been calculated to establish the deviation of the feature center from the datum axis.

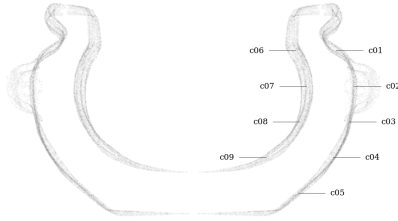


Figure 35: Circularity measurement sample locations, full mesh aligned to exterior surface



Figure 36: Circularity measurement sample location, separately aligned interior mesh

Metric

Tag	Reference	Deviation	Sample size	Circle fit residuals analysis for sample listed in Tag column						Center (x,y)
				Range full	Range inliers	RMSD full	RMDS inliers	SD full	SD inliers	
				mm	mm	mm	mm	mm	mm	
c01	z-axis	0.949	162	4.044	4.044	1.322	1.322	0.556	0.556	−474, 821
c02	z-axis	0.500	149	2.678	2.678	0.857	0.857	0.482	0.482	176, −468
c03	z-axis	0.069	307	1.731	1.731	0.455	0.455	0.260	0.260	56, 41
c04	z-axis	0.541	242	2.683	2.683	0.728	0.728	0.484	0.484	−539, 43
c05	z-axis	0.236	139	1.874	1.874	0.530	0.530	0.300	0.300	−225, −71
c06	z-axis	1.789	273	7.603	7.603	2.112	2.112	0.938	0.938	1559, 879
c06_s	z-axis	1.131	339	3.049	3.049	0.921	0.921	0.439	0.439	1027, −475
c07	z-axis	2.172	276	5.782	5.782	1.848	1.855	0.897	0.895	2137, 393
c07_s	z-axis	0.531	305	2.394	2.394	0.621	0.621	0.365	0.365	398, −351
c08	z-axis	1.401	329	3.247	3.247	1.091	1.091	0.419	0.419	1400, −54
c08_s	z-axis	0.413	290	2.254	2.254	0.499	0.499	0.324	0.324	−320, 261
c09	z-axis	0.597	86	2.948	2.948	0.917	0.918	0.495	0.498	474, −363
c09_s	z-axis	0.410	98	2.153	2.153	0.700	0.700	0.333	0.333	−387, 136
c01	c06_s	1.983								−1502, 1296
c02	c07_s	0.250								−222, −116
c03	c08_s	0.435								375, −221
c04	c09_s	0.178								−152, −93

Imperial

Tag	Reference	Deviation	Sample size	Circle fit residuals analysis for sample listed in Tag column						Center (x,y)
				Range full	Range inliers	RMSD full	RMDS inliers	SD full	SD inliers	
				in	in	in	in	in	in	
c01	z-axis	0.0373	162	0.1592	0.1592	0.0521	0.0521	0.0219	0.0219	−18.7, 32.3
c02	z-axis	0.0197	149	0.1054	0.1054	0.0337	0.0337	0.0190	0.0190	6.9, −18.4
c03	z-axis	0.0027	307	0.0682	0.0682	0.0179	0.0179	0.0102	0.0102	2.2, 1.6
c04	z-axis	0.0213	242	0.1056	0.1056	0.0287	0.0287	0.0191	0.0191	−21.2, 1.7
c05	z-axis	0.0093	139	0.0738	0.0738	0.0209	0.0209	0.0118	0.0118	−8.9, −2.8
c06	z-axis	0.0704	273	0.2993	0.2993	0.0832	0.0832	0.0369	0.0369	61.4, 34.6
c06_s	z-axis	0.0445	339	0.1200	0.1200	0.0363	0.0363	0.0173	0.0173	40.4, −18.7
c07	z-axis	0.0855	276	0.2276	0.2276	0.0728	0.0730	0.0353	0.0352	84.1, 15.5
c07_s	z-axis	0.0209	305	0.0943	0.0943	0.0244	0.0244	0.0144	0.0144	15.7, −13.8
c08	z-axis	0.0552	329	0.1278	0.1278	0.0430	0.0430	0.0165	0.0165	55.1, −2.1
c08_s	z-axis	0.0163	290	0.0888	0.0888	0.0196	0.0196	0.0128	0.0128	−12.6, 10.3
c09	z-axis	0.0235	86	0.1161	0.1161	0.0361	0.0362	0.0195	0.0196	18.7, −14.3
c09_s	z-axis	0.0162	98	0.0848	0.0848	0.0276	0.0276	0.0131	0.0131	−15.3, 5.3
c01	c06_s	0.0781								−59.1, 51.0
c02	c07_s	0.0099								−8.7, −4.6
c03	c08_s	0.0171								14.8, −8.7
c04	c09_s	0.0070								−6.0, −3.7

Table 3: Concentricity analysis of RV003.

Concentricity analysis of c01

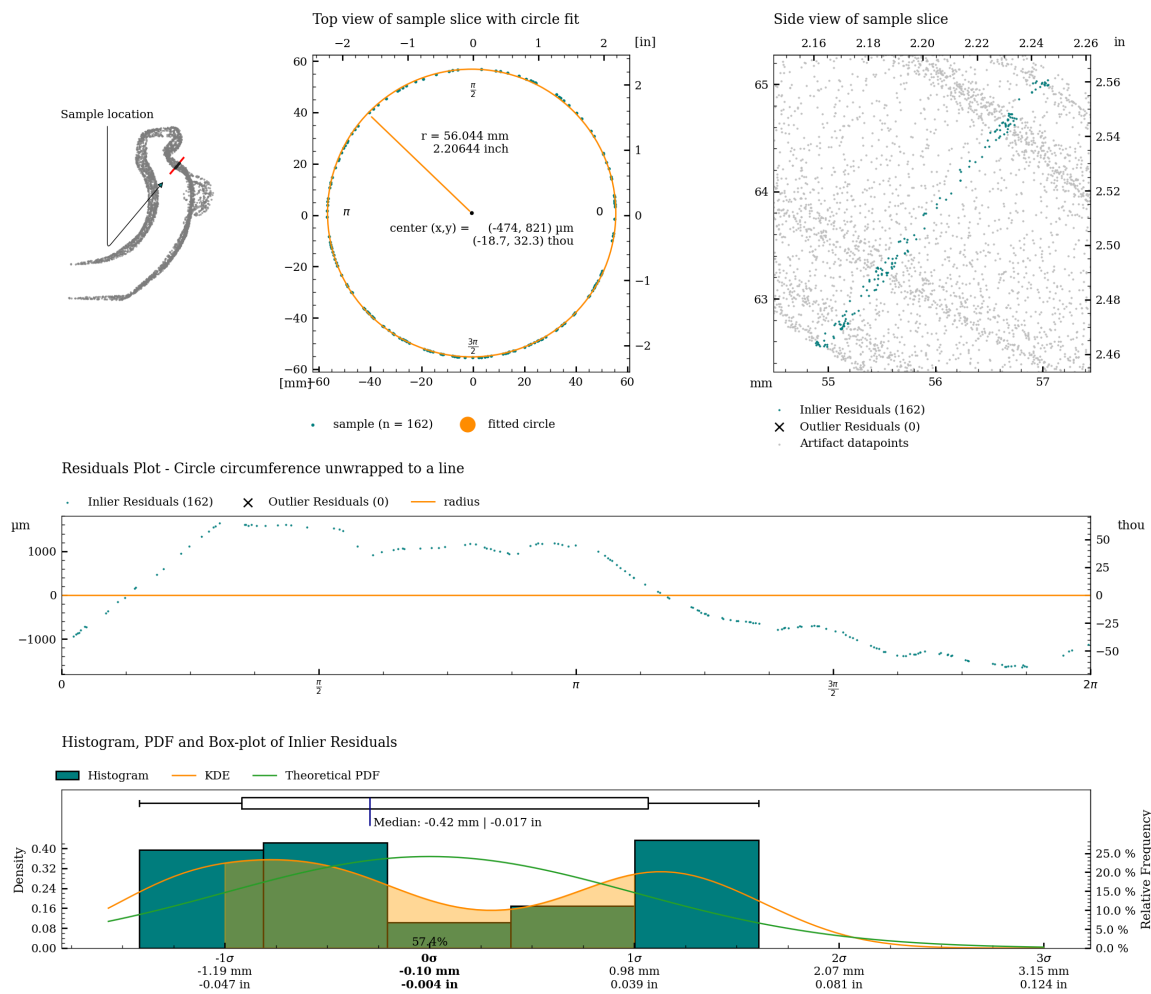


Figure 37: Detailed plot of concentricity measurement for c01.

Concentricity analysis of c02

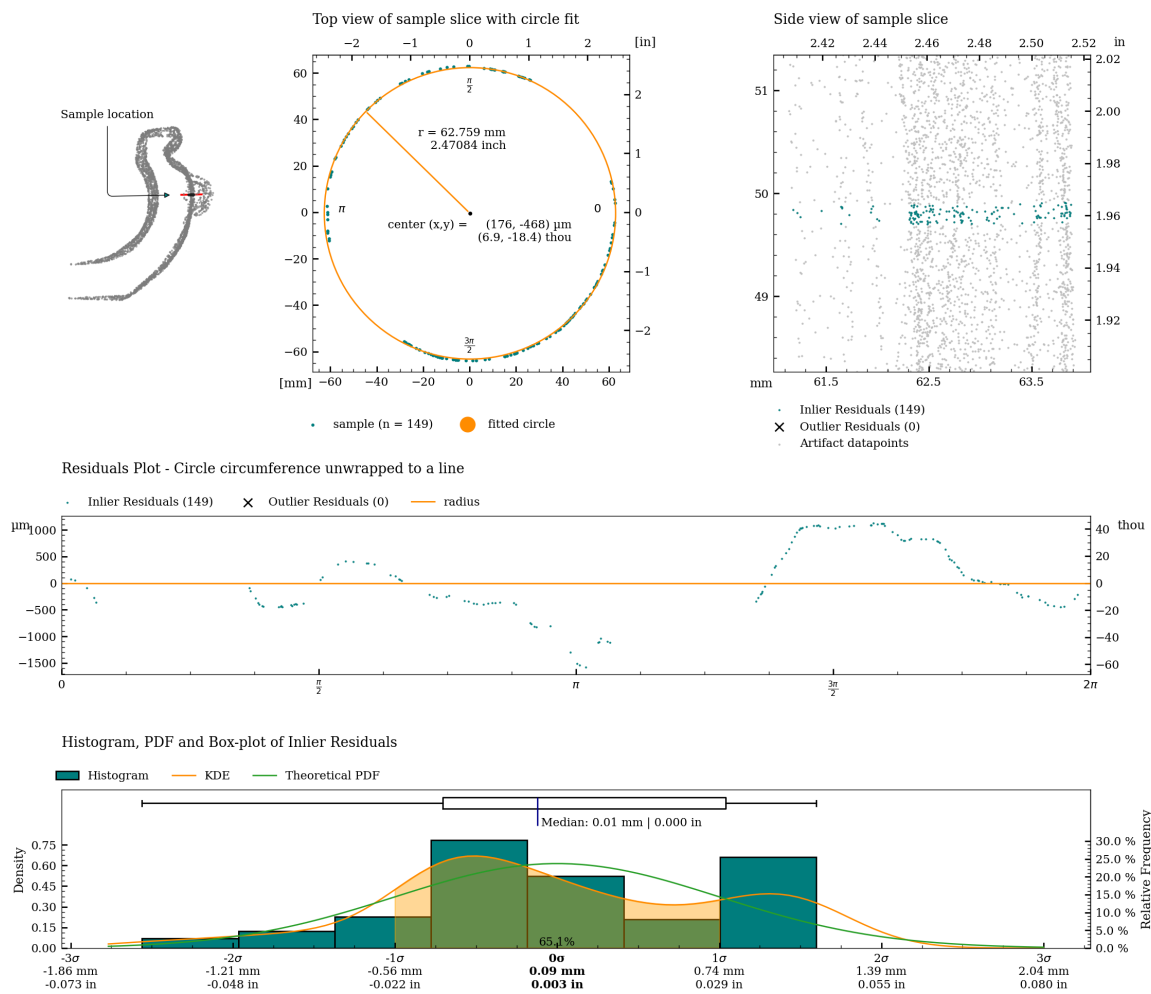


Figure 38: Detailed plot of concentricity measurement for c02.

Concentricity analysis of c03

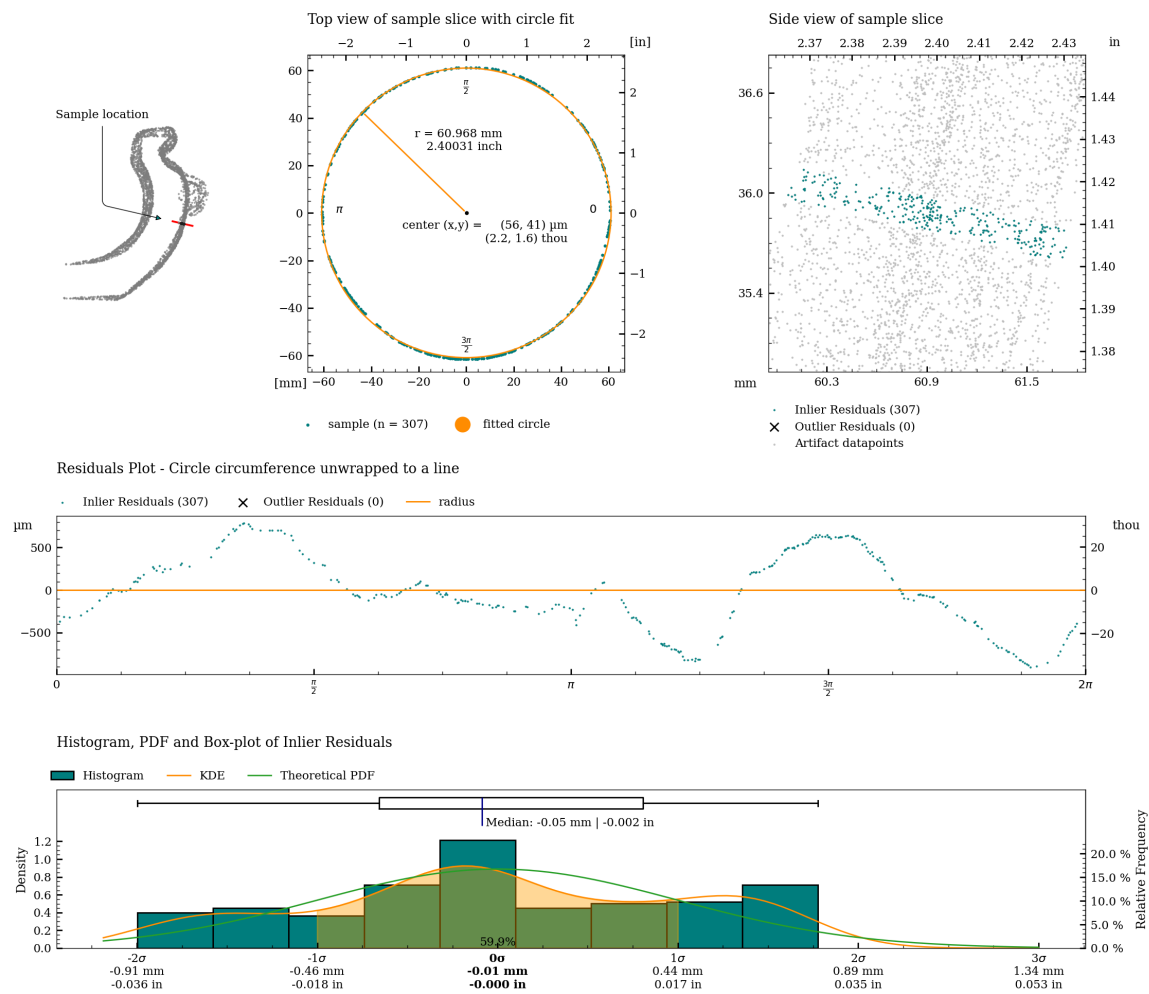


Figure 39: Detailed plot of concentricity measurement for c03.

Concentricity analysis of c04

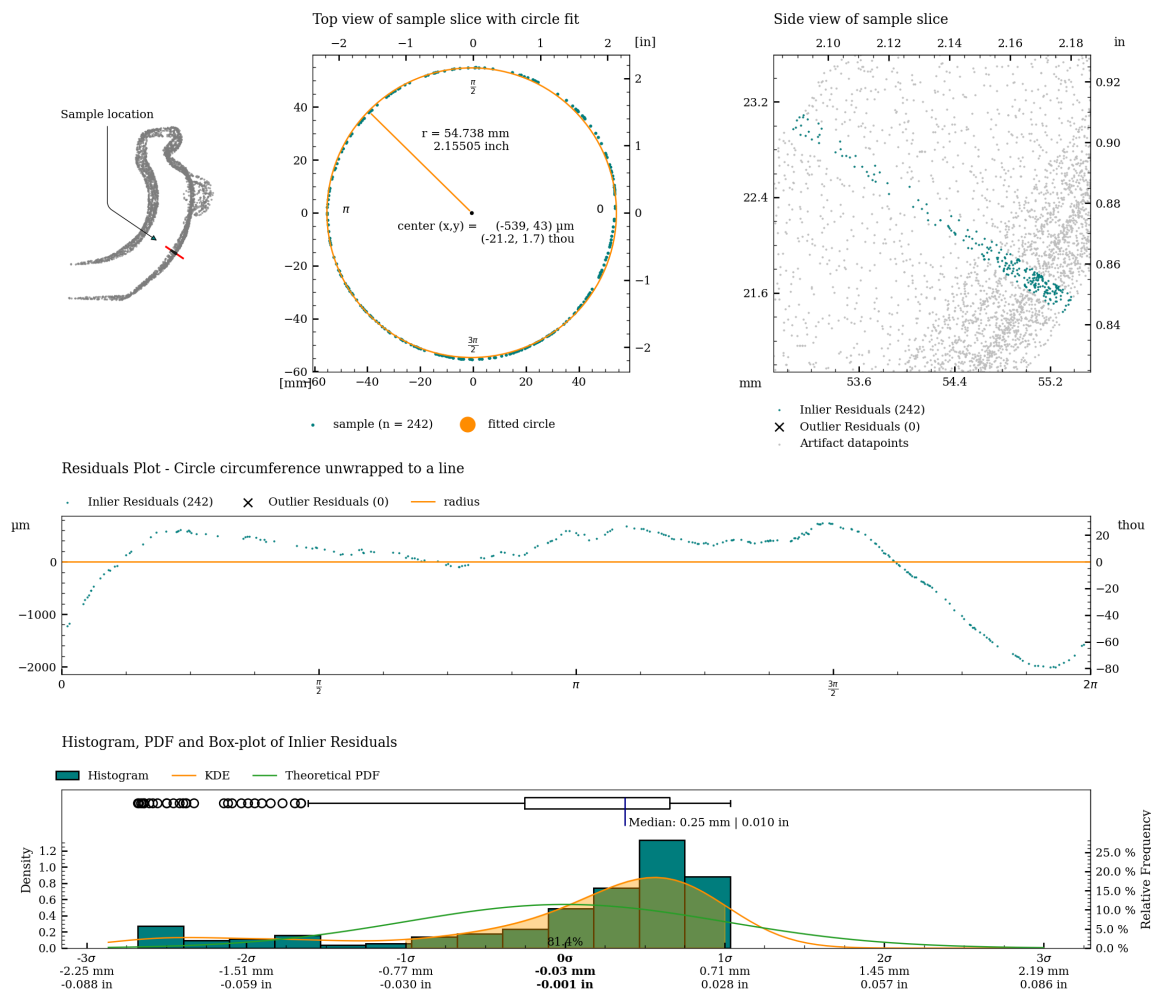


Figure 40: Detailed plot of concentricity measurement for c04.

Concentricity analysis of c05

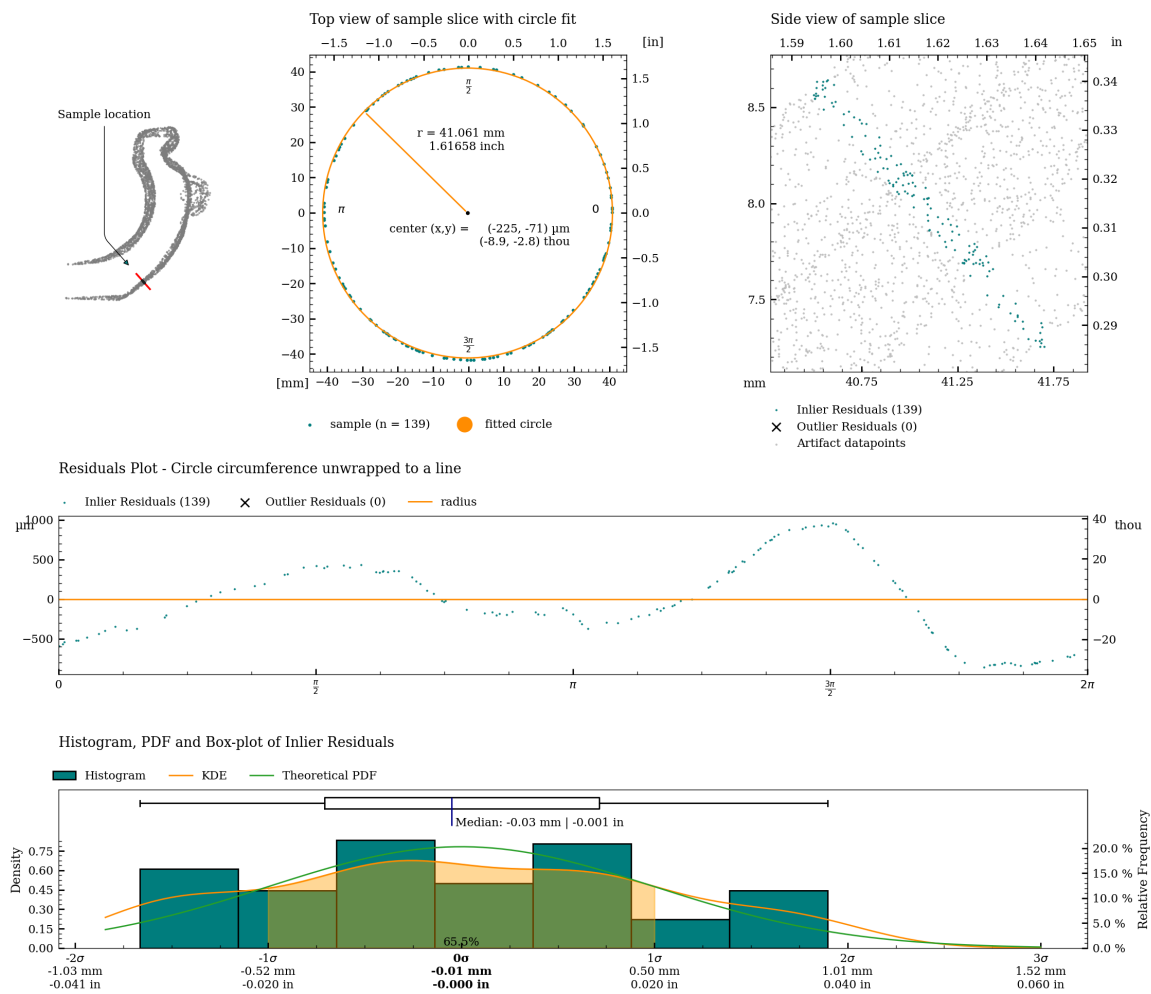


Figure 41: Detailed plot of concentricity measurement for c05.

Concentricity analysis of c06

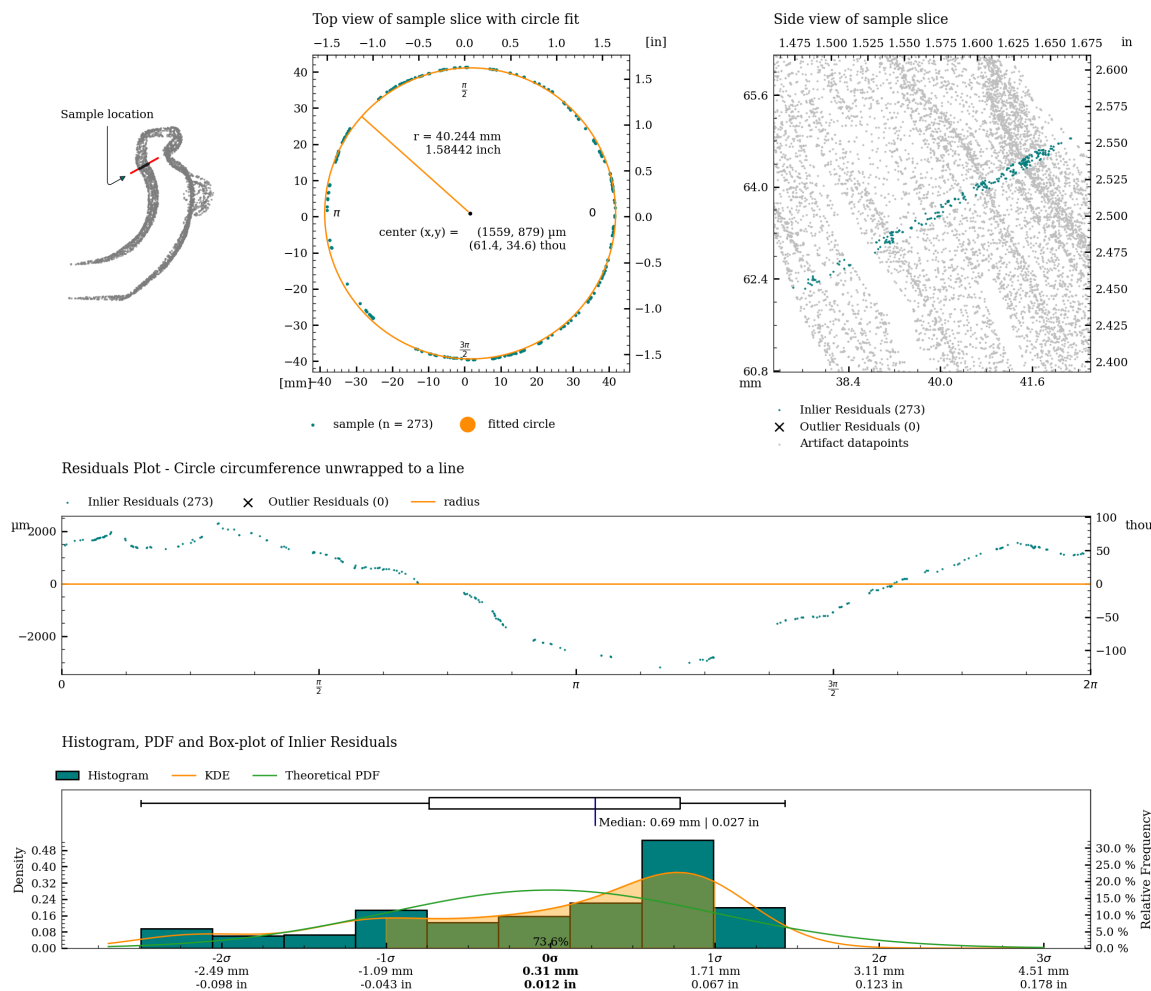


Figure 42: Detailed plot of concentricity measurement for c06.

Concentricity analysis of c06_s

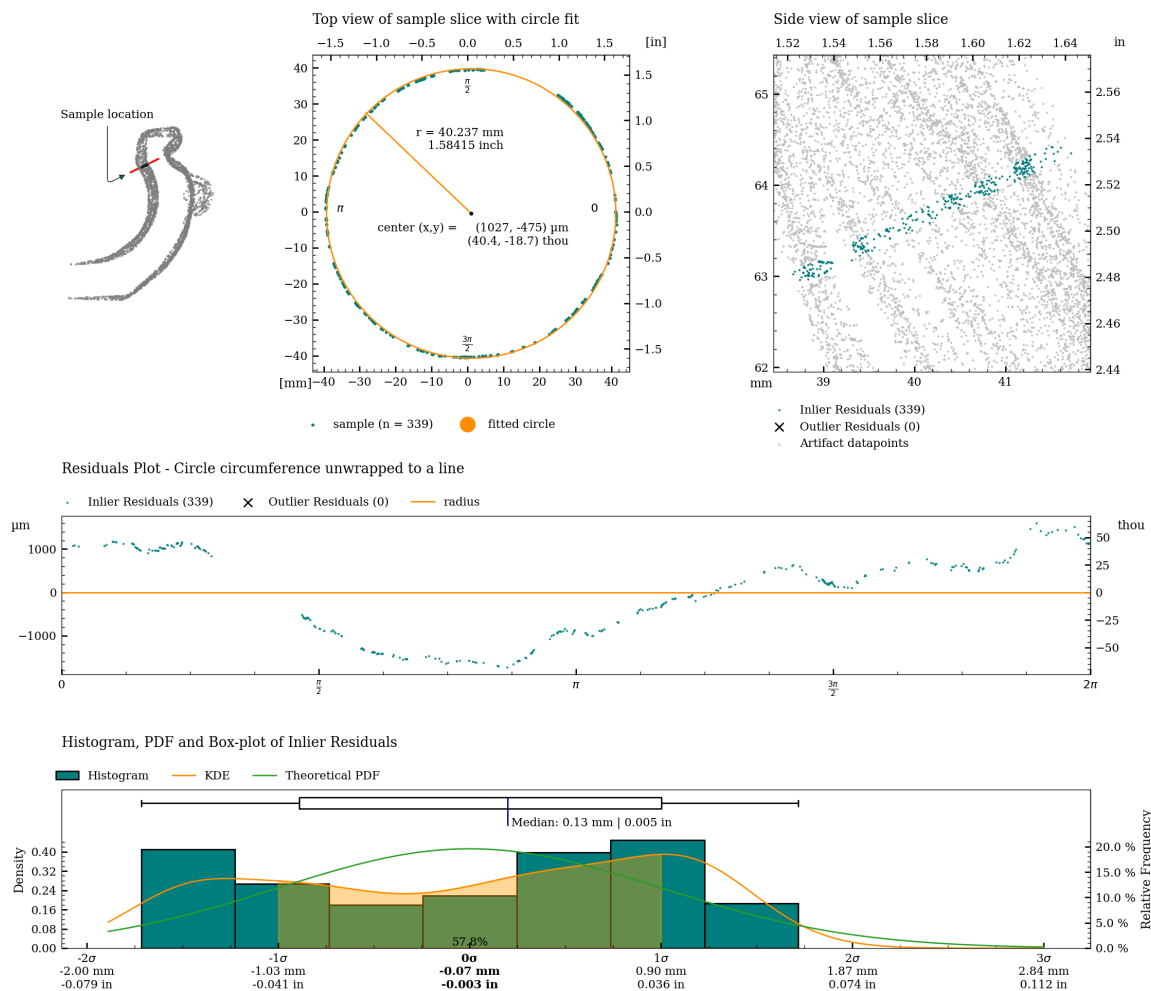


Figure 43: Detailed plot of concentricity measurement for c06_s.

Concentricity analysis of c07

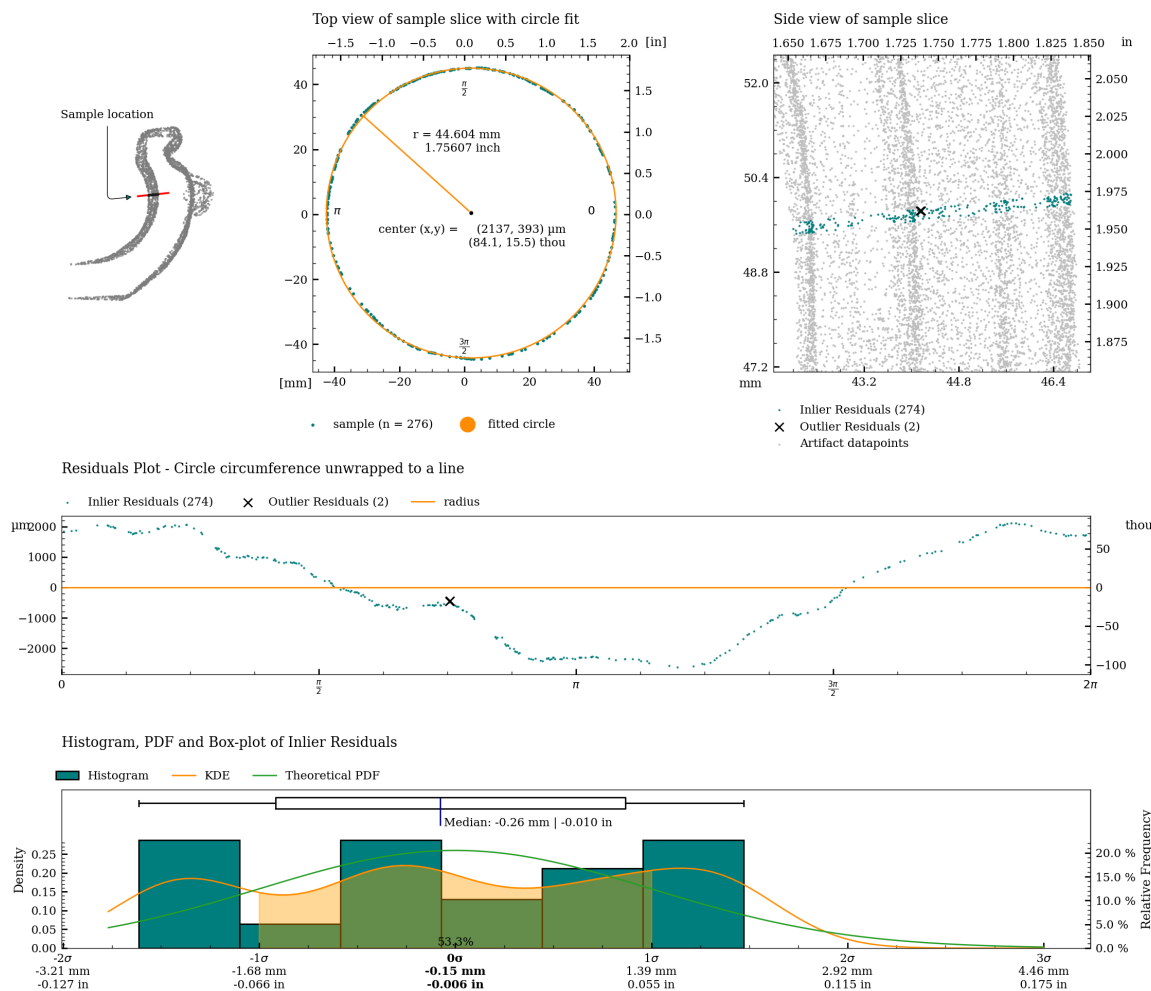


Figure 44: Detailed plot of concentricity measurement for c07.

Concentricity analysis of c07_s

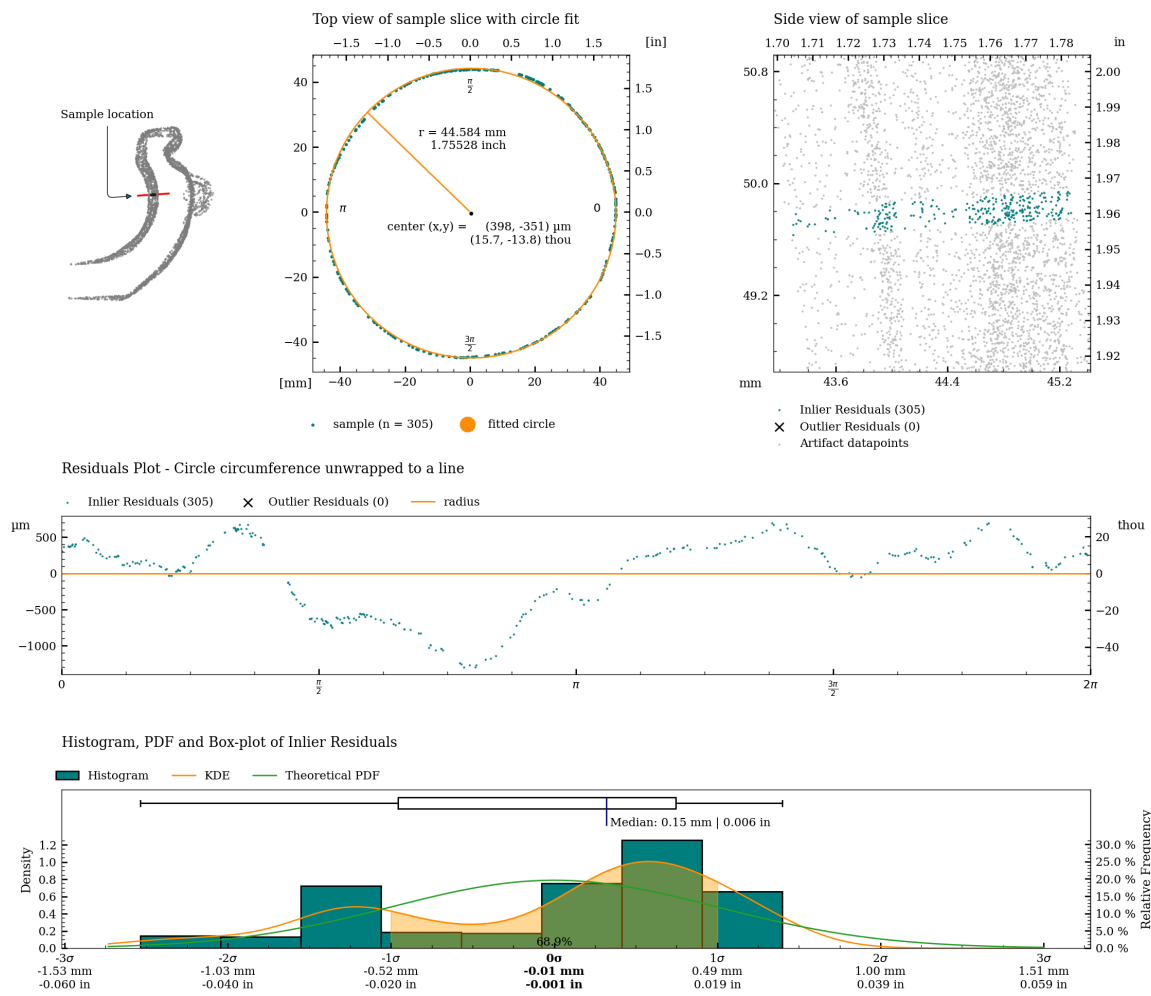


Figure 45: Detailed plot of concentricity measurement for c07_s.

Concentricity analysis of c08

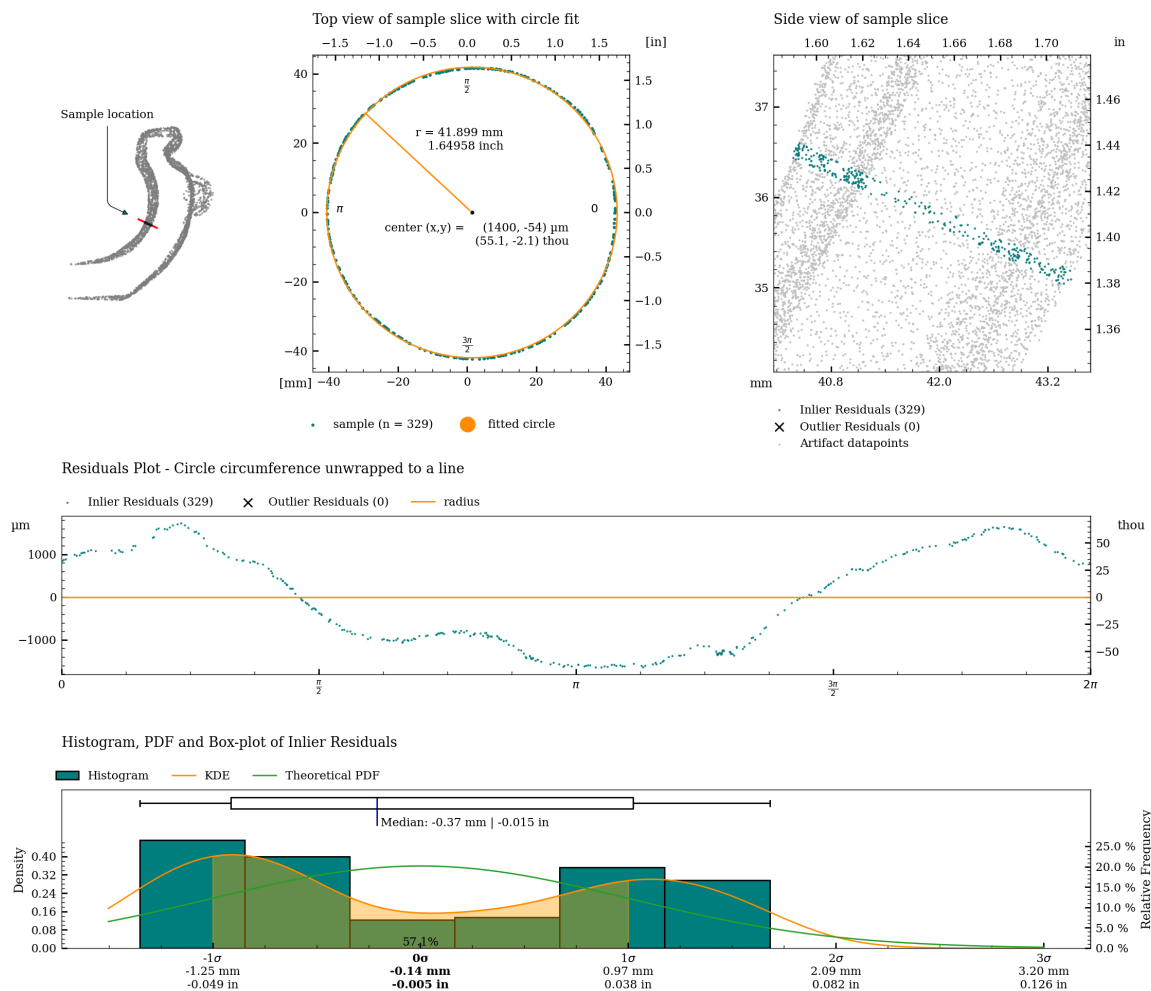


Figure 46: Detailed plot of concentricity measurement for c08.

Concentricity analysis of c08_s

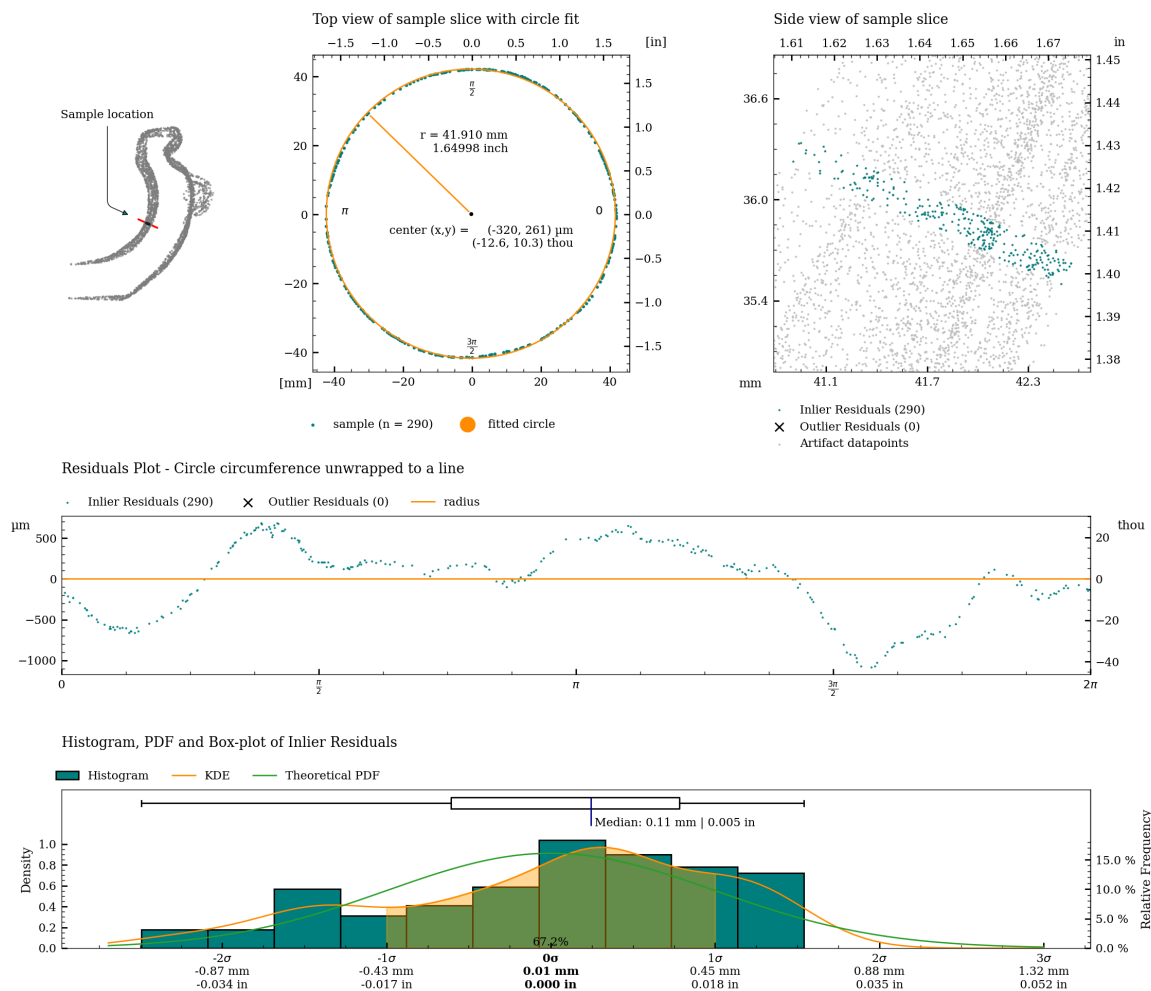


Figure 47: Detailed plot of concentricity measurement for c08_s.

Concentricity analysis of c09

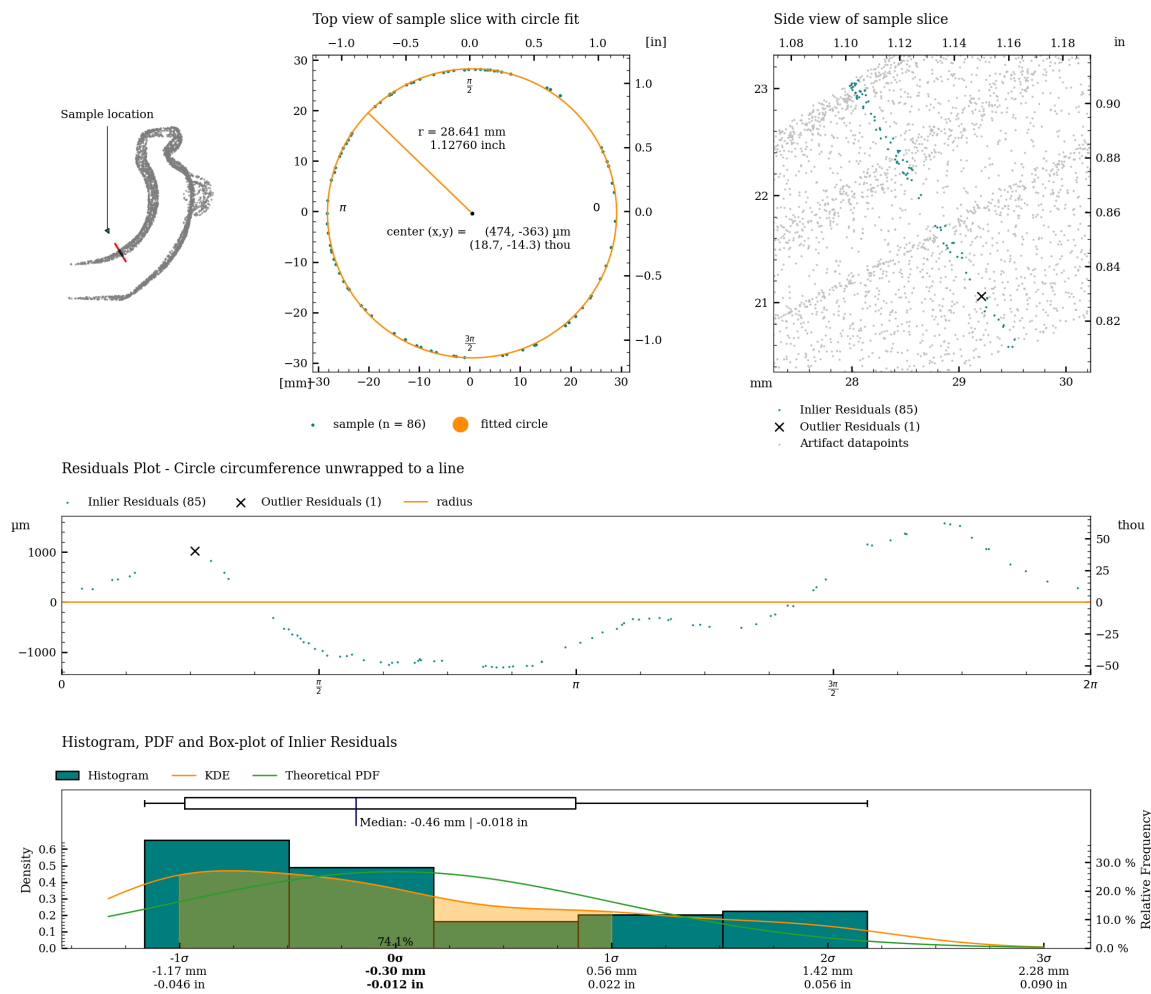


Figure 48: Detailed plot of concentricity measurement for c09.

Concentricity analysis of c09_s

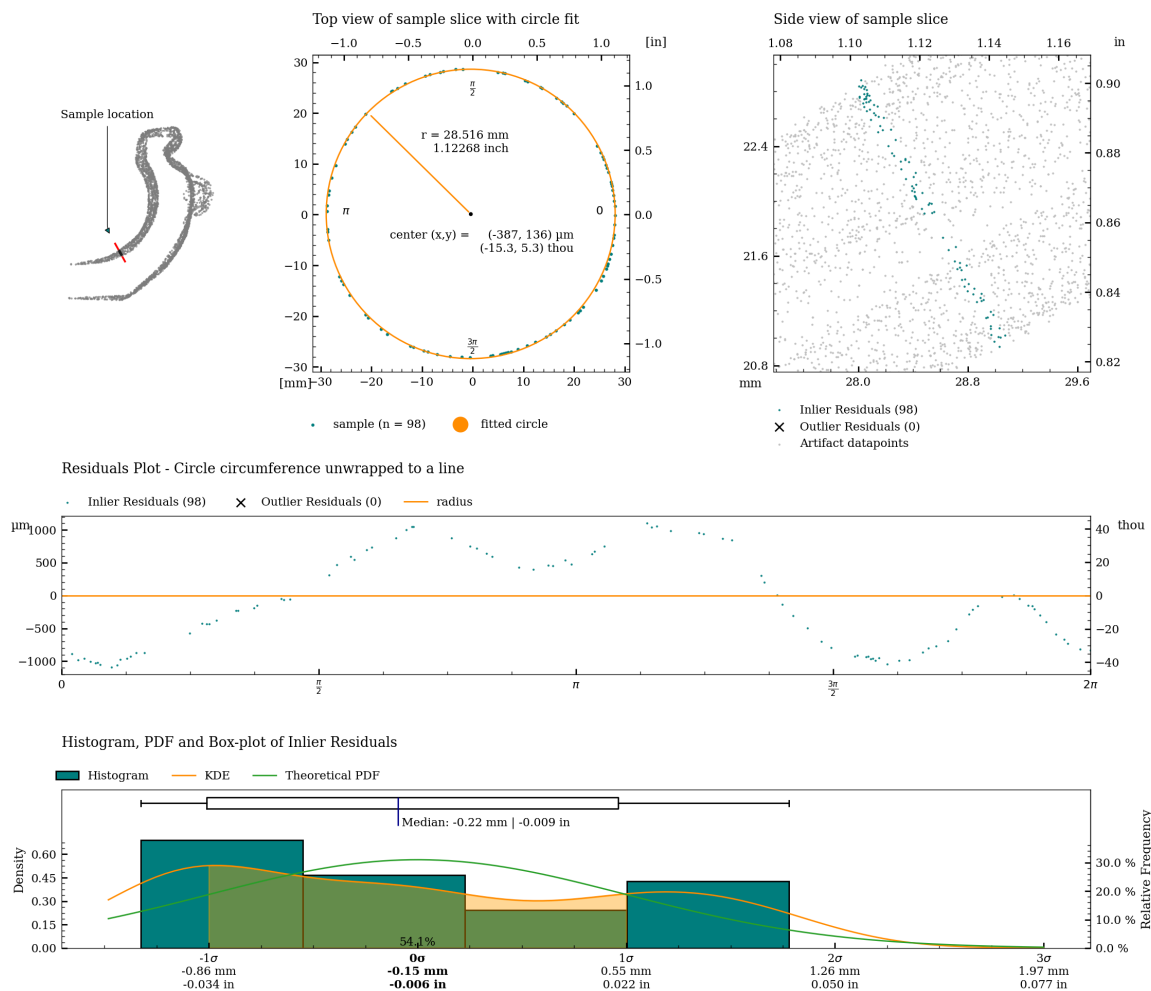


Figure 49: Detailed plot of concentricity measurement for c09_s.

Coaxiality

Coaxiality refers to the straightness and consistency of a central line running through the center of the vase. It measures how aligned the core of the vase remains along its vertical axis.

The coaxiality measurements are calculated using RANSAC (Random sample consensus) algorithm for outlier detection on least squares circle regression on cross-sections of the vessel (excluding potential handles), to estimate the best fit circle centers for each slice of the vessel. A best-fit line connects these centers, showing whether the vessels’s shape twists or remains straight. This concept helps describe the symmetry and structural uniformity in a visual and analytical way.

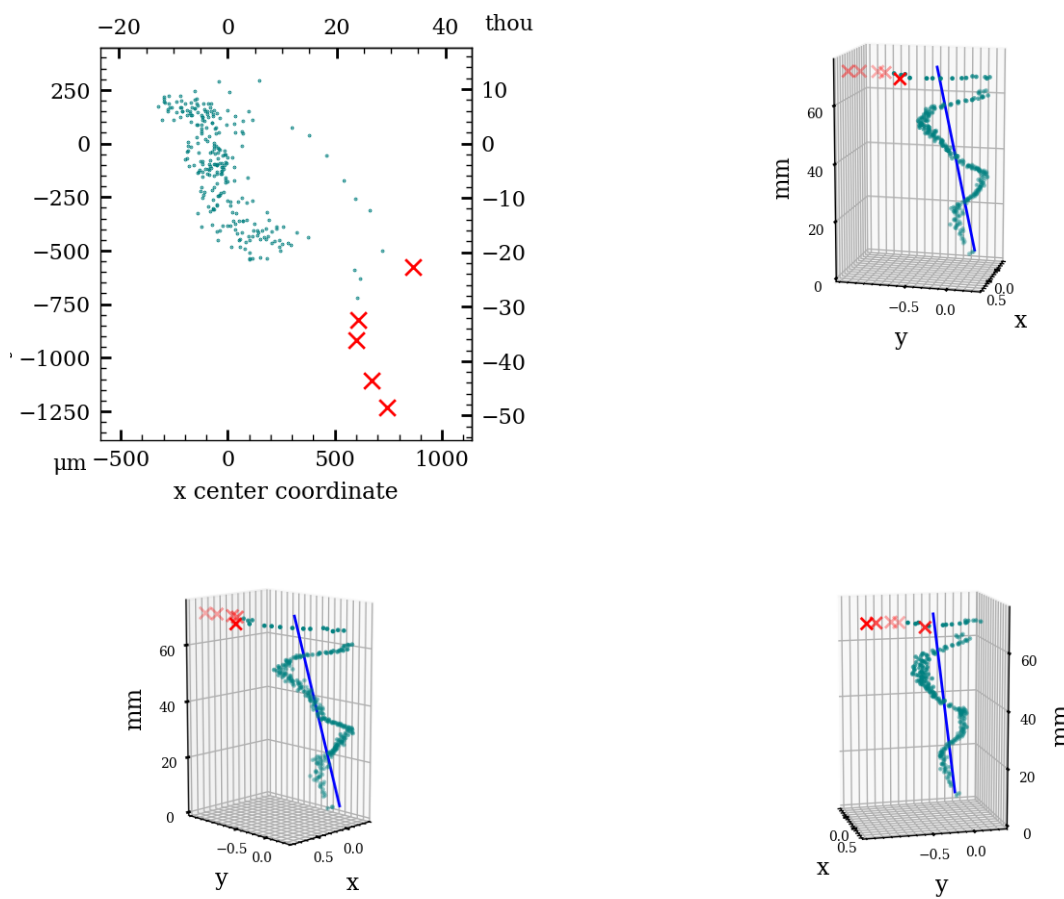
Coaxiality is measured for:

- The exterior surface (excluding handles)
- The interior surface

	Exterior		Interior		Interior separate	
Analyzed Slices	269		213		235	
Median sample size	188		226		279	
Slice Height	200 μm	7.9 thou	200 μm	7.9 thou	200 μm	7.9 thou
Statistics with Z-axis as Reference						
Median Absolute Deviation (MAD)	232 μm	9.1 thou	2017 μm	79.4 thou	523 μm	20.6 thou
Standard Deviation (SD)	204 μm	8.0 thou	383 μm	15.1 thou	253 μm	10.0 thou
Root Mean Square Deviation (RMSD)	349 μm	13.7 thou	1924 μm	75.7 thou	606 μm	23.9 thou
Statistics with Best Fit Central Axis as Reference						
Best fit Central Axis Equation (in metric coordinate system with unit [mm])	x = -0.242 + t0.00585		x = 1.100 + t0.01362		x = -0.774 + t0.01857	
	y = 0.102 + t-0.00575		y = -0.481 + t0.01524		y = -0.024 + t0.00012	
	z = 0.000 + t0.99997		z = 0.000 + t0.99979		z = 0.000 + t0.99983	
Axis tilt	0.337°		0.768°		1.064°	
Median Absolute Deviation (MAD)	204 μm	8.0 thou	360 μm	14.2 thou	396 μm	15.6 thou
Standard Deviation (SD)	151 μm	5.9 thou	152 μm	6.0 thou	270 μm	10.6 thou
Root Mean Square Deviation (RMSD)	280 μm	11.0 thou	380 μm	15.0 thou	531 μm	20.9 thou

Table 4: Coaxiality analysis of vessel RV003.

Coaxiality plots, exterior surface



Coaxiality residuals from fitted axis, exterior surface

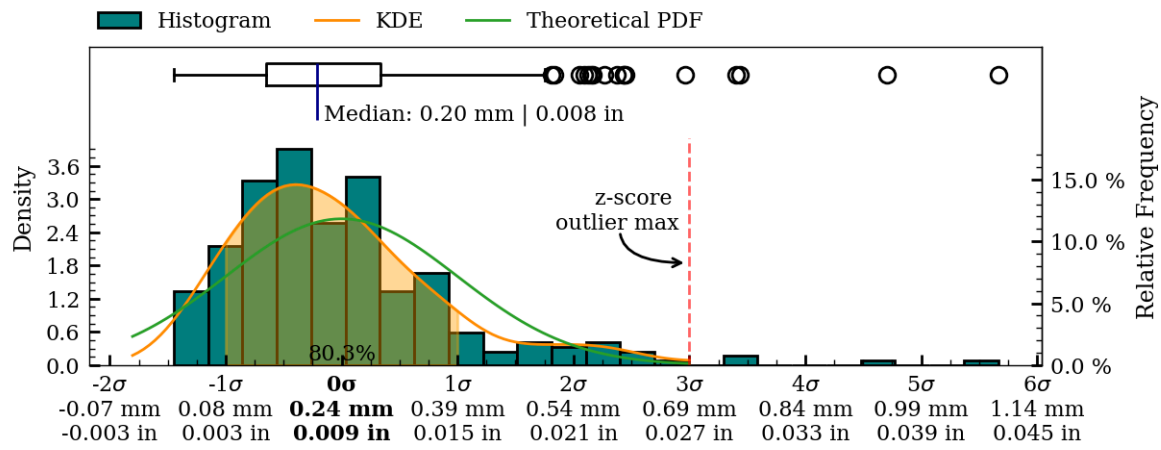
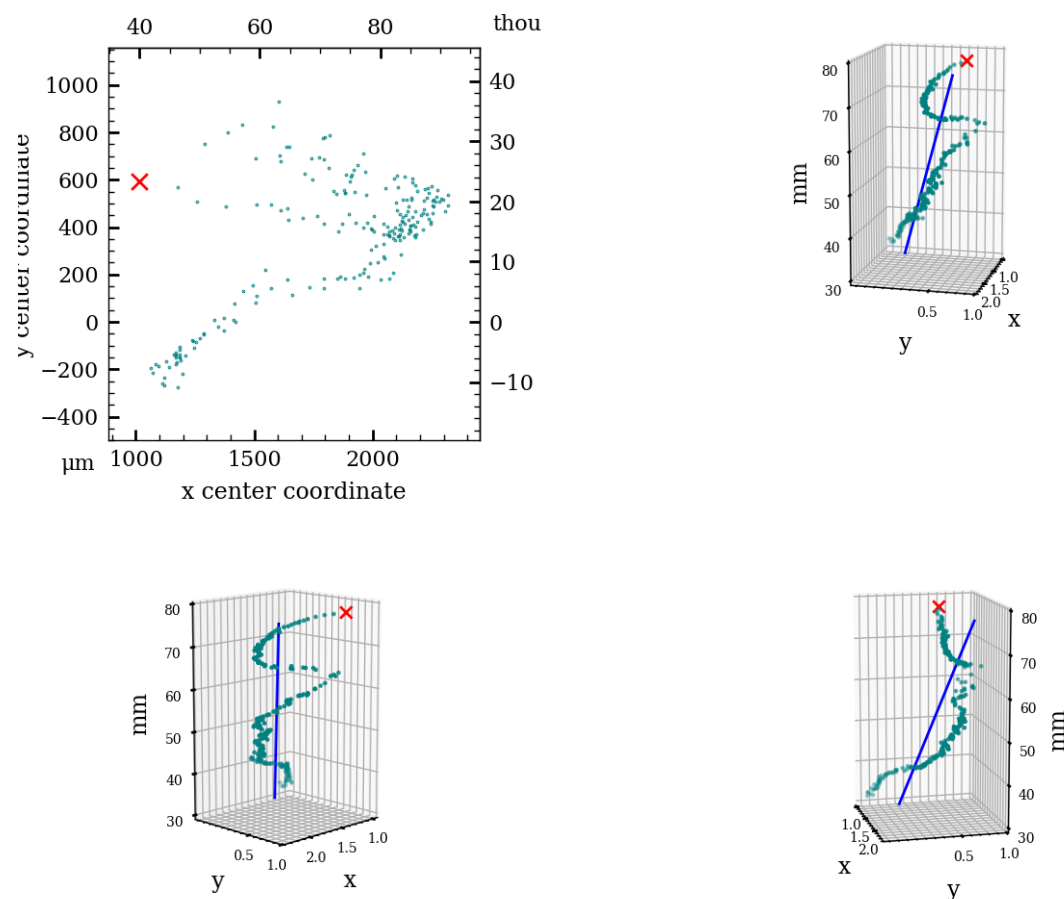


Figure 50: Coaxiality residual plots of exterior surface, RV003.

Coaxiality plots, interior surface



Coaxiality residuals from fitted axis, interior surface

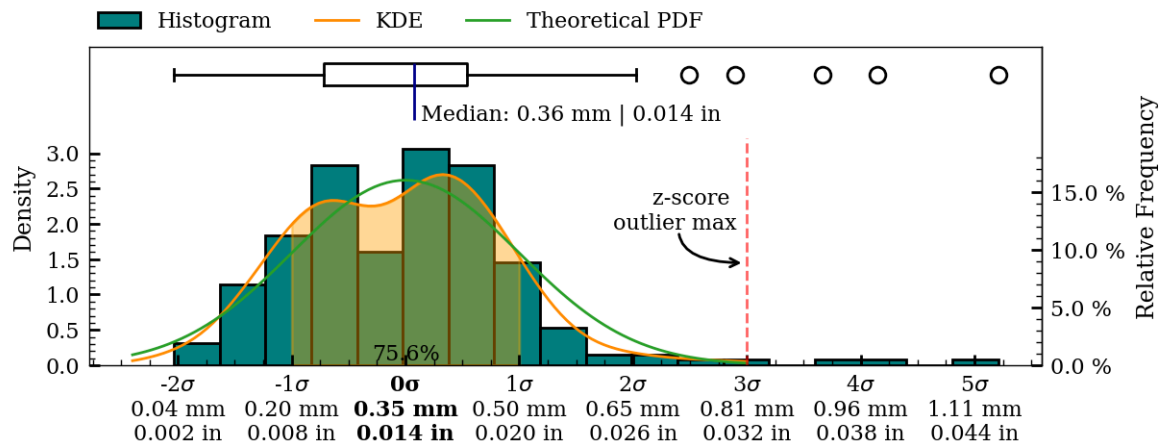
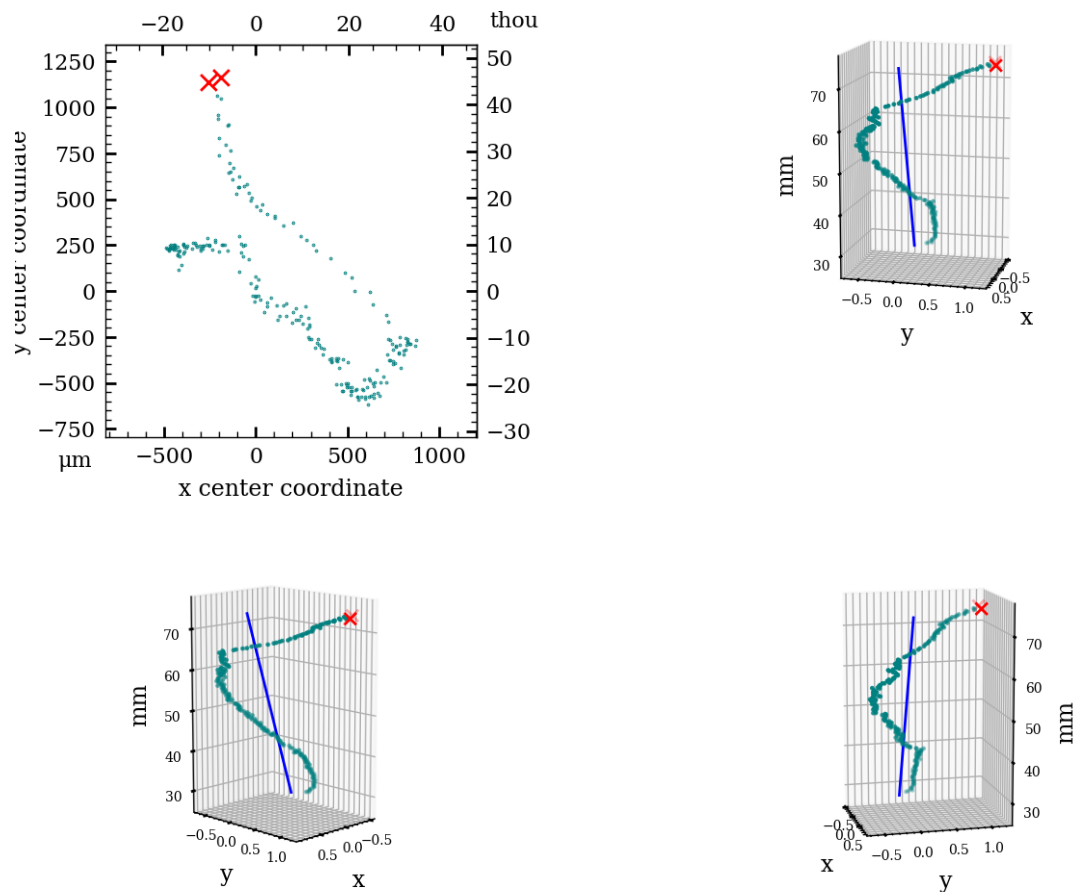


Figure 51: Coaxiality residual plots of interior surface, RV003.

Coaxiality plots, interior separately aligned surface



Coaxiality residuals from fitted axis, interior separately aligned surface

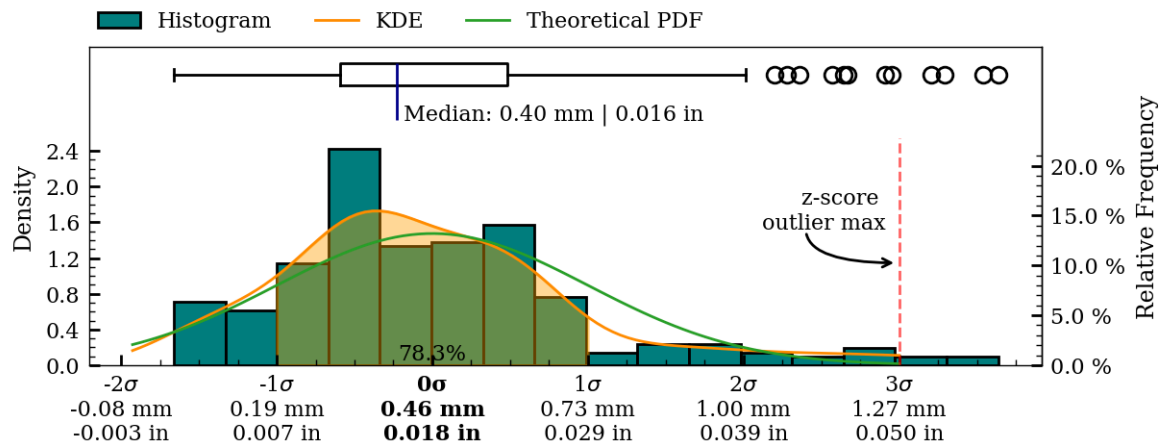


Figure 52: Coaxiality residual plots of interior_separate surface, RV003.

Surface Variability

To illustrate the overall surface deviations of the object, a surface variability heatmap has been created. This heatmap provides an accessible overview of the topography of the manufacturing precision and surface structure of the object.

The surface variability measurements are created by fitting a number of higher-order polynomials to the two-dimensional folded profile of the scan data. This process creates an idealized mathematical representation of actual surface curvature of object, and as such provides a continuous model representation of the actual object. It is important to note that only such a non-discretized representation is sufficient to avoid introducing inconsistently varying errors in the mapping of the final surface deviation results, that the rendered heatmaps are based on.

To produce the final surface variability map, the distance from each scanned vertex to the fitted polynomial is calculated and used as the mapping function input, for applying colours to the surface of the object.

It is important to note that this variability map does not describe deviations from the original *intended* shape of the artifact (if any), as this shape (the *intended design*, so to speak) will have been lost to time. It does however provide a very informative visualization of the texture and structure of the surface and very importantly, *does* highlight potential manufacturing-relevant patterns in the surface texture (if present). Such patterns are, as an example, clearly evident on the interior surface of artifact PV001.

Exterior surface

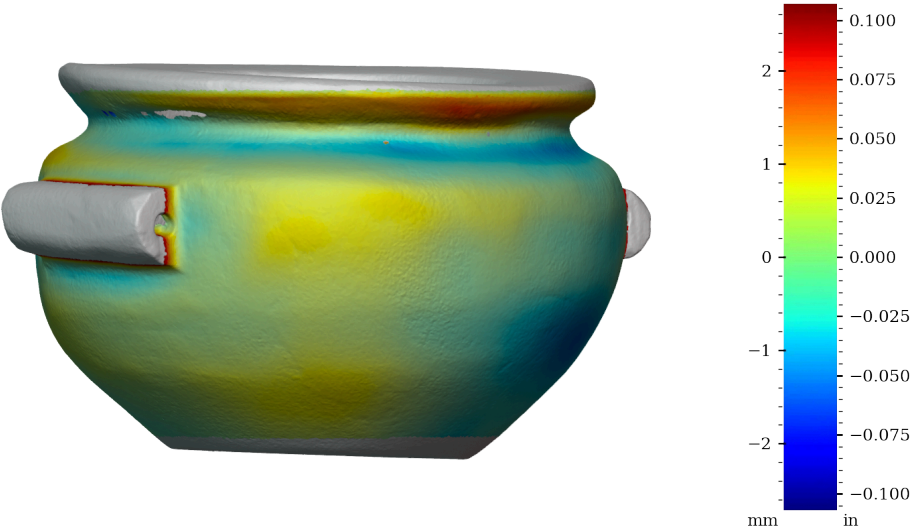


Figure 53: Surface variability heatmap of RV003, front view

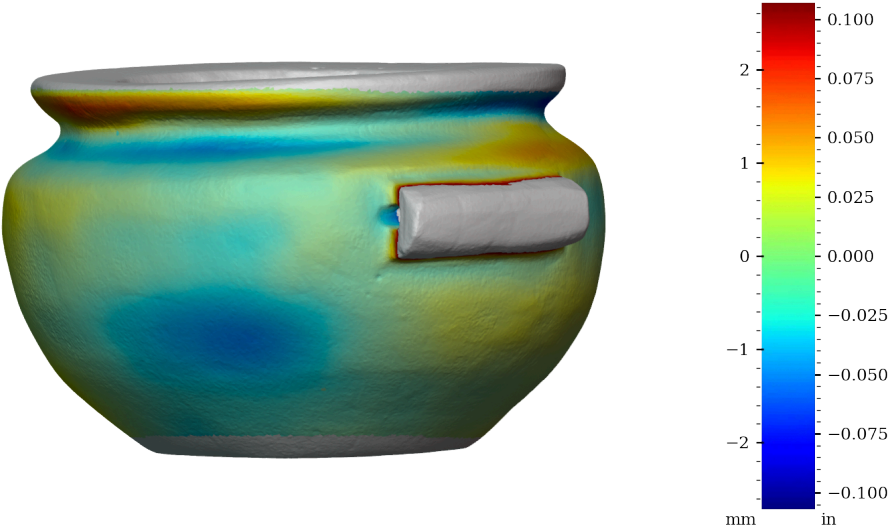


Figure 54: Surface variability heatmap of RV003, rotated 90°

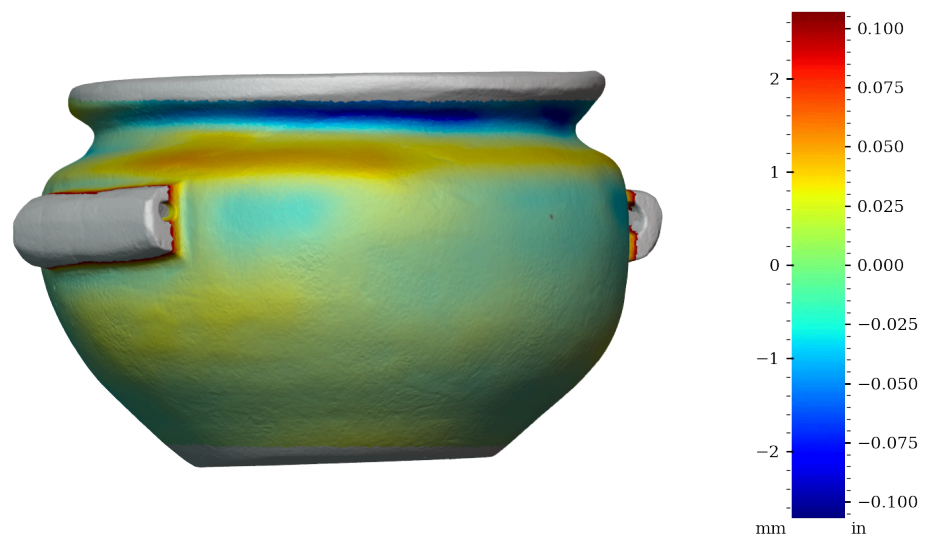


Figure 55: Surface variability heatmap of RV003, rotated 180°

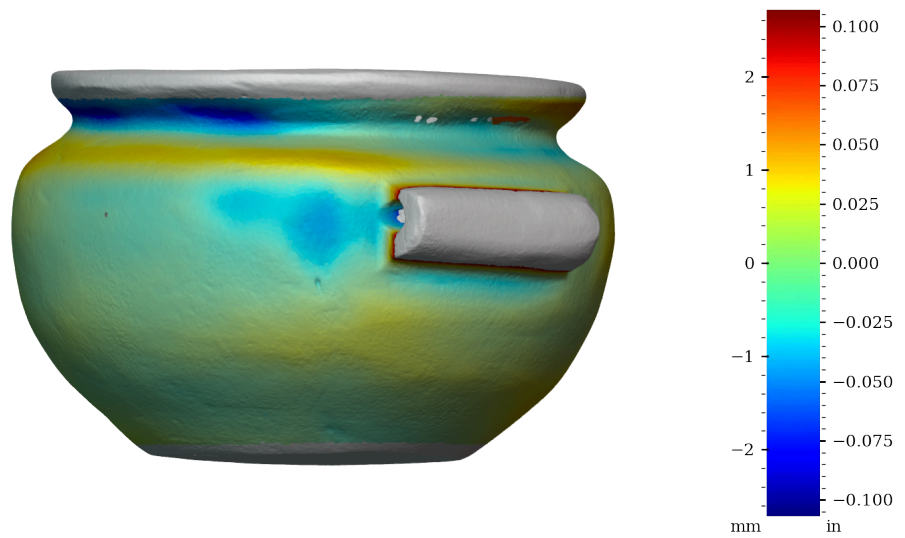


Figure 56: Surface variability heatmap of RV003, rotated 270°

Interior surface

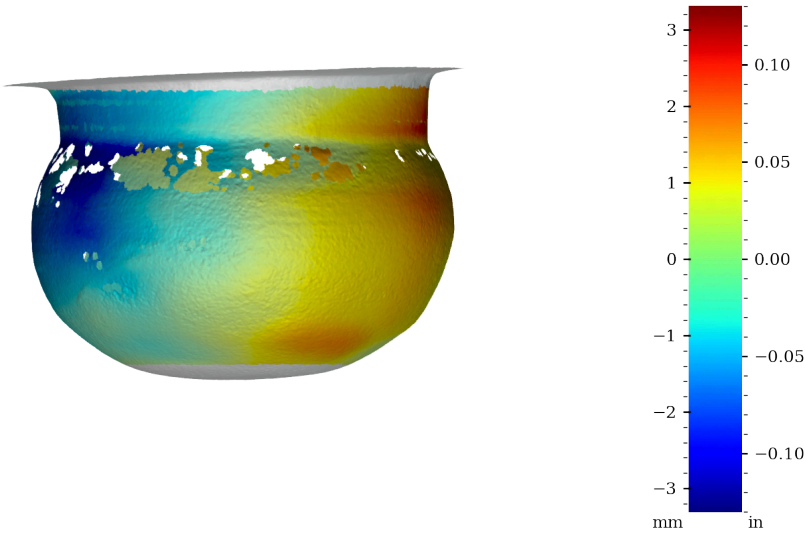


Figure 57: Surface variability heatmap of RV003, front view

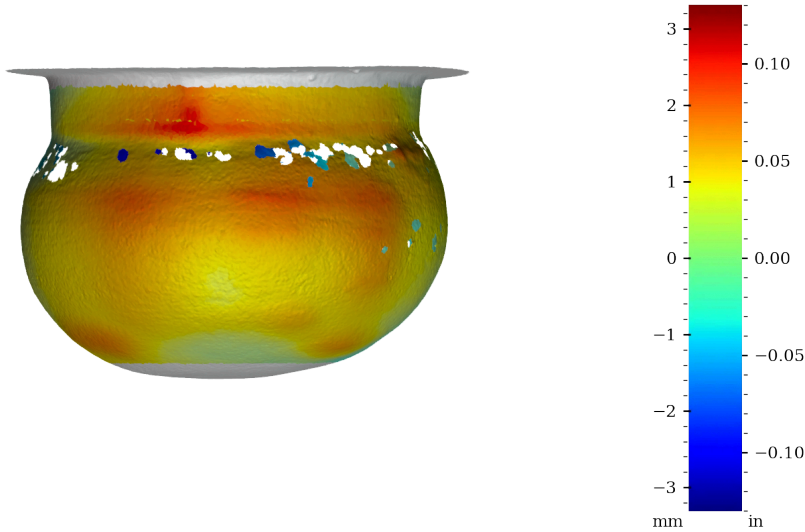


Figure 58: Surface variability heatmap of RV003, rotated 90°

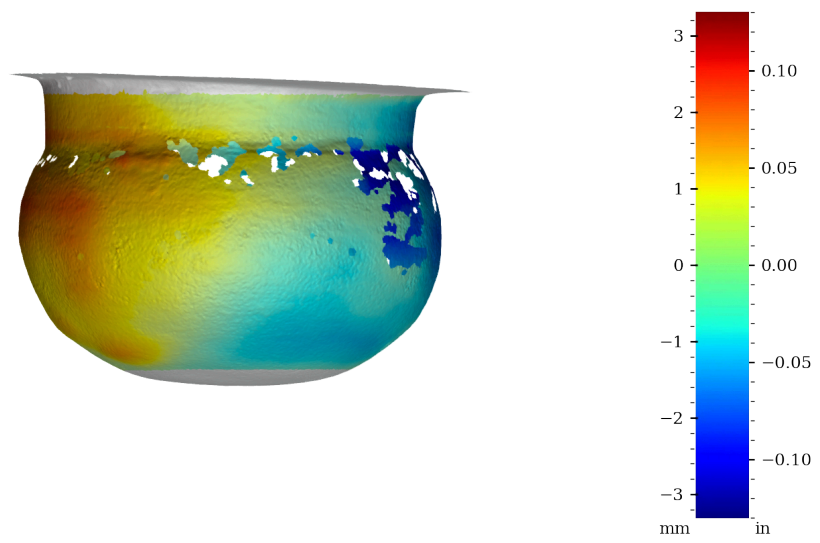


Figure 59: Surface variability heatmap of RV003, rotated 180°

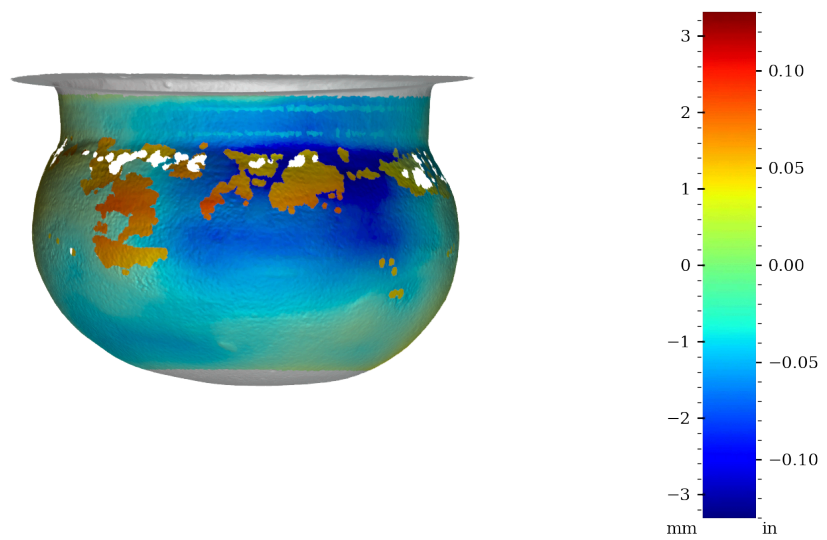


Figure 60: Surface variability heatmap of RV003, rotated 270°

Interior surface aligned separately

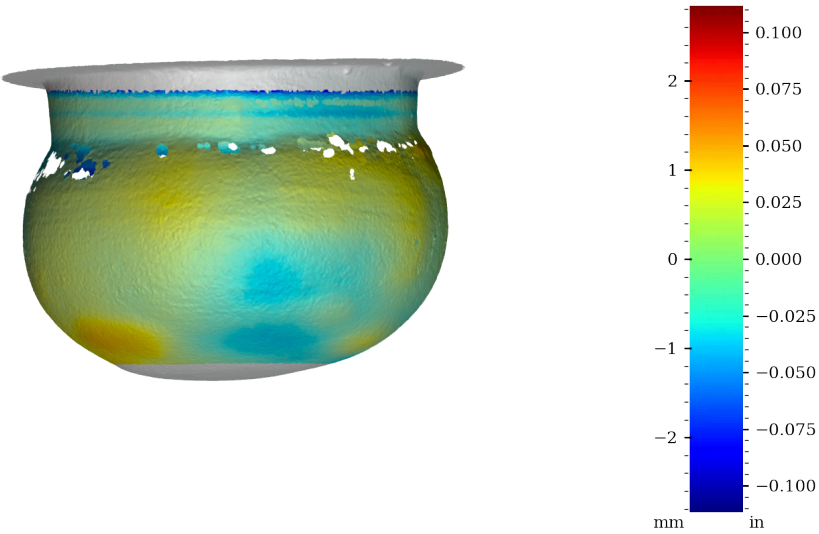


Figure 61: Surface variability heatmap of RV003, front view

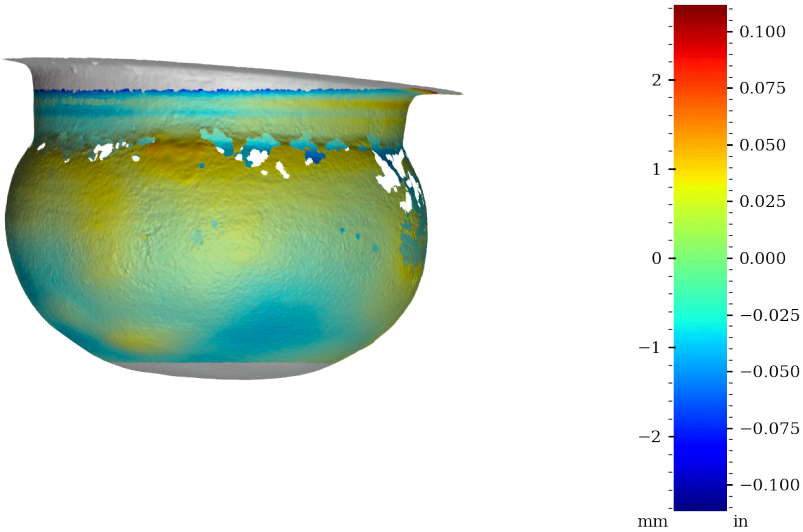


Figure 62: Surface variability heatmap of RV003, rotated 90°

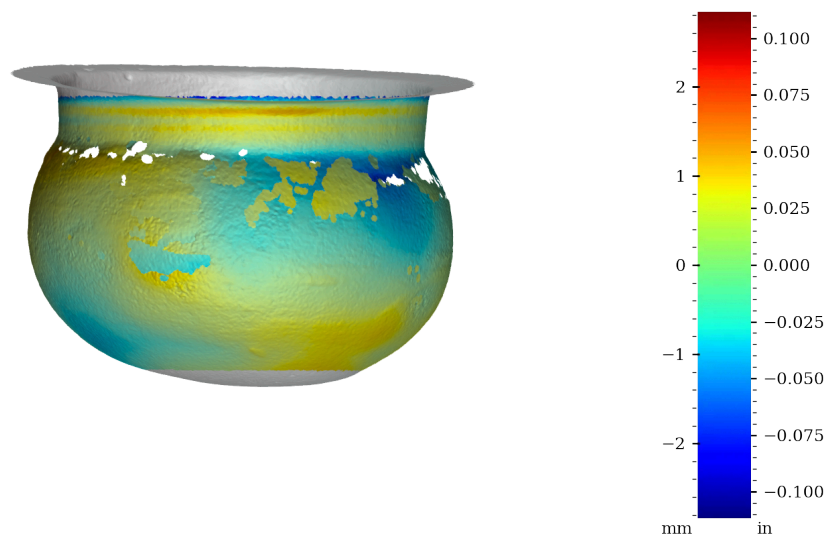


Figure 63: Surface variability heatmap of RV003, rotated 180°

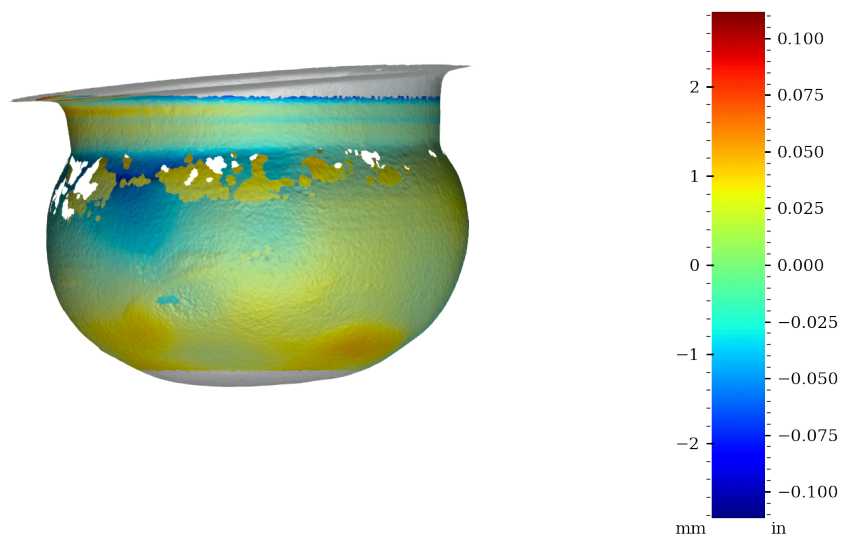


Figure 64: Surface variability heatmap of RV003, rotated 270°

Surface variability statistics

Area	MSD	RMSD	SD	Median AD	Range	Min	Max	Sample size
	mm ²	mm	mm	mm	mm	mm	mm	
Exterior	0.6847	0.827	0.538	0.299	5.346	-2.709	2.638	108882
Interior	1.8634	1.365	0.677	0.514	6.116	-3.310	2.806	91258
Interior separate	0.6520	0.807	0.566	0.253	10.710	-2.854	7.856	93028
	in ²	in	in	in	in	in	in	
Exterior	0.001061	0.0326	0.0212	0.0118	0.2105	-0.1066	0.1038	108882
Interior	0.002888	0.0537	0.0267	0.0202	0.2408	-0.1303	0.1105	91258
Interior separate	0.001011	0.0318	0.0223	0.0099	0.4216	-0.1124	0.3093	93028

Table 5: Surface variability statistics, RV003

Table 5 shows the statistics of the distance from the scan vertices to the best fit object model. These statistics are briefly explained below.

Histogram, KDE and Box-plot of measured surface variability - exterior surface

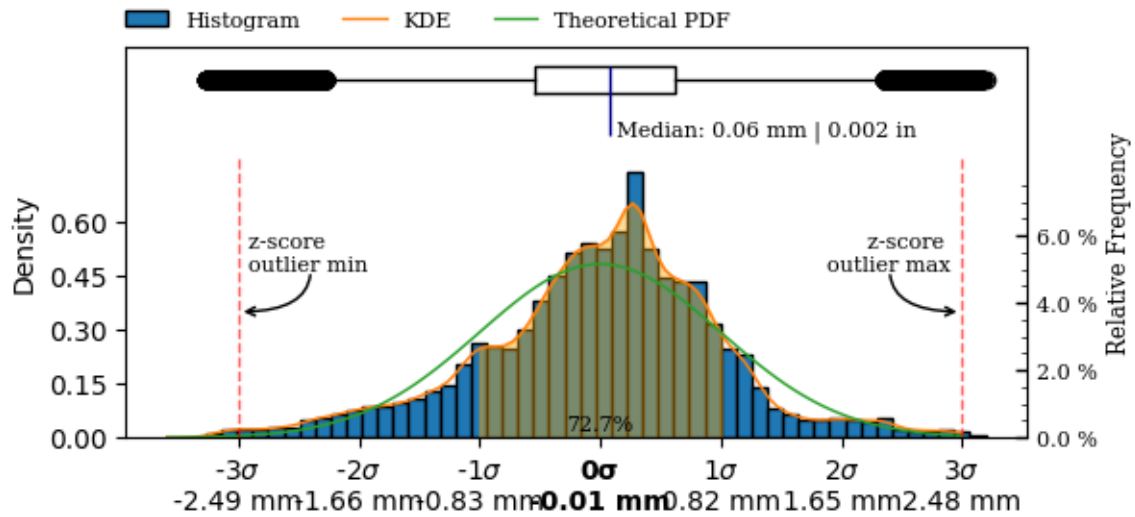


Figure 65: Exterior surface variability boxplot, kds and histogram.

Histogram, KDE and Box-plot of measured surface variability - interior surface

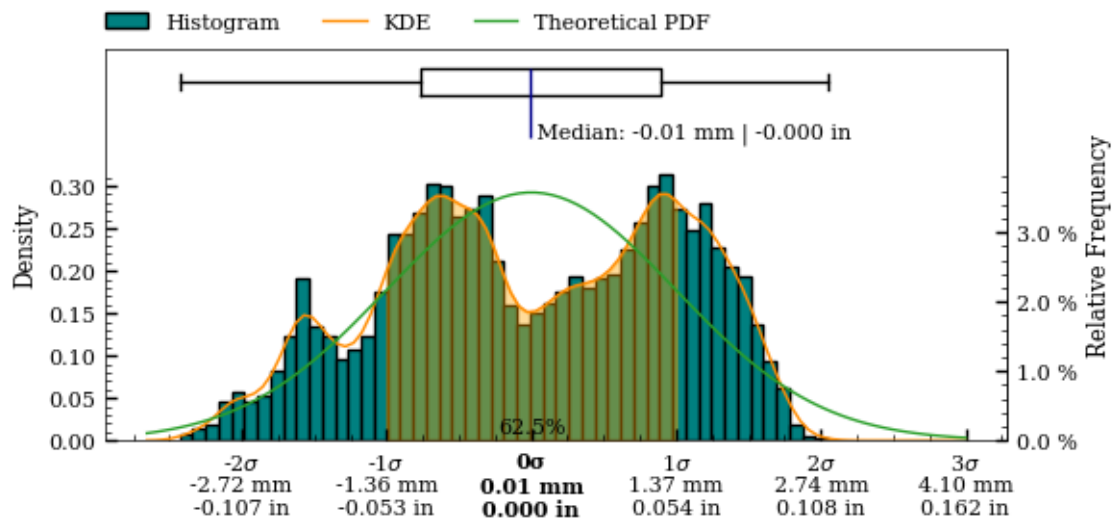


Figure 66: Interior surface variability boxplot, kds and histogram.

Histogram, KDE and Box-plot of measured surface variability - interior separately aligned surface

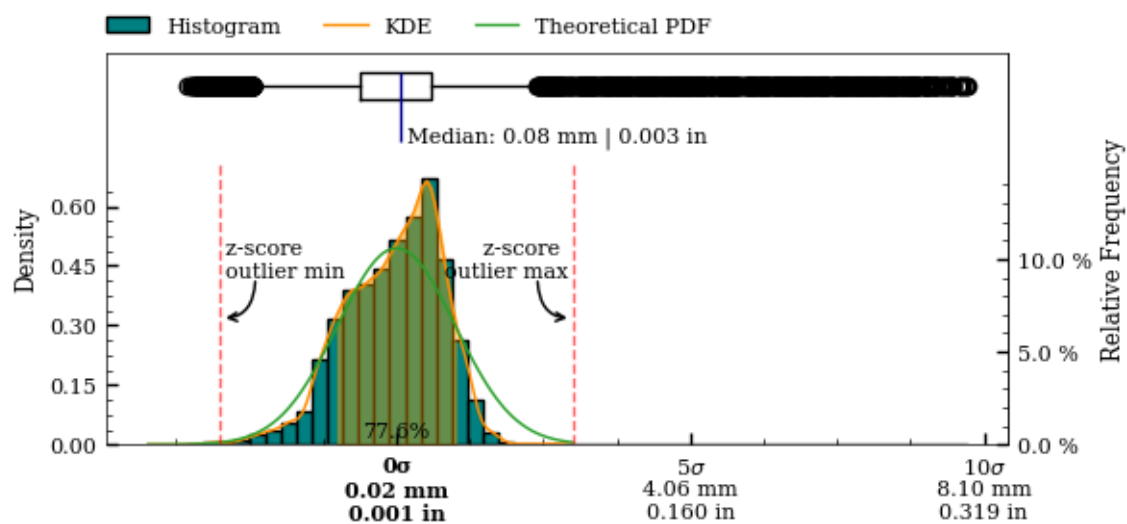


Figure 67: Interior separately aligned surface variability boxplot, kds and histogram.

Precision Score Of The Artifact

To enable valid comparison of the manufacturing precision of different artifacts, a metric that robustly quantifies the overall precision of the object is required. The considerations for such a metric will be explored in this section.

Based on these considerations, a *Precision Score* metric will be defined.

For an object to be described as having been manufactured with high precision, several qualities must be present *concurrently*, and throughout the *entire* geometry of the final object. A given object may exhibit high levels of one or more *components* of precision, but be lacking in others. For example:

- An object may present high levels of coaxiality, but lack circularity.
- An object may exhibit good circularity, but show imperfections in the surface structure.
- An object may be smoothed to perfection *without* any circularity or coaxiality.
- An object may exhibit high levels of all of the above metrics in *some* areas, but not in others.

Therefore, a precision score metric **must** account for *all* aspects of the individual, underlying precision metrics (circularity, concentricity, coaxiality and surface variability) throughout the *entire* surface area of the object.

The composite high order polynomial model, used to generate the surface variability map (described in Surface Variability, p. 52) is the best continuous mathematical representation of the object available to us (lacking any original design plans, as would normally be available in metrological analysis). This idealized model encompasses all of the above component metrics.

In the creation of the model, all scan data-points are taken into account (excluding areas with extensive damage), making it the best possible idealized representation we can achieve. When this model has been accurately created, the deviation between the model and the scanned data-points can be calculated over the non-discretized polynomials, *without* the need for an “original” CAD model (and importantly, unless such a CAD model *actually* corresponded to the original design intent, it would be an insufficient comparison basis).

Within the context of defining a valid, overall precision metric, this approach satisfies the incorporation of all of the necessary metrics:

- **Circularity:** Because the reconstructed polynomial model is revolved around the Z-plane, the idealized representation is perfectly circular, and thus incorporates the circularity component.
- **Concentricity and coaxiality:** Because the Z-axis (datum axis) is the center axis of the model, it incorporates the concentricity and coaxiality components.
- **Surface variability:** Because the model is continuous and non-discretized, it can be used accurately for all points of the scan data, and incorporates the surface variability component.

The level of precision ultimately achieved in a physical object does not share a linear relationship with its manufacturing requirements. Since continuously higher levels of final precision becomes progressively harder to achieve, an overall precision metric must take this relationship into account.

A robust statistical metric that satisfies this requirement is the *Mean Squared Deviation* (MSD or MSE). Here specifically, we can utilize the mean square of the deviations between the model (\hat{y}) and the data-points (y_i).

Combining all of the above considerations, we can express a well-defined *Precision Score* metric, that provides an immediately accessible way to understand the overall precision of an object, while being statistically valid. Since the Mean Squared Deviation tends towards zero as the overall precision increases, the inverse of the Mean Squared Deviation is taken to obtain a precision score metric that increases as precision increases¹²:

$$\text{Precision Score} = \frac{n}{\sum_{i=1}^n (y_i - \hat{y})^2}$$

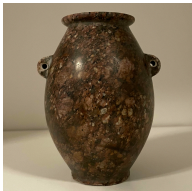
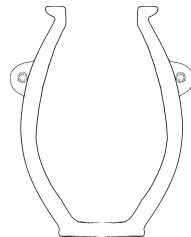

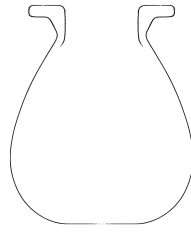




¹²The precision score unit is $\frac{1}{\text{mm}^2}$

The precision score of RV003 have been calculated separately for:

- Precision score, exterior surface: 1.46
- Precision score, separately aligned interior surface: 1.53
- Precision score, interior surface: 0.54
- Precision score, full surface: 1.49

The precision score of a Zeiss 1.00000 inch reference sphere have been calculated to 43,943 (RMSE = 0.00477 mm / 0.00010 in). The scan was obtained by Max Fomitchev-Zamilov using a Keyence VL –500 scanner with a rated accuracy of 10 microns. The precision analysis of the reference sphere scan indicates at the maximum possible precision score obtainable.

Table 6 shows the precision score of this artifact (RV003), compared to the two most precise, and the two least precise vessels currently analyzed.

Artifact		Material	Precision Score	Link to Report
		PV001 Red Granite	1980 Full: 1177 Exterior: 1980 Interior separate: 798 Interior: 722	Report Publication
		PV006 Dark grey granite	621 Full: 610 Exterior: 621 Interior separate: 479 Interior: 152	Report Publication
		RV003 Marble breccia	1.46 Full: 1.49 Exterior: 1.46 Interior separate: 1.53 Interior: 0.54	Report Publication
		MV010 Calcite (Egyptian Alabaster)	1.17 Full: 1.32 Exterior: 1.17 Interior separate: 11 Interior: 0.17	Report Publication

Analysis Roadmap

While the current iteration of this work already provides valuable results, continued future additions and improvements will enhance their utility further. This section details planned iterative updates and improvements, to both the reports themselves, and to the underlying methodology and software they are created with.

Alignment Section

- Detailed exploration of different circle regression algorithms
- If handles are present on the vessel, exploring alignment of the vessels so the handle positions match each other
- Add optimization of the perpendicular surface deviation, with the best results of the coaxial alignment
- Align by minimizing circularity results (of rotated sample slice, to compensate for sample height distortions)

Measurements of Precision

- Section detailing how measurements perpendicular to the surface curvature are obtained
- Detailed surface area analysis, exploring the residual patterns throughout subsequent sample slices of the artifact surface
- Wall thickness deviation color map
- Robust outlier identification on circularity, to better handle analysis of damaged areas of the artifacts in addition to removal of interior crystalline structure points present in CT scans
- Layout updates to the charts and tables

Visibility of Outliers and Damaged Sections

- Identification and marking of damaged parts
- Visualization of outliers on the artifact surface

Exploration of Mathematical Primitives

- Analysis of selected curvatures and flat surfaces on the vessel in both the horizontal and vertical planes
 - Circles
 - Parabolas
 - Ellipsoids
 - Hyperbolas
 - Cones
- Implementation of robust regressions models suitable for this domain, based on RANSAC.

Metrics on Primary Features

- Measurements of features in the horizontal plane
- Measurements of features in the vertical plane
- Measurements of angles
- Measurements of volume

Exploration of Potential Design Ratios

- π , φ , e , 1, 2, 3, 4 etc.

Raw Dataset Attachments

- Including all measurement and sample coordinates as CSV-files embedded in the report
- Including an STL file of the aligned object alongside the report, for easier external replication and validation of the research results

Appendix A - Comparison Of Circularity Measurements (Z-plane vs. surface-perpendicular)

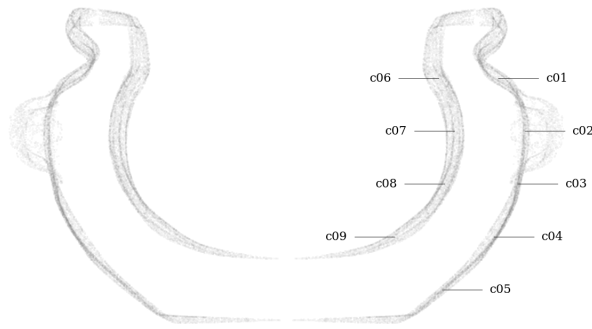


Figure 68: Circularity measurement sample locations, full mesh aligned to exterior surface

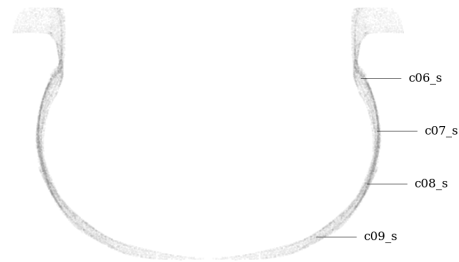


Figure 69: Circularity measurement sample location, separately aligned interior mesh

Samples perpendicular to the surface curvature

Tag	Area	Measured deviation ⁸	Residuals				Sample size	Slice		
			Range	RMSD ⁹	MAD ¹⁰	SD		Height	Z coord.	Radius ¹¹
		mm	mm	mm	mm	mm		mm	mm	mm
c01	exterior	Ø111.834±1.722	3.282	1.085	0.389	0.446	162	0.200	63.743	55.917
c02	exterior	Ø125.763±1.700	2.704	0.651	0.248	0.361	149	0.200	49.799	62.882
c03	exterior	Ø121.976±0.926	1.694	0.450	0.232	0.255	307	0.200	35.856	60.988
c04	exterior	Ø109.485±2.013	2.747	0.740	0.187	0.490	242	0.200	21.912	54.743
c05	exterior	Ø82.190±0.936	1.817	0.511	0.207	0.276	139	0.200	7.969	41.095
c06	interior	Ø80.516±3.192	5.489	1.433	0.416	0.687	273	0.200	63.743	40.258
c06_s	interior sep.	Ø80.571±1.770	3.326	0.974	0.405	0.471	339	0.200	63.743	40.285
c07	interior	Ø88.855±2.447	4.734	1.529	0.764	0.768	276	0.200	49.799	44.428
c07_s	interior sep.	Ø89.099±1.262	1.992	0.507	0.180	0.259	305	0.200	49.799	44.549
c08	interior	Ø83.652±1.798	3.373	1.115	0.299	0.438	329	0.200	35.856	41.826
c08_s	interior sep.	Ø83.803±1.076	1.766	0.438	0.189	0.247	290	0.200	35.856	41.902
c09	interior	Ø57.403±1.549	2.884	0.925	0.381	0.409	86	0.200	21.912	28.701
c09_s	interior sep.	Ø57.052±1.098	2.194	0.724	0.263	0.330	98	0.200	21.912	28.526

Table 7: Detailed circularity measurements at selected samples in z-plane, vessel RV003.

Samples in the Z-plane

Tag	Area	Measured deviation ⁸	Residuals				Sample size	Slice		
			Range	RMSD ⁹	MAD ¹⁰	SD		Height	Z coord.	Radius ¹¹
		mm	mm	mm	mm	mm		mm	mm	mm
c01	exterior	Ø110.816±3.691	6.042	1.891	0.790	0.963	469	0.200	63.743	55.408
c02	exterior	Ø125.495±1.568	2.703	0.656	0.258	0.388	153	0.200	49.799	62.748
c03	exterior	Ø121.836±0.902	1.745	0.440	0.217	0.259	302	0.200	35.856	60.918
c04	exterior	Ø110.137±2.774	3.340	0.974	0.172	0.766	335	0.200	21.912	55.069
c05	exterior	Ø82.189±1.570	3.055	0.749	0.317	0.432	290	0.200	7.969	41.094
c06	interior	Ø80.805±3.511	6.179	2.000	0.807	1.002	358	0.200	63.743	40.402
c06_s	interior sep.	Ø80.937±2.039	3.375	1.044	0.405	0.545	400	0.200	63.743	40.469
c07	interior	Ø88.233±2.630	4.823	1.594	0.712	0.840	312	0.200	49.799	44.116
c07_s	interior sep.	Ø89.459±1.497	2.092	0.562	0.204	0.375	312	0.200	49.799	44.730
c08	interior	Ø83.686±1.987	3.733	1.182	0.271	0.460	377	0.200	35.856	41.843
c08_s	interior sep.	Ø84.036±1.316	2.031	0.512	0.250	0.315	364	0.200	35.856	42.018
c09	interior	Ø56.920±3.942	6.378	1.912	0.707	0.934	362	0.200	21.912	28.460
c09_s	interior sep.	Ø56.840±2.602	4.847	1.459	0.534	0.711	361	0.200	21.912	28.420

Table 8: Detailed circularity measurements at selected samples perpendicular to vessel curvature, vessel RV003.

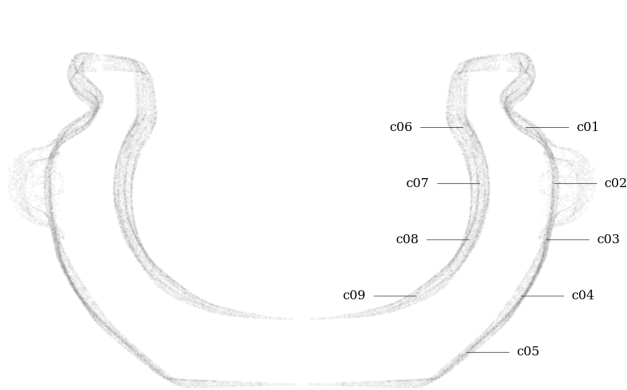


Figure 70: Circularity measurement sample locations, full mesh aligned to exterior surface

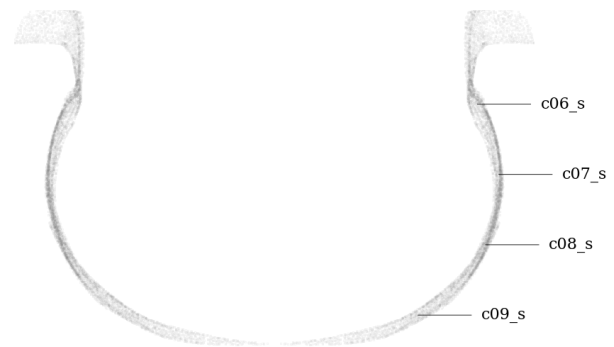


Figure 71: Circularity measurement sample location, separately aligned interior mesh

Samples perpendicular to the surface curvature

Tag	Area	Measured deviation ⁸	Residuals				Sam-ple size	Slice		
			Range	RMSD ⁹	MAD ¹⁰	SD		Height	Z coord.	Radius ¹¹
		in	in	in	in	in		in	in	in
c01	exterior	Ø4.4029±0.0678	0.1292	0.0427	0.0153	0.0176	162	0.0079	2.5096	2.2014
c02	exterior	Ø4.9513±0.0669	0.1065	0.0256	0.0098	0.0142	149	0.0079	1.9606	2.4756
c03	exterior	Ø4.8022±0.0365	0.0667	0.0177	0.0091	0.0101	307	0.0079	1.4116	2.4011
c04	exterior	Ø4.3105±0.0793	0.1081	0.0291	0.0074	0.0193	242	0.0079	0.8627	2.1552
c05	exterior	Ø3.2358±0.0368	0.0715	0.0201	0.0082	0.0109	139	0.0079	0.3137	1.6179
c06	interior	Ø3.1699±0.1257	0.2161	0.0564	0.0164	0.0270	273	0.0079	2.5096	1.5850
c06_s	interior sep.	Ø3.1721±0.0697	0.1309	0.0384	0.0160	0.0186	339	0.0079	2.5096	1.5860
c07	interior	Ø3.4982±0.0963	0.1864	0.0602	0.0301	0.0302	276	0.0079	1.9606	1.7491
c07_s	interior sep.	Ø3.5078±0.0497	0.0784	0.0200	0.0071	0.0102	305	0.0079	1.9606	1.7539
c08	interior	Ø3.2934±0.0708	0.1328	0.0439	0.0118	0.0172	329	0.0079	1.4116	1.6467
c08_s	interior sep.	Ø3.2993±0.0424	0.0695	0.0173	0.0074	0.0097	290	0.0079	1.4116	1.6497
c09	interior	Ø2.2599±0.0610	0.1135	0.0364	0.0150	0.0161	86	0.0079	0.8627	1.1300
c09_s	interior sep.	Ø2.2461±0.0432	0.0864	0.0285	0.0104	0.0130	98	0.0079	0.8627	1.1231

Table 9: Detailed circularity measurements at selected samples in z-plane, vessel RV003.

Samples in the Z-plane

Tag	Area	Measured deviation ⁸	Residuals				Sam-ple size	Slice		
			Range	RMSD ⁹	MAD ¹⁰	SD		Height	Z coord.	Radius ¹¹
		in	in	in	in	in		in	in	in
c01	exterior	Ø4.3628±0.1453	0.2379	0.0744	0.0311	0.0379	469	0.0079	2.5096	2.1814
c02	exterior	Ø4.9408±0.0617	0.1064	0.0258	0.0101	0.0153	153	0.0079	1.9606	2.4704
c03	exterior	Ø4.7967±0.0355	0.0687	0.0173	0.0085	0.0102	302	0.0079	1.4116	2.3983
c04	exterior	Ø4.3361±0.1092	0.1315	0.0384	0.0068	0.0302	335	0.0079	0.8627	2.1681
c05	exterior	Ø3.2358±0.0618	0.1203	0.0295	0.0125	0.0170	290	0.0079	0.3137	1.6179
c06	interior	Ø3.1813±0.1382	0.2433	0.0787	0.0318	0.0394	358	0.0079	2.5096	1.5906
c06_s	interior sep.	Ø3.1865±0.0803	0.1329	0.0411	0.0159	0.0215	400	0.0079	2.5096	1.5933
c07	interior	Ø3.4737±0.1035	0.1899	0.0628	0.0280	0.0331	312	0.0079	1.9606	1.7369
c07_s	interior sep.	Ø3.5220±0.0589	0.0824	0.0221	0.0080	0.0147	312	0.0079	1.9606	1.7610
c08	interior	Ø3.2947±0.0782	0.1470	0.0465	0.0107	0.0181	377	0.0079	1.4116	1.6474
c08_s	interior sep.	Ø3.3085±0.0518	0.0800	0.0202	0.0098	0.0124	364	0.0079	1.4116	1.6542
c09	interior	Ø2.2409±0.1552	0.2511	0.0753	0.0278	0.0368	362	0.0079	0.8627	1.1205
c09_s	interior sep.	Ø2.2378±0.1024	0.1908	0.0575	0.0210	0.0280	361	0.0079	0.8627	1.1189

Table 10: Detailed circularity measurements at selected samples perpendicular to vessel curvature, vessel RV003.

Comparison of circularity on the full vessel surface

Metric

Samples perpendicular to the surface curvature

Area	Range			Standard Deviation			RMSD			Slices	Slice height
	Median	Min.	Max.	Median	Min.	Max.	Median	Min.	Max.		
	mm	mm	mm	mm	mm	mm	mm	mm	mm		mm
Exterior	1.913	1.205	3.721	0.251	0.140	0.489	0.457	0.235	0.916	269	0.200
Interior	4.381	1.959	5.168	0.636	0.254	0.857	1.374	0.549	1.739	213	0.200
Interior separate	1.962	1.070	3.129	0.266	0.118	0.603	0.501	0.314	1.057	235	0.200

Table 11: Detailed circularity measurements at selected samples in z-plane, vessel RV003.

Samples in the z-plane

Area	Range			Standard Deviation			RMSD			Slices	Slice height
	Median	Min.	Max.	Median	Min.	Max.	Median	Min.	Max.		
	mm	mm	mm	mm	mm	mm	mm	mm	mm		mm
Exterior	2.952	1.545	6.739	0.482	0.212	1.103	0.766	0.401	2.289	363	0.200
Interior	4.867	3.444	6.447	0.772	0.414	1.325	1.540	0.863	2.065	288	0.200
Interior separate	2.351	1.130	14.025	0.388	0.152	2.554	0.680	0.316	4.560	288	0.200

Table 12: Detailed circularity measurements at selected samples perpendicular to vessel curvature, vessel RV003.

Imperial

Samples perpendicular to the surface curvature

Area	Range			Standard Deviation			RMSD			Slices	Slice height
	Median	Min.	Max.	Median	Min.	Max.	Median	Min.	Max.		
	in	in	in	in	in	in	in	in	in		in
Exterior	1.913	1.205	3.721	0.251	0.140	0.489	0.457	0.235	0.916	269	0.200
Interior	4.381	1.959	5.168	0.636	0.254	0.857	1.374	0.549	1.739	213	0.200
Interior separate	1.962	1.070	3.129	0.266	0.118	0.603	0.501	0.314	1.057	235	0.200

Table 13: Detailed circularity measurements at selected samples in z-plane, vessel RV003.

Samples in the z-plane

Area	Range			Standard Deviation			RMSD			Slices	Slice height
	Median	Min.	Max.	Median	Min.	Max.	Median	Min.	Max.		
	in	in	in	in	in	in	in	in	in		in
Exterior	2.952	1.545	6.739	0.482	0.212	1.103	0.766	0.401	2.289	363	0.200
Interior	4.867	3.444	6.447	0.772	0.414	1.325	1.540	0.863	2.065	288	0.200
Interior separate	2.351	1.130	14.025	0.388	0.152	2.554	0.680	0.316	4.560	288	0.200

Table 14: Detailed circularity measurements at selected samples perpendicular to vessel curvature, vessel RV003.

Circularity analysis of exterior surface - perpendicular to surface curvature

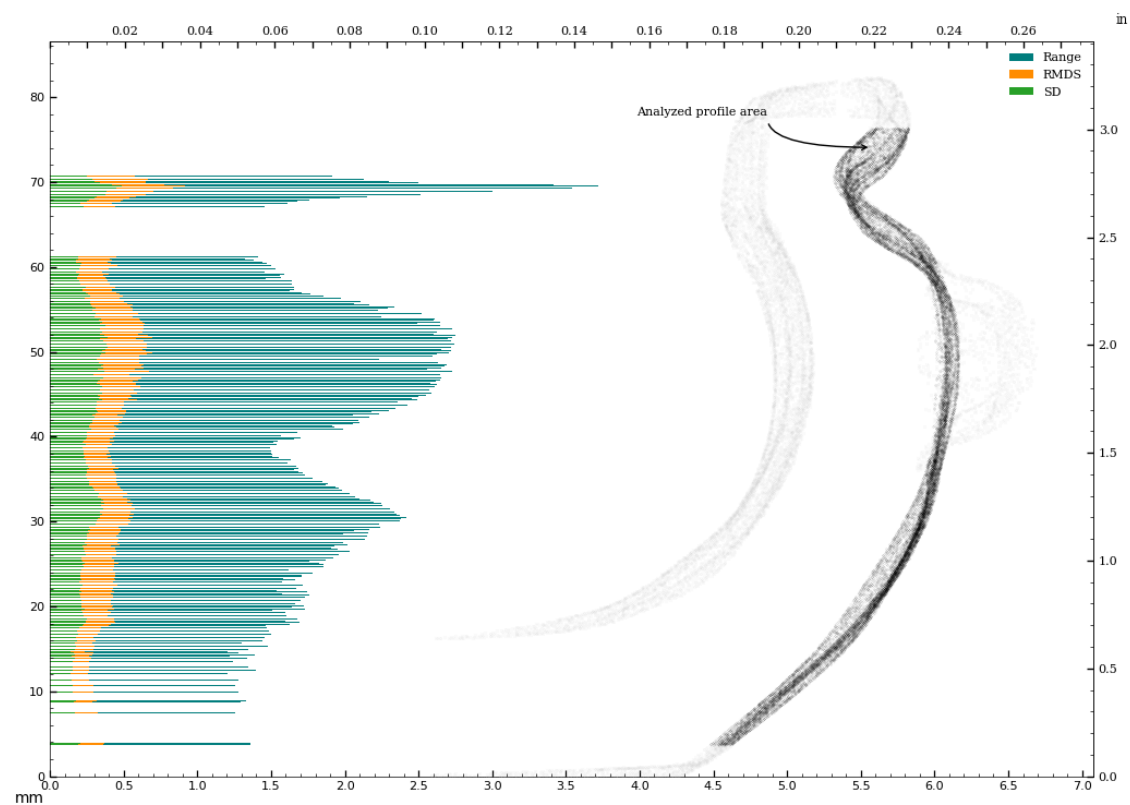


Figure 72: Circularity of exterior surface - perpendicular to surface curvature.

Circularity analysis of exterior surface - in z-plane

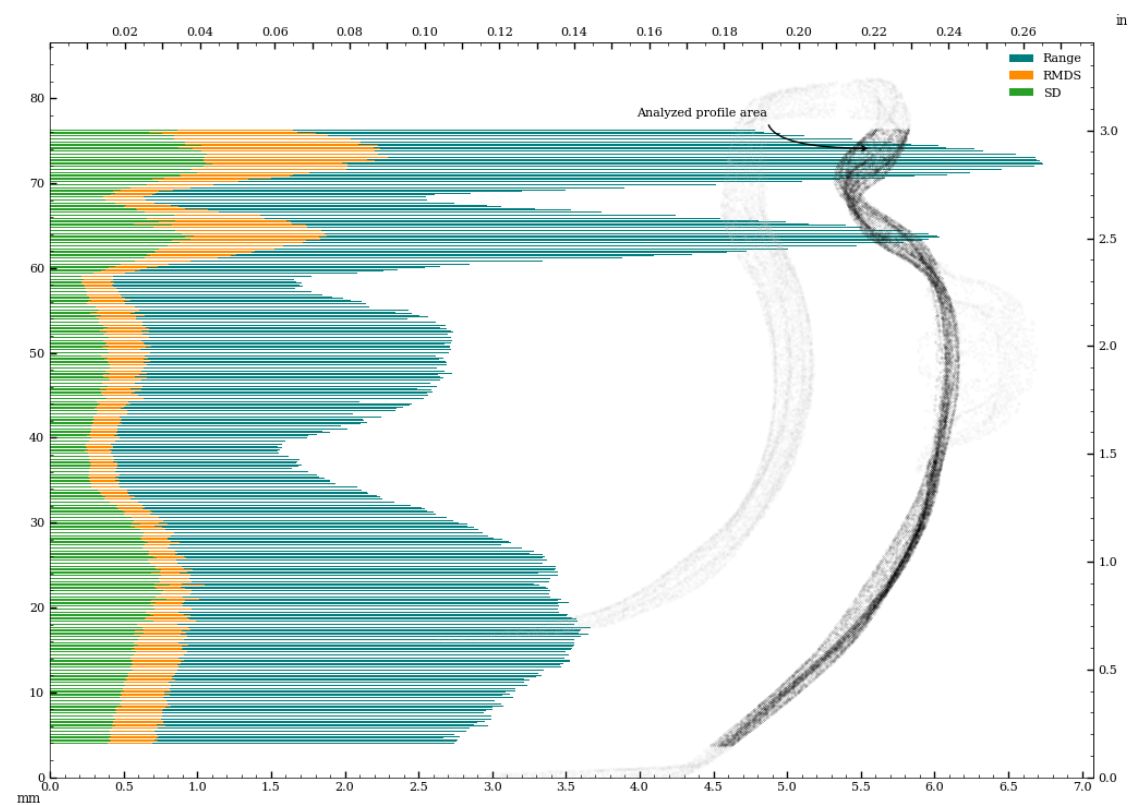


Figure 73: Circularity of exterior surface - in z-plane.

Circularity analysis of exterior surface, perpendicular to surface curvature, Standard Deviation and Root Mean Squared Deviation

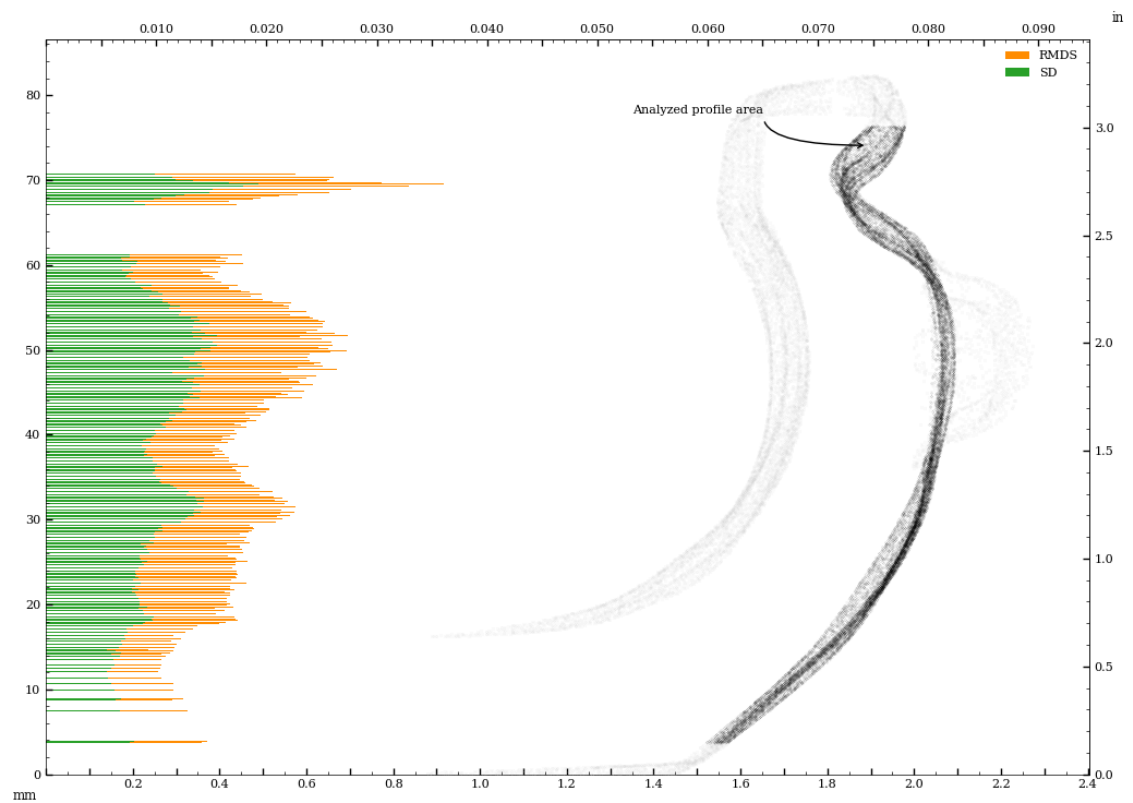


Figure 74: Vessel circularity of exterior surface, perpendicular to surface curvature, standard deviation and median absolute deviation.

Circularity analysis of exterior surface, in z-plane, Standard Deviation and Root Mean Squared Deviation

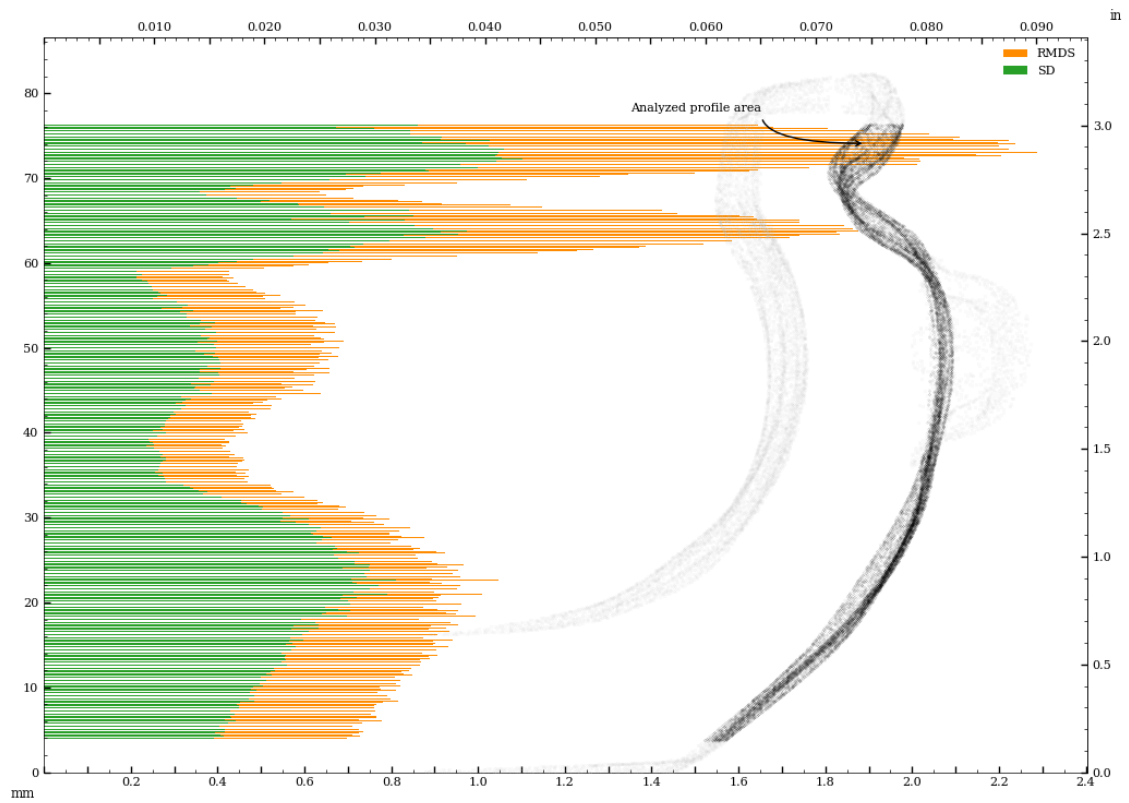


Figure 75: Vessel circularity of exterior surface, in z-plane, standard deviation and median absolute deviation.

Circularity analysis of interior surface - perpendicular to surface curvature

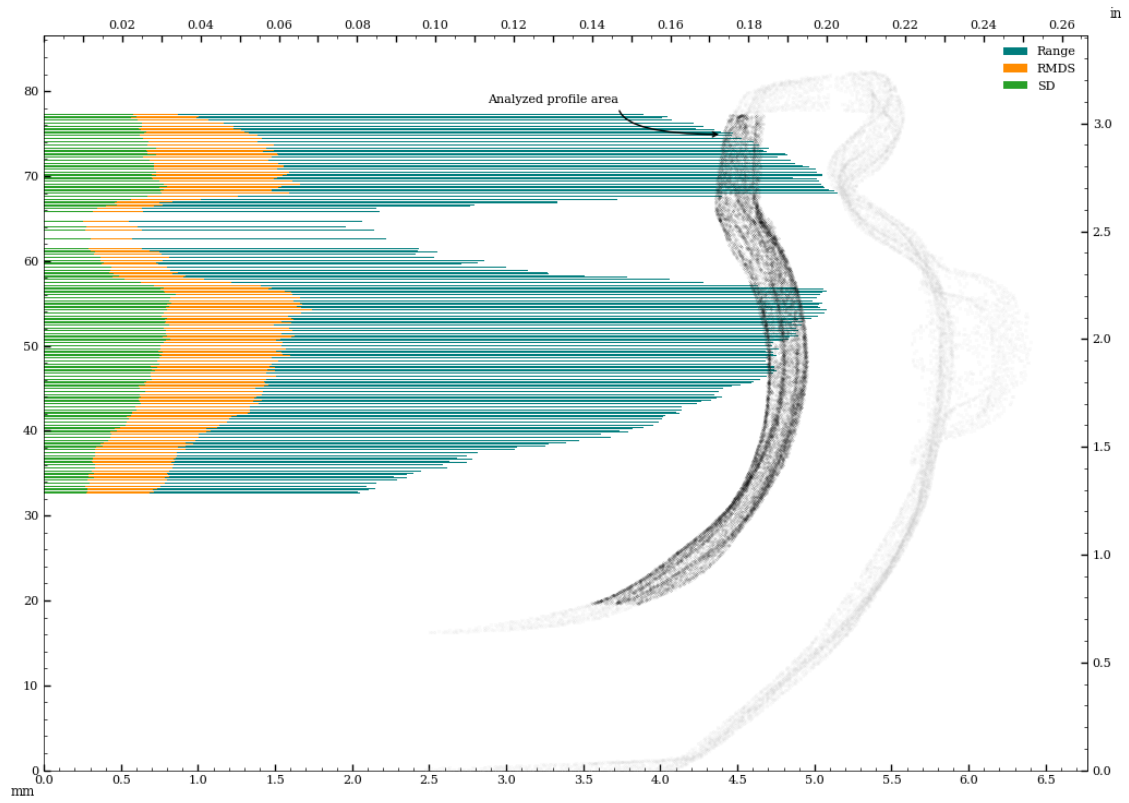


Figure 76: Circularity of interior surface - perpendicular to surface curvature.

Circularity analysis of interior surface - in z-plane

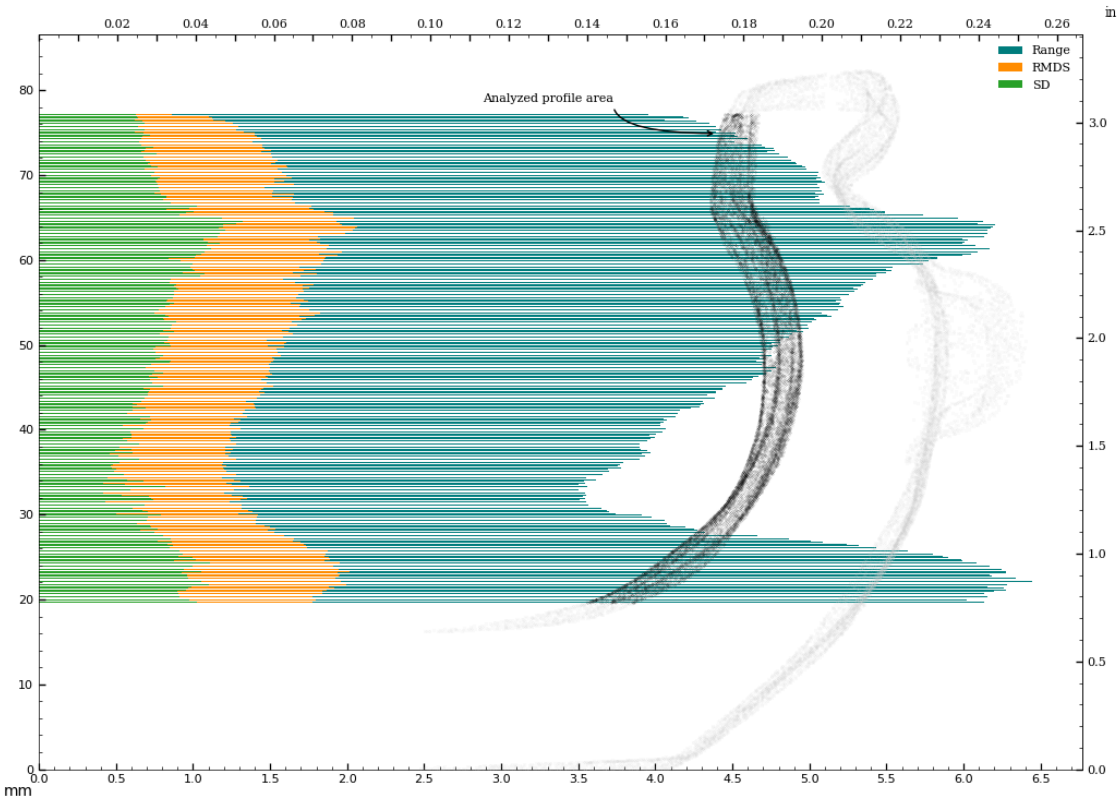


Figure 77: Circularity of interior surface - in z-plane.

Circularity analysis of interior surface, perpendicular to surface curvature, Standard Deviation and Root Mean Squared Deviation

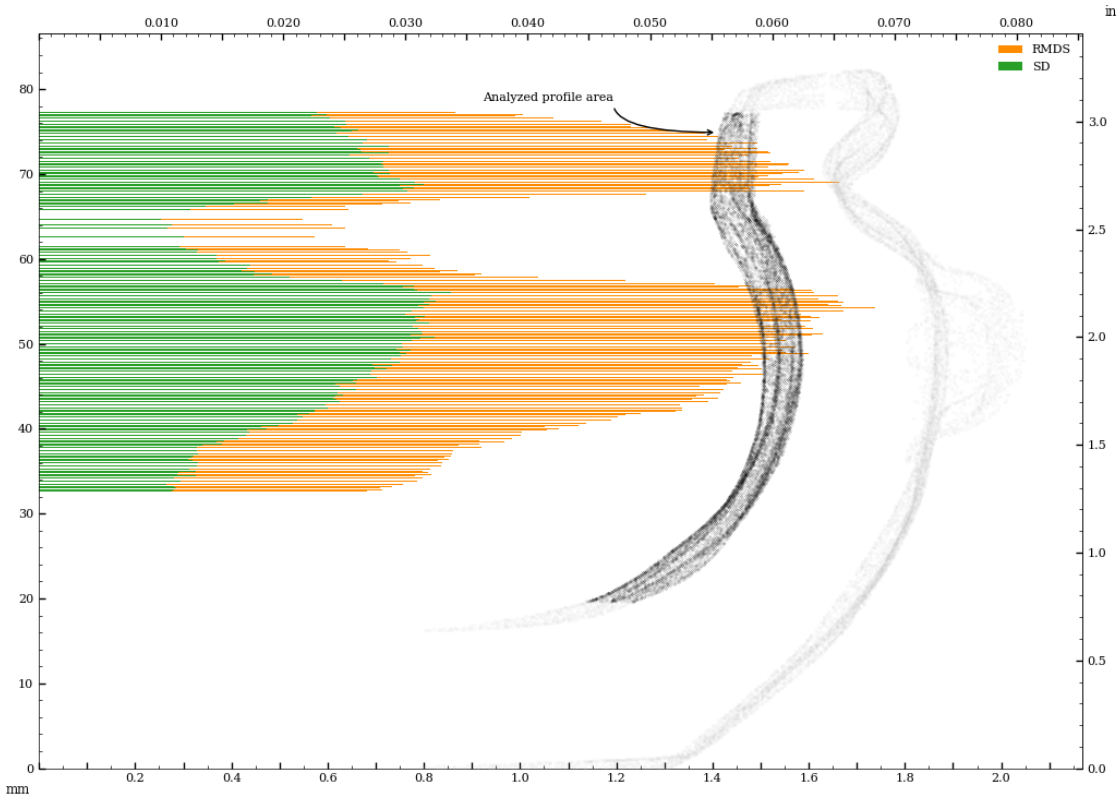


Figure 78: Vessel circularity of interior surface, perpendicular to surface curvature, standard deviation and median absolute deviation.

Circularity analysis of interior surface, in z-plane, Standard Deviation and Root Mean Squared Deviation

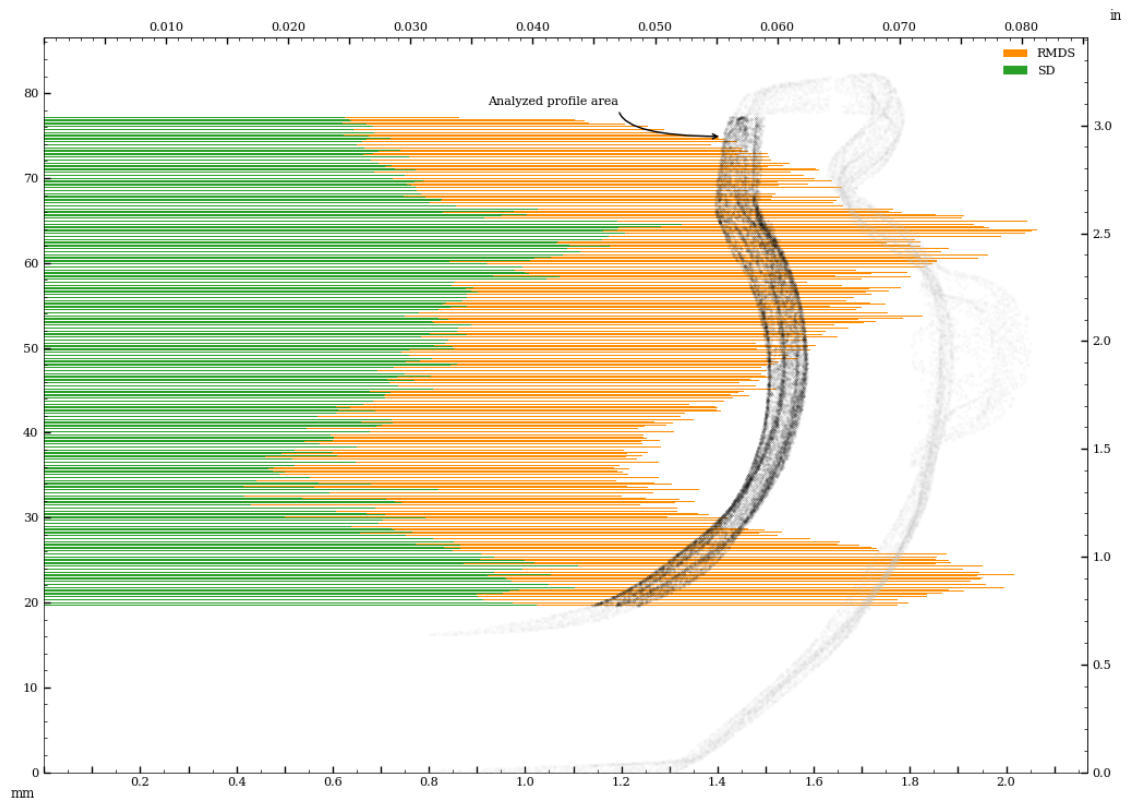


Figure 79: Vessel circularity of interior surface, in z-plane, standard deviation and median absolute deviation.

Circularity analysis of interior separately aligned surface - perpendicular to surface curvature

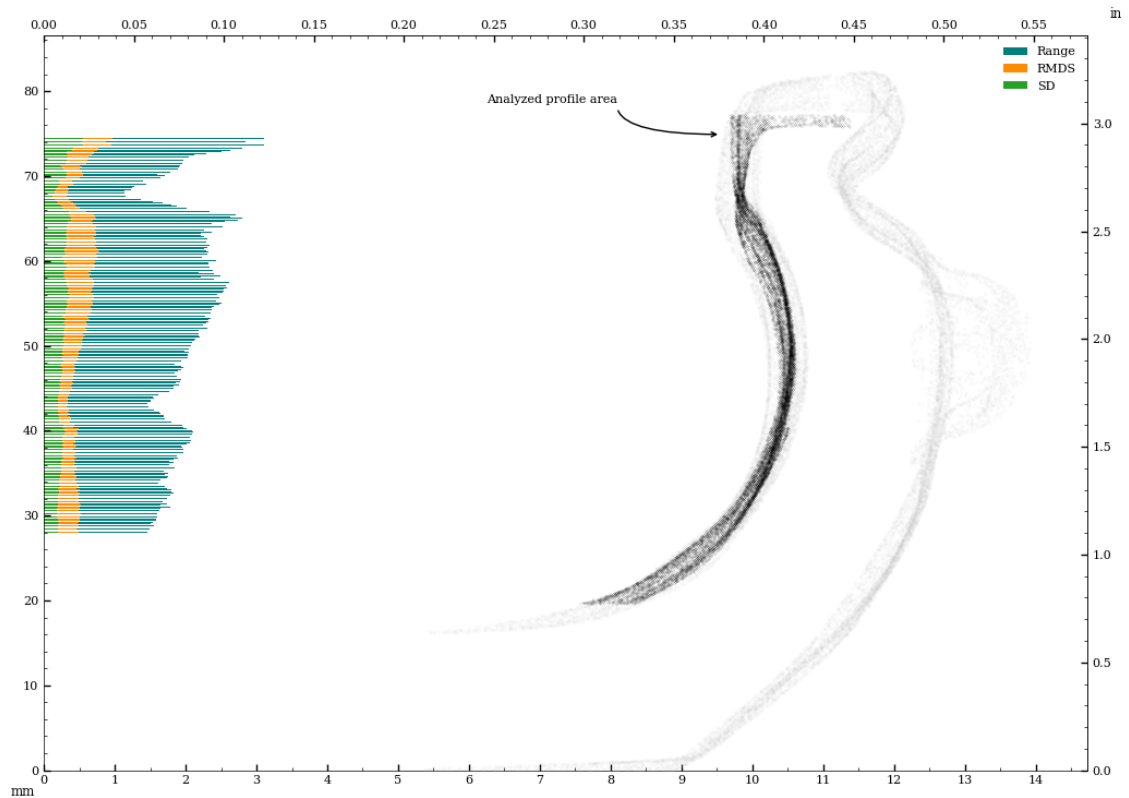


Figure 80: Circularity of interior_separate surface - perpendicular to surface curvature.

Circularity analysis of interior separately aligned surface - in z-plane

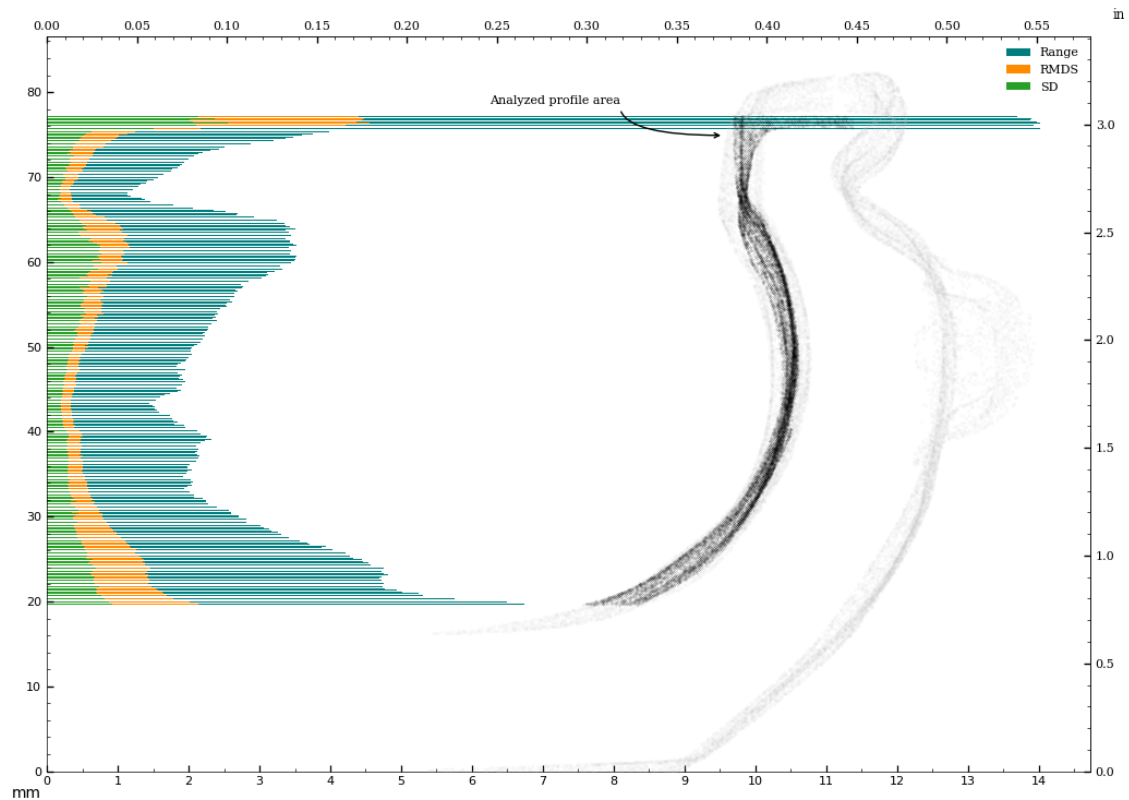


Figure 81: Circularity of interior_separate surface - in z-plane.

Circularity analysis of interior separately aligned surface, perpendicular to surface curvature, Standard Deviation and Root Mean Squared Deviation

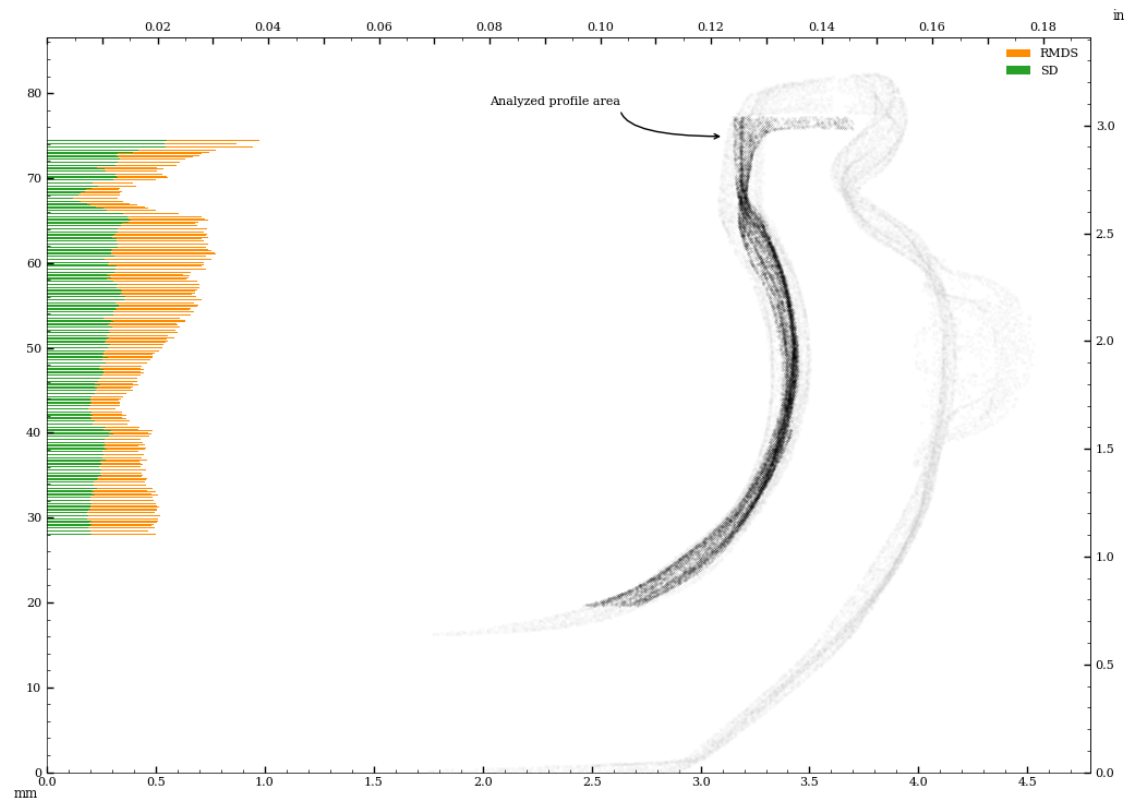


Figure 82: Vessel circularity of interior_separate surface, perpendicular to surface curvature, standard deviation and median absolute deviation.

Circularity analysis of interior separately aligned surface, in z-plane, Standard Deviation and Root Mean Squared Deviation

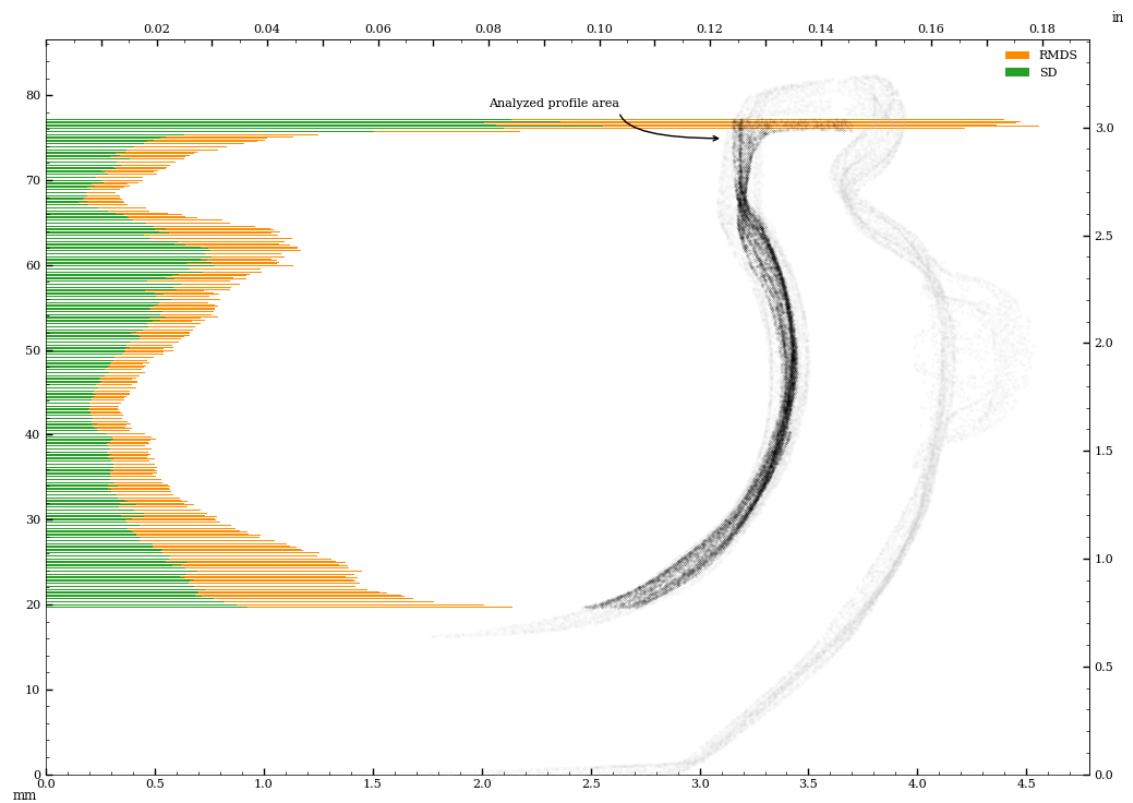


Figure 83: Vessel circularity of interior_separate surface, in z-plane, standard deviation and median absolute deviation.

Appendix B - Comparison Of Concentricity Measurements (Z-plane vs. surface-perpendicular)

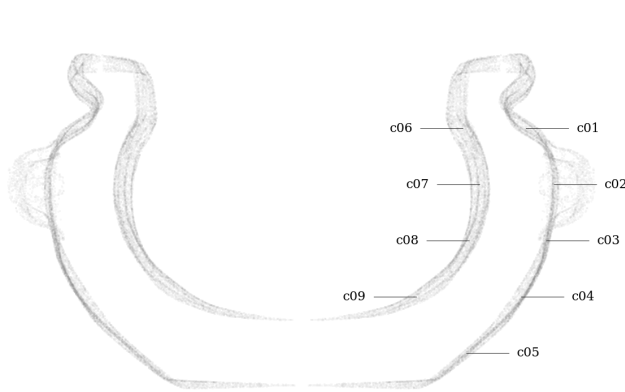


Figure 84: Circularity measurement sample locations, full mesh aligned to exterior surface



Figure 85: Circularity measurement sample location, separately aligned interior mesh

Concentricity measurements perpendicular to surface curvature

Tag	Reference	Deviation	Sample size	Circle fit residuals analysis for sample listed in Tag column						
				Range full	Range inliers	RMSD full	RMSD inliers	SD full	SD inliers	Center (x,y)
		mm		mm	mm	mm	mm	mm	mm	μm
c01	z-axis	2.522	469	10.561	10.561	3.425	3.425	1.578	1.578	−1183, 2227
c02	z-axis	0.502	153	2.700	2.700	0.858	0.858	0.485	0.485	165, −474
c03	z-axis	0.102	302	1.899	1.899	0.465	0.465	0.273	0.273	23, 99
c04	z-axis	0.812	335	3.267	3.267	0.876	0.876	0.575	0.575	−807, 91
c05	z-axis	0.477	290	3.281	3.281	0.843	0.843	0.502	0.502	−439, −186
c06	z-axis	2.615	358	9.711	9.711	3.205	3.205	1.345	1.345	2283, 1275
c06_s	z-axis	1.346	400	3.362	3.362	1.007	1.007	0.496	0.496	1208, −592
c07	z-axis	2.183	312	6.018	6.018	1.951	1.951	0.938	0.938	2137, 447
c07_s	z-axis	0.567	312	2.500	2.500	0.655	0.655	0.375	0.375	423, −378
c08	z-axis	1.665	377	3.445	3.445	1.113	1.113	0.415	0.415	1659, −135
c08_s	z-axis	0.515	364	2.641	2.641	0.565	0.565	0.372	0.372	−412, 309
c09	z-axis	2.374	362	7.226	7.226	2.018	2.018	1.117	1.117	2062, −1176
c09_s	z-axis	1.759	361	4.494	4.494	1.343	1.343	0.676	0.676	−1742, 245
c01	c06	3.595								−3466, 952
c02	c07	2.176								−1971, −922
c03	c08	1.653								−1636, 234
c04	c09	3.137								−2869, 1267

Concentricity measurements in z-plane

Tag	Reference	Deviation	Sample size	Circle fit residuals analysis for sample listed in Tag column						
				Range full	Range inliers	RMSD full	RMDS inliers	SD full	SD inliers	Center (x,y)
		mm		mm	mm	mm	mm	mm	mm	μm
c01	z-axis	2.522	469	10.561	10.561	3.425	3.425	1.578	1.578	−1183, 2227
c02	z-axis	0.502	153	2.700	2.700	0.858	0.858	0.485	0.485	165, −474
c03	z-axis	0.102	302	1.899	1.899	0.465	0.465	0.273	0.273	23, 99
c04	z-axis	0.812	335	3.267	3.267	0.876	0.876	0.575	0.575	−807, 91
c05	z-axis	0.477	290	3.281	3.281	0.843	0.843	0.502	0.502	−439, −186
c06	z-axis	2.615	358	9.711	9.711	3.205	3.205	1.345	1.345	2283, 1275
c06_s	z-axis	1.346	400	3.362	3.362	1.007	1.007	0.496	0.496	1208, −592
c07	z-axis	2.183	312	6.018	6.018	1.951	1.951	0.938	0.938	2137, 447
c07_s	z-axis	0.567	312	2.500	2.500	0.655	0.655	0.375	0.375	423, −378
c08	z-axis	1.665	377	3.445	3.445	1.113	1.113	0.415	0.415	1659, −135
c08_s	z-axis	0.515	364	2.641	2.641	0.565	0.565	0.372	0.372	−412, 309
c09	z-axis	2.374	362	7.226	7.226	2.018	2.018	1.117	1.117	2062, −1176
c09_s	z-axis	1.759	361	4.494	4.494	1.343	1.343	0.676	0.676	−1742, 245
c01	c06	3.595								−3466, 952
c02	c07	2.176								−1971, −922
c03	c08	1.653								−1636, 234
c04	c09	3.137								−2869, 1267

Figure 86: Circularity measurement sample locations, full mesh aligned to exterior surface

Figure 87: Circularity measurement sample location, separately aligned interior mesh

Concentricity measurements perpendicular to surface curvature

Tag	Reference	Deviation	Sample size	Circle fit residuals analysis for sample listed in Tag column						
				Range full	Range inliers	RMSD full	RMDS inliers	SD full	SD inliers	Center (x,y)
		in		in	in	in	in	in	in	thou
c01	z-axis	0.0993	469	0.4158	0.4158	0.1349	0.1349	0.0621	0.0621	−46.6, 87.7
c02	z-axis	0.0198	153	0.1063	0.1063	0.0338	0.0338	0.0191	0.0191	6.5, −18.7
c03	z-axis	0.0040	302	0.0748	0.0748	0.0183	0.0183	0.0107	0.0107	0.9, 3.9
c04	z-axis	0.0320	335	0.1286	0.1286	0.0345	0.0345	0.0226	0.0226	−31.8, 3.6
c05	z-axis	0.0188	290	0.1292	0.1292	0.0332	0.0332	0.0198	0.0198	−17.3, −7.3
c06	z-axis	0.1030	358	0.3823	0.3823	0.1262	0.1262	0.0530	0.0530	89.9, 50.2
c06_s	z-axis	0.0530	400	0.1324	0.1324	0.0396	0.0396	0.0195	0.0195	47.6, −23.3
c07	z-axis	0.0859	312	0.2369	0.2369	0.0768	0.0768	0.0369	0.0369	84.1, 17.6
c07_s	z-axis	0.0223	312	0.0984	0.0984	0.0258	0.0258	0.0148	0.0148	16.7, −14.9
c08	z-axis	0.0655	377	0.1356	0.1356	0.0438	0.0438	0.0163	0.0163	65.3, −5.3
c08_s	z-axis	0.0203	364	0.1040	0.1040	0.0222	0.0222	0.0146	0.0146	−16.2, 12.2
c09	z-axis	0.0935	362	0.2845	0.2845	0.0795	0.0795	0.0440	0.0440	81.2, −46.3
c09_s	z-axis	0.0692	361	0.1769	0.1769	0.0529	0.0529	0.0266	0.0266	−68.6, 9.7
c01	c06	0.1415								−136.5, 37.5
c02	c07	0.0857								−77.6, −36.3
c03	c08	0.0651								−64.4, 9.2
c04	c09	0.1235								−113.0, 49.9

Concentricity measurements in z-plane

Tag	Reference	Deviation	Sample size	Circle fit residuals analysis for sample listed in Tag column						
				Range full	Range inliers	RMSD full	RMDS inliers	SD full	SD inliers	Center (x,y)
		in		in	in	in	in	in	in	thou
c01	z-axis	0.0993	469	0.4158	0.4158	0.1349	0.1349	0.0621	0.0621	−46.6, 87.7
c02	z-axis	0.0198	153	0.1063	0.1063	0.0338	0.0338	0.0191	0.0191	6.5, −18.7
c03	z-axis	0.0040	302	0.0748	0.0748	0.0183	0.0183	0.0107	0.0107	0.9, 3.9
c04	z-axis	0.0320	335	0.1286	0.1286	0.0345	0.0345	0.0226	0.0226	−31.8, 3.6
c05	z-axis	0.0188	290	0.1292	0.1292	0.0332	0.0332	0.0198	0.0198	−17.3, −7.3
c06	z-axis	0.1030	358	0.3823	0.3823	0.1262	0.1262	0.0530	0.0530	89.9, 50.2
c06_s	z-axis	0.0530	400	0.1324	0.1324	0.0396	0.0396	0.0195	0.0195	47.6, −23.3
c07	z-axis	0.0859	312	0.2369	0.2369	0.0768	0.0768	0.0369	0.0369	84.1, 17.6
c07_s	z-axis	0.0223	312	0.0984	0.0984	0.0258	0.0258	0.0148	0.0148	16.7, −14.9
c08	z-axis	0.0655	377	0.1356	0.1356	0.0438	0.0438	0.0163	0.0163	65.3, −5.3
c08_s	z-axis	0.0203	364	0.1040	0.1040	0.0222	0.0222	0.0146	0.0146	−16.2, 12.2
c09	z-axis	0.0935	362	0.2845	0.2845	0.0795	0.0795	0.0440	0.0440	81.2, −46.3
c09_s	z-axis	0.0692	361	0.1769	0.1769	0.0529	0.0529	0.0266	0.0266	−68.6, 9.7
c01	c06	0.1415								−136.5, 37.5
c02	c07	0.0857								−77.6, −36.3
c03	c08	0.0651								−64.4, 9.2
c04	c09	0.1235								−113.0, 49.9